

https://dspace.org/

Mechanistic insights into cholesterol depletion in an in vivo model of pancreatic cancer

van Wyk, Lize-Marie

2025-05

University of the Witwatersrand, Johannesburg

https://hdl.handle.net/10539/48371

van Wyk, Lize-Marie. (2025). Mechanistic insights into cholesterol depletion in an in vivo model of pancreatic cancer. [Master's dissertation, University of the Witwatersrand, Johannesburg]. WIReDSpace. https://hdl.handle.net/10539/48371

Downloaded from a DSpace repository. https://dspace.org/



MECHANISTIC INSIGHTS INTO CHOLESTEROL DEPLETION IN AN *IN VIVO* MODEL OF PANCREATIC CANCER

by

Lize-Marie van Wyk

(1619251)

DISSERATION

Submitted in fulfilment of the requirements for the degree

MASTERS IN SCIENCE

in

Molecular and Cell Biology

in the Faculty of Science, University of the Witwatersrand, Johannesburg, South Africa

Supervisor: Prof. Mandeep Kaur

Co-supervisor: Dr Liang Gu

May 2025

CANDIDATE DECLARATION

I declare that this dissertation is my own, unaided work. It is being submitted for the Degree of Masters in Science at the University of the Witwatersrand, Johannesburg. It has not been submitted before for any degree or examination at any other University.



(Lize-Marie van Wyk)

22nd day of May 2025 at Roodepoort

ACKNOWLEDGEMENTS

This research project would not have been feasible without the support and assistance of the following individuals and institutions:

I would like to express my gratitude to Prof. Mandeep Kaur and Dr Liang Gu, for their invaluable and constructive suggestions throughout my research project and dissertation writing. In Prof. Kaur's laboratory, I have acquired numerous skills and am profoundly appreciative of the opportunity to contribute to her research team.

I would like to express my gratitude to my colleagues in GH519, especially Thea du Plessis and Andrea Breytenbach for their assistance and support. They have provided invaluable guidance, encouragement, and memorable experiences. Their contributions extend beyond professional relationships, as they have become valued friends. Additionally, I wish to convey my appreciation to the Pancreatic cancer team, whose support has been instrumental in the completion of this work.

I hereby acknowledge the University of the Witwatersrand for providing the infrastructure to conduct my research and for funding the tuition for my degree of Masters in Science through the Postgraduate Merit Award. The financial funding for this research project was received from the South African Medical Research Council (Self-Initiated Research Grant to Prof. M Kaur) for the *in vivo* xenograft study.

ETHICAL CLEARANCE

Clearance was received from the Wits Animal Research Ethics Committee (clearance number: 2019/09/52/D).

TABLE OF CONTENTS

ABSTRACT ……11
1 INTRODUCTION 12
1.1 Pancreatic Cancer Epidemiology 12
1.2 PC pathogenesis and progression 12
1.3 Current Chemotherapeutic Treatment Regimens 14
1.4 Resistance to chemotherapies in PDAC 17
1.4.1 Drug transport 17
1.4.2 Drug metabolism 18
1.4.3 Tumour heterogeneity 18
1.4.4 Reprogrammed cellular metabolism 19
1.5 Cholesterol homeostasis and its role in PDAC 19
1.5.1 Cholesterol *de novo* biosynthesis 21
1.5.1.1 Uptake of cholesterol 22
1.5.1.2 Efflux of cholesterol 23
1.5.1.3 Storage and transport of cholesterol 24
1.6 Targeting cholesterol for anticancer therapy 26
1.6.1 Statins 27
1.6.2 Cyclodextrins 28
1.7 Rationale for the present study 29
2 AIMS AND OBJECTIVES 30
2.1 Aim 30
2.2 Objectives 30
2.3 Workflow 30
3 METHODS 31
3.1 Pancreatic Cancer Mice Xenograft Model 31
3.2 Protein Extraction from Cryopreserved PDAC Xenograft Tissue 33

3.2.1 Protein Extraction Protocol 33
3.3 Protein Identification and Quantification with Western Blotting 34
3.3.1 Protein Quantification: BCA Assay 34
3.3.2 Protein separation: SDS-PAGE 36
3.3.3 Protein identification: Western Blotting 39
3.4 Statistical Analysis 42
4 RESULTS 43
4.1 Tumour volume 43
4.2 Relative protein expression in xenograft tumour tissue 45
4.2.1 β-tubulin normalization 45
4.2.2 Cholesterol storage: ACAT1 46
4.2.3 Cholesterol Synthesis: HMGCR 48
4.2.4 Cholesterol Uptake: LDLR & PCSK9 49
4.2.5 Regulation of cholesterol synthesis and uptake: SREBP2 51
4.2.6 Cholesterol Efflux: ABCG1 53
5 DISCUSSION 54
5.1 Tumour volume and metastasis 54
5.1.1 HPβCD was not effective as monotherapy and possibly induced epithelial-mesenchymal transition (EMT) 55
5.1.2 Combination with HPβCD did not significantly improve 5-FU efficacy 55
5.1.3 Single and combination treatments of GEM and HPβCD potentially induced metastasis in PDAC 56
5.2 Effects on cholesterol homeostasis using HPβCD monotherapy and in combination with first-line chemotherapies: 5-FU and GEM 57
5.2.1 Cholesterol storage 59
5.2.2 Cholesterol synthesis 60
5.2.3 Cholesterol uptake 62

5.2.4 SREBP2 mediated transcriptional regulation of cholesterol synthesis and uptake…..64
5.2.5 Cholesterol efflux....66
5.3 Conclusion....68
5.4 Limitations and future work....70
6 TROUBLESHOOTING....72
6.1 Protein Extraction....72
6.2 Western Blots....73
7 REFERENCES....74
8 APPENDIX....109
8.1 Mice Xenograft Study....109
8.1.1 Cell Culture....109
8.1.2 Xenograft Mice Model Study....109
8.2 Mice eliminated from the study....112
8.3 Gene expression....113
8.4 Mouse serum analysis of total cholesterol....114
8.5 Tumour volume and relative protein expression of vehicle control DMSO....115

LIST OF EQUATIONS

Equation 1: Calculation for concentration of protein lysate....36
Equation 2: Calculation of tumour volume....110

LIST OF FIGURES

Figure 1: Progression of low-grade PanIN-1 to PDAC....13
Figure 2: Molecular mechanism of action of GEM....15
Figure 3: Molecular mechanism and action of 5-FU....16
Figure 4: Simplistic overview of enzyme catalysed reactions of the Mevalonate Pathway....21
Figure 5: Cholesterol homeostasis in PDAC....26
Figure 6: Computational configuration of HPβCD with cholesterol....28
Figure 7: Workflow used in the present study....31

Figure 8: A prototypical standard curve used in a BCA assay 35
Figure 9: PDAC tumours from xenograft mice 44
Figure 10: Normalization of loading with β-tubulin.....46
Figure 11: Relative protein expression levels of ACAT1.....47
Figure 12: Relative protein expression levels of HMGCR.....48
Figure 13: Relative protein expression levels of LDLR 50
Figure 14: Relative protein expression levels of PCSK9.....51
Figure 15: Relative protein expression level of SREBP2 active and precursor form.....52
Figure 16: Relative protein expression level of ABCG1 53
Figure 17: A heat map summarising the protein expression profiles (%) of key proteins involved in cholesterol homeostasis 58
Figure 18: Visual summary on cholesterol depletion and PDAC tumour response 70

LIST OF TABLES

Table 1: Cell-derived Xenograft Treatment Regimens.....32
Table 2: RIPA lysis buffer components.....34
Table 3: SDS-PAGE resolving and stacking gel components.....38
Table 4: Running buffer components 39

LIST OF SYMBOLS

α	alpha
β	beta
©	copyright
°C	celsius
κ	kappa
μ	micro
μL	microlitres
μM	micromolar
mM	milimolar

ABBREVIATIONS

5-FU	5-Fluorouracil
ABC	ATP-binding cassette
ABCG1	ATP Binding Cassette Transporter Subfamily G 1
ACAT1	Acyl-CoA: Cholesterol Acyltransferase 1
acetoacetyl-CoA	Acetoacetyl-Coenzyme A
ADM	acinar-to-ductal metaplasia
AP	Acetyl Plumbagin
apoA-I	Apolipoprotein A-I
apoB	Apolipoprotein B
Cav-1	Caveolin-1
CDs	Cyclodextrins
CDA	Cytidine Deaminase
CDK	Cyclin dependent kinase
CDKN	Cyclin-Dependent Kinase Inhibitor
CDs	Cyclodextrins
CE	Cholesteryl Ester
CETP	Cholesterol Ester Transport Protein
CNT	Concentrative Nucleoside Transporters
CSC	Cancer Stem Cell

CtBP	C-terminal-binding protein
DCK	Deoxycytidine Kinase
dFdC	2 2-Difluorodeoxycytidine
dFdCDP	dFdC Diphosphate
dFdCMP	dFdC Monophosphate
dFdCTP	dFdC Triphosphate
dFdUMP	2 2-Difluorodeoxyuridine Monophosphate
DMEM	Dulbecco's Modified Eagle Medium
DNA	Deoxyribonucleic acid
DPD	Dihydropyrimidine dehydrogenase
dTMP	Deoxythymidine Monophosphate
dTTP	Deoxythymidine Triphosphate
dUMP	Deoxyuridine Monophosphate
dUTP	Deoxyuridine Triphosphate
EDTA	Ethylenediaminetetraacetic acid
EGF	Epidermal Growth Factor
EGFR	Epidermal Growth Factor Receptor
EMT	Epithelial To Mesenchymal Transition
ER	Endoplasmic Reticulum
ERK	Extracellular Signal-Regulated Kinase
FBS	Foetal Bovine Serum
FdUDP	16-Fluorodeoxyuridine Diphosphate
FdUMP	Fluorodeoxyuridine Monophosphate
FdUTP	Fluorodeoxyuridine Triphosphate
FGF	Fibroblast Growth Factor
FPP	Farnesyl pyrophosphate
FUDP	Fluorouridine Diphosphate
FUDR	Fluorodeoxyuridine
FUMP	Fluorouridine Monophosphate
FUR	Fluorouridine
FUTP	Fluorouridine Triphosphate
GEM	Gemcitabine
GGPP	Geranylgeranyl pyrophosphate

GPCRs	G-protein Coupled Receptors
GSK3	Glycogen Synthase Kinase 3 Protein
HDL	High Density Lipoprotein
HDLR	HDL receptor
hENT	Human Equilibrative Nucleoside Transporters
HIF1α	Hypoxia-Inducible Factor 1 A
HMG-CoA	3-hydroxy-3-methyl-glutaryl CoA
HMGCR	HMG-CoA reductase
hOAT2	organic anionic transporter 2
HPβCD	2-Hydroxypropyl-β-Cyclodextrin
KRAS	Kirsten Rat Sarcoma Viral Oncogene Homolog
LDL	Low Density Lipoprotein
LDLR	LDL Receptor
LXR	Liver X Receptor
MAPK	Mitogen-Activated Protein Kinase
MDR	Multi-drug resistance
MEK	Mitogen-Activated Protein Kinase
MP	Mevalonate Pathway
mTOR	Mammalian Target Of Rapamycin
mTORC1	Mechanistic Target of Rapamycin Complex 1
MTT	4,5-Dimethylthiazol-2-yl)-2,5-Diphenyltetrazolium Bromide
MβCD	Methyl-β-Cyclodextrin
NF-κB	Nuclear Factor Kappa-Light-Chain-Enhancer of Activated B Cells
PanIN	Pancreatic Intraepithelial Neoplasia
PARP	Poly-Adp Ribose Polymerase
PBS	Phosphate Buffered Saline
PC	Pancreatic Cancer
PCR	Polymerase Chain Reaction
PCSK9	Proprotein convertase subtilisin/kexin type 9
PDAC	Pancreatic Ductal Adenocarcinoma
PI3K	Phosphatidyl Inositol 3-Kinase
PRPP	Phosphoribosyl Pyrophosphate
PTEN	Phosphatase and Tensin Homolog

RNA	Ribonucleic Acid
RT-qPCR	Real Time-Quantitative PCR
RTKs	Receptor Tyrosine Kinases
SCAP	SREBP-Cleavage Activating Protein
SDS	Sodium Dodecyl Sulphate
SMAD	Mothers Against Decapentaplegic Homolog 4
SR-B1	Scavenger Receptor B1
SRE	Sterol Regulatory Element
SREBP	Sterol Regulatory Element-Binding Protein
SREBP2	Sterol Regulatory Element Binding Protein 2
STAT-3	Signal Transducer and Activator of Transcription
TGF-β	Transforming Growth Factor-β
TME	Tumour Microenvironment
TP53	Tumour Protein 53
TS	Thymidylate Synthase
UK	Uridine Kinase
UP	Uridine Phosphorylase
WHO	World Health Organization

ABSTRACT

Pancreatic ductal adenocarcinoma (PDAC) is a silent global burden with a poor survival rate and highly drug resistant. It is believed that its altered cholesterol metabolism, which results from metabolic changes in PDAC, may influence treatment response. Cholesterol depleting agents, also known as cyclodextrins, provide a novel therapeutic strategy to improve treatment response and potentially overcome drug resistance in PDAC. Using 2-hydroxypropyl-β-cyclodextrin (HPβCD) to deplete cholesterol has shown promising results in *in vitro* PDAC studies. In our lab, HPβCD alone, and the combination of HPβCD with chemotherapeutic drugs has shown improved treatment response from *in vivo* studies for triple negative breast cancer and colorectal cancer, respectively. Nevertheless, no study has yet examined the impact of using HPβCD in conjunction with chemotherapy on the cholesterol homeostasis and treatment response of PDAC *in vivo*. Therefore, the aim of this study was to investigate the effects of adjuvant cholesterol depletion, with HPβCD, on the expression of key proteins in cholesterol metabolism and treatment response from cryopreserved PDAC tumour tissue. A PDAC mice xenograft served as the *in vivo* model for this study. Mice tumours were subjected to treatments consisting of mono- and combination therapies of Gemcitabine, 5-Fluorouracil, and HPβCD. Following successful completion of treatment regimens, tumours were excised and volume was measured. Whole protein was extracted from snap-frozen PDAC mice tumours and quantified using BCA assay, followed by Western blots to quantify the relative protein expression of key proteins involved in cholesterol homeostasis. 5-Fluorouracil monotherapy and its combination with HPβCD significantly reduced tumor volume to a greater extent than Gemcitabine and HPβCD therapies. ACAT1 expression indicates that Gemcitabine upregulated cholesterol storage, which was mitigated by HPβCD, whereas 5-Fluorouracil did not induce a cellular dependence on cholesterol storage. The combination of HPβCD with both Gemcitabine and 5-Fluorouracil reduced cellular dependence on cholesterol synthesis and uptake, as evidenced by decreased HMGCR and LDLR expression. Notably, HPβCD activated the SREBP2 negative feedback loop without increasing cholesterol uptake or synthesis. Furthermore, HPβCD enhanced cholesterol export via ABCG1, whether utilized alone or in combination. These findings elucidate the complex relationship between cholesterol homeostasis and drug response. Further investigation of cholesterol depletion using HPβCD, either as monotherapy or combination therapy in PDAC, is essential to comprehensively understand the mechanisms of drug resistance.

1 INTRODUCTION

1.1 Pancreatic Cancer Epidemiology

The World Health Organization (WHO) has reported that cancer is the most prevalent cause of death worldwide (Sung *et al.*, 2021). The most rapid increase in cancer cases occurs in sub-Saharan Africa, including South Africa (Sung *et al.*, 2021). Pancreatic cancer (PC) is the "silent global burden", which has doubled in the past two decades (Lippi and Mattiuzzi, 2020; Klein, 2021). Its low five-year survival rate of 9% has made it among the most lethal cancers worldwide (Lippi and Mattiuzzi, 2020), with over 450 000 deaths recorded globally in 2020 (Li *et al.*, 2022), and it is projected to be the 2nd primary cause of cancer-related deaths by 2030 (Z Zhang *et al.*, 2023). The global PC burden is expected to increase dramatically in the coming years (Klein, 2021). This is largely attributed to hereditary factors (cancer gene variants and familial pancreatitis) linked to a fast-growing population, as well as modifiable lifestyle factors (tobacco smoke, diabetes, obesity and alcohol) associated with a westernized lifestyle (Lippi and Mattiuzzi, 2020; Klein, 2021). The lethality of PC is attributed to its late diagnosis as symptoms only surface at an advanced malignant stage, which is currently incurable, highlighting the importance of PC research (Lippi and Mattiuzzi, 2020).

1.2 PC pathogenesis and progression

Malignant transformation comprises several steps, including accumulation of somatic mutations, epigenetic alterations, uncontrolled cell proliferation, and reprogramming of cell metabolism (Göbel *et al.*, 2020). The pancreas forms part of both the exocrine and endocrine system and is composed of several glands (Grant *et al.*, 2016). Pancreatic neoplasms commonly arise from the epithelial exocrine cells (Grant *et al.*, 2016). The most prominent subtype of exocrine PC, that accounts for 90% of all pancreatic malignancies, is Pancreatic Ductal Adenocarcinoma (PDAC) (Grant *et al.*, 2016). PDAC originates from the epithelial layer lining of the pancreatic duct where precursor lesions form (Grant *et al.*, 2016). Pancreatic intraepithelial neoplasia (PanINs) are the precursor lesions mostly associated with PDAC (Grant *et al.*, 2016). The other main precursor lesions of PDAC include intraductal papillary mucinous neoplasia (IPMN) and mucinous cystic neoplasia (MCN) (Noë and Brosens, 2016). The formation of precursor lesions is initiated by mutations in the Kristen rat sarcoma viral oncogene homolog (*KRAS*) gene (Grant *et al.*, 2016; Lai *et al.*, 2020; Z Zhang *et al.*, 2023). The *KRAS* gene has a 95% mutation rate in PDAC and is therefore associated with its pathogenesis and progression (Z Zhang *et al.*, 2023). The initial precursor lesions, formed as a

result of mutated *KRAS*, are classified as low-grade. They require the subsequent accumulation of mutations in tumour suppressor genes to progress to PDAC (Grant *et al.*, 2016; Noë and Brosens, 2016). These tumour suppressor genes contribute to the progression to higher grade lesions and include cyclin-dependent kinase inhibitor 2A (*CDKN2A*); tumour protein 53 (*TP53*); and Mothers against decapentaplegic homolog 4 (*SMAD4*) (Fig 1) (Hu *et al.*, 2021).

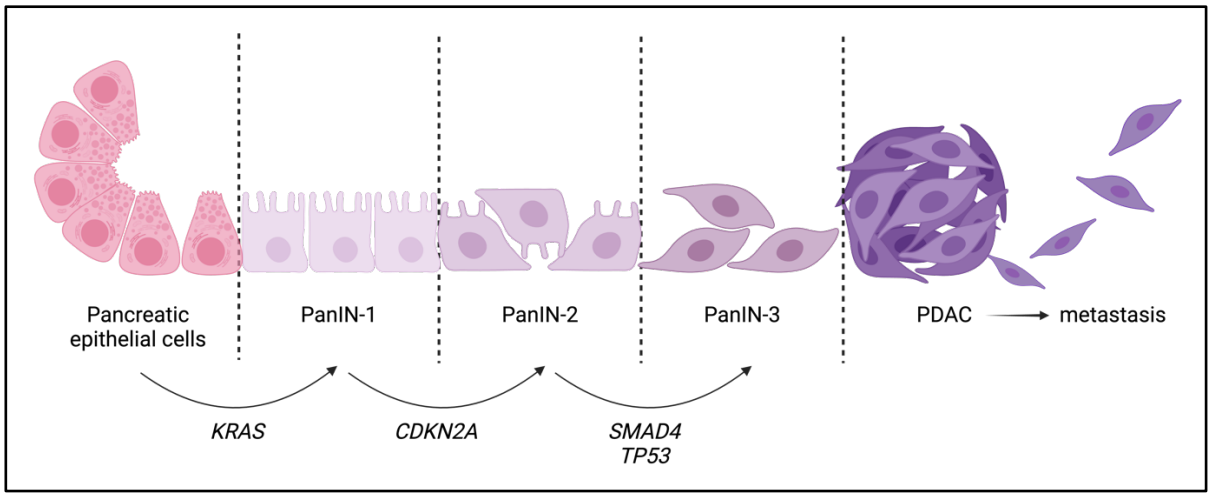


Figure 1: Progression of low-grade PanIN-1 to PDAC

Four main mutagenic events lead to the formation of PDAC from low-grade PanINs (PanIN-1). The mutation in the *KRAS* oncogene initiates the pathogenesis of PDAC. Loss of function mutations in *CDKN2A* and *SMAD4* follow subsequently and progression to high-grade PanINs (PanIN-3) are finalised with the gain of function mutation in *TP53*. *CDK2NA* encodes a cyclin-dependent kinase inhibitor, which is responsible for inhibiting entry into the S-phase of the cell cycle (Grant *et al.*, 2016). Consequently, a loss-of-function mutation in *CDK2NA* will induce senescence following *KRAS* oncogene activation. *SMAD4's* loss-of-function mutation results in the promotion of invasion and apoptosis (Grant *et al.*, 2016). *TP53* acquires a functional mutation that impedes the expression of genes related to cell cycle arrest and apoptosis, thereby contributing to the metastatic nature of PDAC (Grant *et al.*, 2016). High-grade PanINs are associated with PDAC (Hu *et al.*, 2021). (Adapted from Grant *et al.,* 2016; Created with Biorender.com).

The *KRAS* gene encodes for small guanosine-5'-triphosphatases (GTPases), responsible for regulating cell proliferation, differentiation, survival and migration pathways (Grant *et al.*, 2016). KRAS is a guanine-nucleotide binding protein (Gillette *et al.*, 2015), which cycles between a GTP-bound active state (stimulated by growth factors) and a GDP-bound inactive state (Grant *et al.*, 2016). In PDAC, the mutant KRAS protein is permanently activated in a GTP-bound state, since the mutation impairs its ability to hydrolyse GTP into GDP (Grant *et al.*, 2016), this leads to the continuous activation of its downstream effector pathways of which include the mitogen-activated protein kinase (MAPK), phosphatidylinositol 3-kinase (PI3K),

Ras like guanine nucleotide exchange factors (RAL-GEFs) and nuclear factor kappa-light-chain-enhancer of activated B cells (NF-κB) pathways (Mann *et al.*, 2016; Mizrahi *et al.*, 2020; Z Zhang *et al.*, 2023). The mutant KRAS protein is therefore central to PDAC initiation, development, proliferation, angiogenesis, metastasis, metabolic reprogramming, drug resistance and remodelling of the tumour microenvironment (TME) (Grant *et al.*, 2016; Göbel *et al.*, 2020; Lai *et al.*, 2020; Hu *et al.*, 2021; Z Zhang *et al.*, 2023). Thus, KRAS provides the ultimate drug target. However, KRAS remains "undruggable" since it lacks a binding pocket and has a high affinity towards GTP (Göbel *et al.*, 2020). The current treatment regimens for PDAC remain largely ineffective and do not directly target these driver-mutations.

1.3 Current Chemotherapeutic Treatment Regimens

The late-stage diagnosis of PDAC render surgical resection an ineffective first-line approach, therefore pervasive chemotherapy is the chosen approach (Orth *et al.*, 2019). The current first-line treatment for PDAC consists of a choice between Gemcitabine (GEM) or 5-Fluorouracil (5-FU) (Principe *et al.*, 2021; C Liu *et al.*, 2023). GEM is generally administered in combination with capecitabine or nab-paclitaxel (Ciccolini *et al.*, 2016; Principe *et al.*, 2021; C Liu *et al.*, 2023). 5-FU forms part of a multi-drug regimen named FOLFIRINOX (leucovorin, oxaliplatin, irinotecan and 5-FU) (C Liu *et al.*, 2023). Both GEM and 5-FU rely on the utilization of proteins, such as human concentrative nucleoside transporters (hCNT) and human equilibrative nucleoside transporters (hENT), to enter the cancer cell. Although both are nucleoside transporters, they differ in that hCNT employs unidirectional sodium-dependent active transport, whereas hENT utilizes bidirectional facilitated diffusion (Young *et al.*, 2013).

GEM (2',2'-difluorodeoxycytidine, dFdC, Gemzar®) is one of the most prescribed antimetabolite chemotherapeutic drugs and used to treat several cancer types, and is a deoxycytidine analogue, distinguished by the presence of two fluoride atoms at the 2' position (Ciccolini *et al.*, 2016; C Liu *et al.*, 2023). GEM employs hCNT1, hCNT3, and particularly hENT1 to gain entry into the cell (Principe *et al.*, 2021). GEM is converted into its active form by tumour cells, where it interferes with DNA synthesis via chain termination and inhibits the activity of ribonucleotide reductase, leading to impeded cancer cell proliferation (Fig 2) (Ciccolini *et al.*, 2016; C Liu *et al.*, 2023).

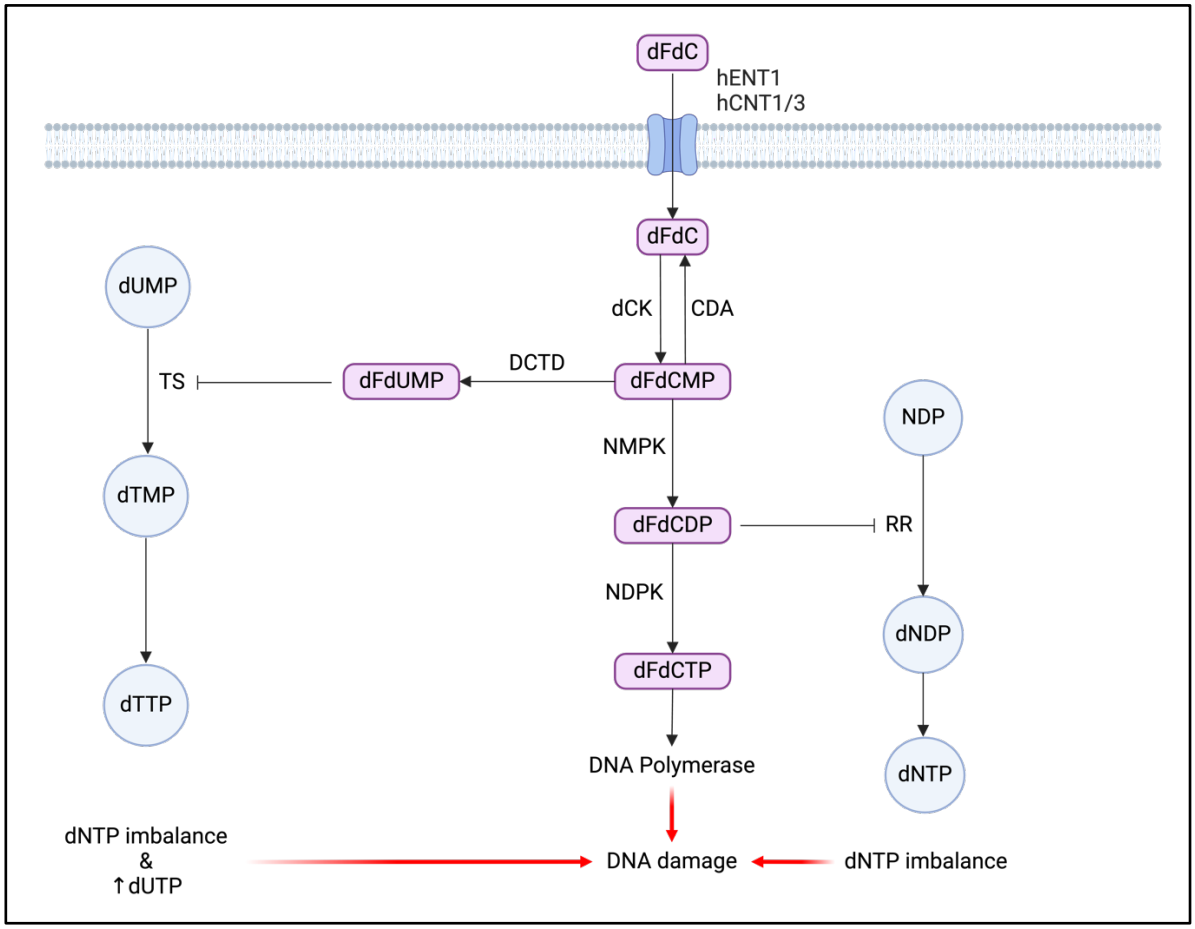


Figure 2: Molecular mechanism of action of GEM

Upon entering the cancer cell, GEM is initially phosphorylated by deoxycytidine kinase (dCK) into GEM monophosphate (dFdCMP), which is the rate-limiting step in GEM metabolism (Principe *et al.*, 2021). This initial phosphorylation step can also be carried out by the extra-mitochondrial thymidine kinase 2, but to a lesser extent (Ciccolini *et al.*, 2016). Cytidine deaminase (CDA) is responsible for catalyzing the reverse of this reaction. CDA is mostly expressed in the liver where it regulates cellular GEM toxicity. dFdCMP will either be deaminated into dFdUMP, or further phosphorylated to GEM diphosphate (dFdCDP). dFdUMP inhibits thymidylate synthase (TS), increasing DNA damage and disrupting DNA synthesis, contributing to PC cell death (Principe *et al.*, 2021). dFdCDP impedes ribonucleotide reductase (RR), a nucleotide pathway enzyme that is vital for cancer cells to manage their pools of deoxynucleotides (Ciccolini *et al.*, 2016). Alternatively, dFdCDP can be further be phosphorylated into GEM triphosphate (dFdCTP) that inhibits DNA polymerase (Principe *et al.*, 2021). (Adapted from Ciccolini *et al.,* 2016 and Principe *et al.,* 2021; Created in BioRender.com).

Similar to GEM, 5-FU is also an antimetabolite chemotherapeutic agent. It is a fluoropyrimidine uracil analogue, where a fluorine atom substitutes the hydrogen atom at the carbon-5 position (Longley *et al.*, 2003). 5-FU enters the cell via a similar mechanism to that of uracil, utilizing hENT1 and hENT2, and some studies suggest that human organic anion transporter 2 (hOAT2) may also be involved (Kobayashi *et al.*, 2010; Mafi *et al.*, 2023). After

entering, it is transformed into three active metabolites, namely: fluorouridine triphosphate (FUTP), fluorodeoxyuridine triphosphate (FdUTP), and fluorodeoxyuridine monophosphate (FdUMP). 5-FU's anticancer effects result from its ability to inhibit thymidylate synthase (TS), interfering with DNA and protein synthesis, and incorporation of its metabolites into RNA and DNA, interfering with nucleic acid synthesis (Fig 3) (Longley *et al.*, 2003; C Liu *et al.*, 2023).

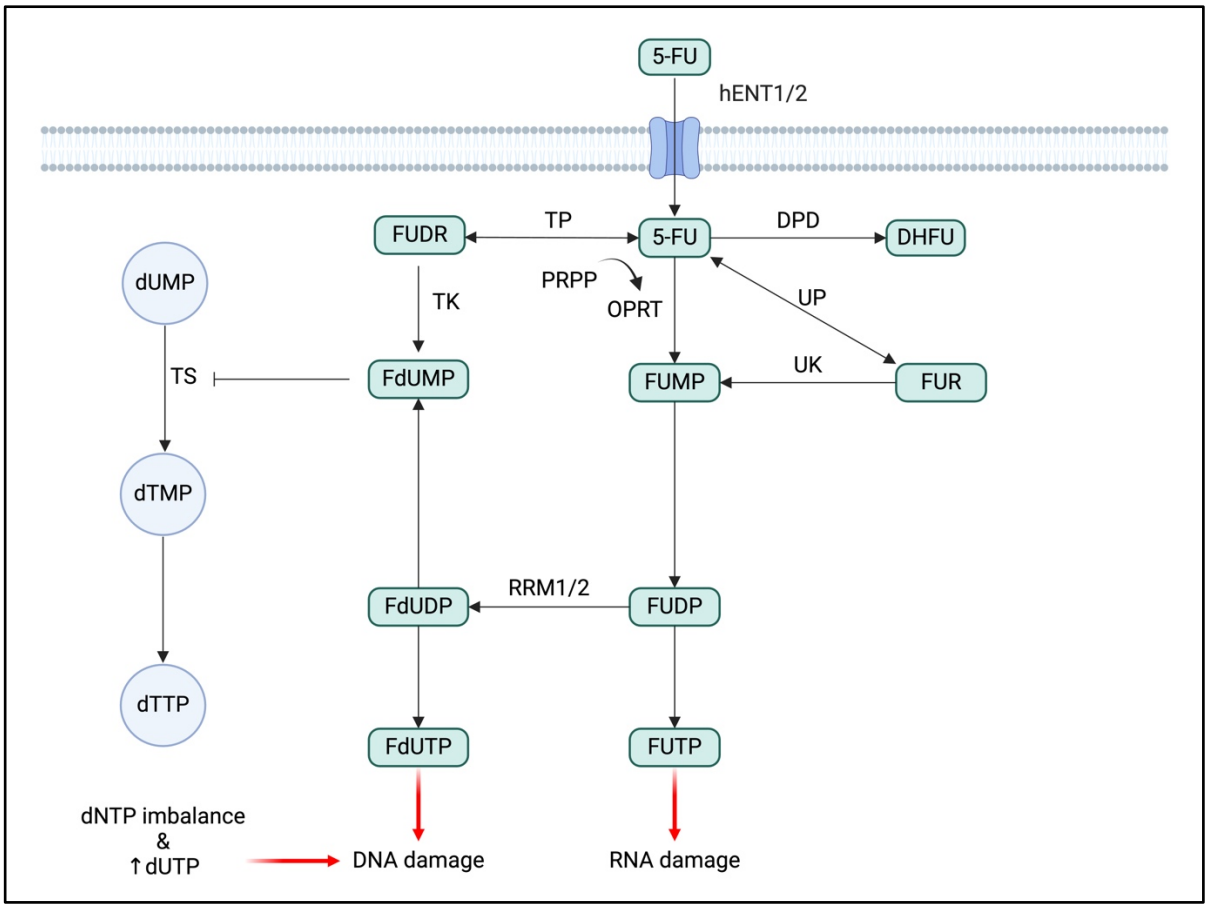


Figure 3: Molecular mechanism and action of 5-FU

The primary method of activating 5-FU involves its conversion to fluorouridine monophosphate (FUMP). This process can occur through two pathways: a direct route utilizing orotate phosphoribosyltransferase (OPRT) with the help of the cofactor phosphoribosyl pyrophosphate (PRPP), or an indirect route via fluorouridine (FUR). The indirect pathway requires the consecutive actions of uridine phosphorylase (UP) and uridine kinase (UK). In the presence of ribose-1-phosphate, UP facilitates the transformation of 5-FU into FUR, which is considered the forward reaction. Although the reverse process, converting FUR back to 5-FU, is possible under specific circumstances, it is not the primary direction observed *in vivo*. The reaction's equilibrium tends to favor the production of FUR over that of 5-FU. Phosphorylation of FUMP, leads to the formation of fluorouridine diphosphate (FUDP). Thereafter, FUDP can either be phosphorylated to the active metabolite FUTP, or converted to fluorodeoxyuridine diphosphate (FdUDP) through ribonucleotide reductase (RR). FUTP is incorporated into RNA, disrupting normal RNA processing and function. FdUDP can be phosphorylated to FdUTP or dephosphorylated to FdUMP, where FdUTP results in DNA damage. A different activation

route involves the conversion of 5-FU to fluorodeoxyuridine (FUDR) through thymidine phosphorylase (TP). Subsequently, thymidine kinase (TK) phosphorylates FUDR to produce FdUMP. FdUMP inhibits thymidylate synthase (TS), leading to decreased deoxythymidine monophosphate (dTMP) synthesis from deoxyuridine monophosphate (dUMP) and subsequent decrease in deoxythymidine triphosphate (dTTP). This results in an imbalance in the deoxynucleotide pool and increased levels of deoxyuridine triphosphate (dUTP), hindering DNA synthesis and repair. The deactivation route involves the transformation of 5-FU into dihydrofluorouracil (DHFU) by the enzyme dihydropyrimidine dehydrogenase (DPD). DPD catalyses the rate-limiting step in the catabolism of 5-FU in normal and tumour cells (Adapted from Longley *et al*., 2003; Created in BioRender.com).

GEM and 5-FU are well studied chemotherapeutic agents, unfortunately, they have shown limited success in PDAC patients displaying resistance within a week of initiating treatment (Binenbaum *et al.*, 2015). In recent years, novel therapeutic strategies have been tested on PDAC, but with no success. Immunotherapies, such as vaccines, inhibition of immune checkpoint, and therapy with CAR-T cells, also did not show expected responses due to the highly immunosuppressive TME of PDAC (Alshememry *et al.*, 2022). Alternative methods, such as nanoparticles, also show limited success (Alshememry *et al.*, 2022). The failure of current and novel strategies is due to the drug-resistant nature of PDAC, of which the underlying mechanisms are poorly understood (Orth *et al.*, 2019).

1.4 Resistance to chemotherapies in PDAC

In addition to the late-stage diagnosis of PDAC, its intrinsic and acquired drug-resistance provides a large barrier to improve therapeutic treatment (C Wang *et al.*, 2016). Furthermore, the lack of drug-resistance biomarkers makes it difficult to predict patient outcome (Grasso *et al.*, 2017). Drug resistance in PDAC is a complex phenomenon and is influenced by several mechanisms (drug transport, drug metabolism, tumour heterogeneity and reprogrammed cellular metabolism) which show an interplay with one another. These mechanisms modulate regulatory pathways controlling apoptosis, autophagy, inflammation, cell proliferation and differentiation (Alshememry *et al.*, 2022).

1.4.1 Drug transport

Drug transport proteins exert a large influence on resistance, in that they are involved in the entry and exit of drugs into and out of the cells. GEM resistance has been linked to decreased expression of hENT1 and hCNT1, which results in only partial uptake of GEM (Principe *et al.*, 2021). On the other hand, higher levels of hENT1 have been found to be associated with a better prognosis and improved overall survival for both GEM and 5-FU treated PC patients

(Elander *et al.*, 2018; Principe *et al.*, 2021). In conjunction, PDAC cells can also increase their expression of drug efflux transporters to further reduce intracellular drug concentrations. ATP binding cassette (ABC) transporters are responsible for the efflux of active agents and determine the chemosensitivity of tumours (Marin *et al.*, 2022). ABC transporters are overexpressed and highly active in PDAC cells in comparison to normal pancreatic cells. This is due to the overactive glycolytic pathway (Warburg effect) in cancer cells, which results in elevated ATP availability for ABC transporter functional requirements (Kimmelman, 2015; Adamska and Falasca, 2018), and several studies have shown that it is linked to GEM and 5-FU resistance (Alshememry *et al.*, 2022; Marin *et al.*, 2022).

1.4.2 Drug metabolism

Alterations in drug metabolism pathways provide another means of acquired drug resistance. In the case of GEM resistance, low expression levels of dCK, which catalyses the rate-limiting step in GEM activation, are observed (Saiki *et al.*, 2012; Koltai *et al.*, 2022). Furthermore, CDA, responsible for converting active GEM back into its inactive form (dFdU), is overexpressed, thereby limiting drug availability (Bjånes *et al.*, 2020). The expression of RR isoforms is also increased, counteracting GEM, and increasing the production of nucleotides for DNA synthesis (Koltai *et al.*, 2022). Interestingly, TS inhibition has been demonstrated to stimulate hENT1 activation, and its overexpression could potentially result in reduced hENT1 expression (Fig 2) (Komori *et al.*, 2011). TS overexpression is also linked to 5-FU resistance (Zhang *et al.*, 2011). Furthermore, high levels of DPD, the enzyme responsible for inactivating 5-FU, contribute to increased resistance to 5-FU (Kurata *et al.*, 2011). On the other hand, when DPD levels are insufficient, it can result in fatal toxicity from 5-FU (Fig 3) (Fidai *et al.*, 2018).

1.4.3 Tumour heterogeneity

Tumour heterogeneity provide a means of acquired drug resistance, as tumours are exposed to drugs, they become more genomically complex (Dagogo-Jack and Shaw, 2017). The oncogenic landscape of PDAC (consisting of *KRAS*, *TP53*, *CDKN2A* and *SMAD4*) drive transcriptomic alterations, producing phenotypic subtypes of PDAC (Cros *et al.*, 2018). One such subtype is pancreatic cancer stem cells, which have a high degree of plasticity and are maintained through *KRAS* (Hermann and Sainz, 2018). PC stem cells exist in a dynamic state influenced by the TME (Alshememry *et al.*, 2022). PDAC TME is classified by extensive fibrosis, lack of vascularization, hypoxic conditions, and infiltration of the immune system

(Espiau-Romera *et al.*, 2020). These characteristics reinforce KRAS protein expression, cell proliferation, cell survival and metastasis (Grant *et al.*, 2016; Sherman and Beatty, 2023).

1.4.4 Reprogrammed cellular metabolism

The reprogramming of the cellular metabolism is proven to be a key regulator of tumourigenesis and is considered a new hallmark of cancer (Göbel *et al.*, 2020; D Zhang *et al.*, 2021; Kaoutari *et al.*, 2021). Reprogrammed metabolic pathways interact with oncogenes causing downstream effects on protein expression; signalling pathways, TME and drug resistance (C Liu *et al.*, 2023). The mevalonate pathway, responsible for cholesterol production, is identified as a key regulator of tumour biology (Göbel *et al.*, 2020). Cholesterol serves a crucial role as one of the principal components in the plasma membrane, alongside phospholipids and signalling proteins, which are vital for proper cell function and proliferation (Lu and Martí, 2020). Since cancer cells are continuously proliferating, they have a high demand of cholesterol and lipids in order to maintain and supply membrane components for infinite cell division (Park *et al.*, 2020). The involvement of cholesterol in PDAC drug resistance has been reported in literature.

1.5 Cholesterol homeostasis and its role in PDAC

Cholesterol ($C_{27}H_{46}O$) is a sterol lipid, and is a key player in several biological processes, such as bile acid synthesis, Vitamin-D synthesis, steroid hormone production and is a constituent of plasma lipoproteins (Karlic and Varga, 2019; Riscal *et al.*, 2019; Luo *et al.*, 2020; Mayengbam *et al.*, 2021; Vona *et al.*, 2021). PDAC cells maintain a higher concentration of cholesterol inside the cell as compared to normal pancreatic duct epithelial cells (Yuchuan Li *et al.*, 2023). Thus, PDAC cells exhibit a strong reliance on cholesterol, as it not only provides nutrients for uncontrolled cell proliferation, but supports: tumourigenesis; disease progression; invasion and migration (Huang *et al.*, 2020; Lu and Martí, 2020; Giacomini *et al.*, 2021). Cholesterol homeostasis is achieved through several extracellular and intracellular regulators (Gu *et al.*, 2019), which dynamically balance the biosynthesis, uptake, export and storage of cholesterol (Luo *et al.*, 2020). The *KRAS* oncogene plays a significant role in altering cholesterol homeostasis in PDAC. Through the activation of the PI3K pathway, the KRAS mutant promotes cholesterol synthesis and uptake to establish a high concentration intracellular cholesterol (Kuzu *et al.*, 2016; Ruiz *et al.*, 2020; Yuchuan Li *et al.*, 2023). In turn, membrane-associated cholesterol renders the KRAS-4b mutant in a constitutively active state (Lu and

Martí, 2020). The fluidity and permeability of cell membranes are influenced by membrane-associated cholesterol, which may also play a role in drug resistance. Elevated concentrations of cholesterol within membranes are often linked to increased membrane rigidity and reduced drug permeability (Peetla *et al.*, 2013; Lu and Martí, 2020; Yan *et al.*, 2020). Moreover, high membrane-cholesterol levels further support invasiveness, which is crucial for rapidly proliferating cancer cells which require large amounts of cholesterol for continuous membrane synthesis (Göbel *et al.*, 2020).

In addition, cholesterol aids in the facilitation of specialised microdomains within the plasma membrane, such as lipid rafts (Huang *et al.*, 2020). Lipid rafts (10 to 200 nm microdomains) serve as "signalling platforms" as they house several receptors and are crucial for membrane trafficking (Cruz *et al.*, 2013; Vona *et al.*, 2021). Lipid rafts are also key to conferring drug resistance and are known to be increased in cancer cells that exhibit chemoresistance (Yan *et al.*, 2020). PDAC cells are abundant in caveolae, a sub-class of lipid rafts, which contain the cholesterol binding protein, caveolin-1 (Yan *et al.*, 2020). The increased caveolin-1 levels in PDAC cells have been linked to GEM and 5-FU resistance (Yan *et al.*, 2020). Furthermore, cholesterol-rich lipid rafts are reported to be involved in cancer cell adhesion and migration, since lipid rafts house cell adhesion machinery (Li *et al.*, 2016; Göbel *et al.*, 2020). When lipid rafts are disrupted in PDAC cells their metastatic capabilities are impeded (Kaoutari *et al.*, 2021). Moreover, cholesterol performs several functions inside the cell, as it is distributed amongst organelles inside the cell (Vona *et al.*, 2021).

For instance, cholesterol is implicated in the cell cycle as it aids in G1 to S-phase transitioning, which is a crucial step for proliferating cells (Singh *et al.*, 2013). Interestingly, cholesterol has also recently been implicated in the modulation of the immune system, and literature suggests that cholesterol performs several other intrinsic functions which are yet to be investigated (Vona *et al.*, 2021). The abundance of functions, performed by cholesterol, requires a balance in cholesterol homeostasis, since the maintenance of intracellular cholesterol is paramount for normal cell function and proliferation (Riscal *et al.*, 2019). In PDAC, metabolic changes lead to unbalanced cholesterol levels, which enhance PDAC progression and promote cellular functions such as proliferation, invasion, migration, and drug resistance. This imbalance stems from disturbances in key processes governing cholesterol homeostasis (Fig 5).

1.5.1 Cholesterol *de novo* biosynthesis

Free cholesterol (FC) is produced from the mevalonate pathway (MP) through anabolic metabolism and consists of a cascade of enzyme catalysed reactions (Cruz *et al.*, 2013; Karlic and Varga, 2019). The primary rate limiting step, of the MP, entails the conversion of 3-hydroxy-3-methylglutaryl-CoA (HMG-CoA) to mevalonate, which is catalysed by HMG-CoA Reductase (HMGCR) (Karlic and Varga, 2019). HMGCR is therefore considered the master regulator of cholesterol biosynthesis. HMGCR, along with several other MP enzymes, are regulated by sterol regulatory element binding proteins (SREBP), a class of transcriptional regulators (Riscal *et al.*, 2019). SREBP2 is responsible for controlling MP gene expression and is synthesized in the endoplasmic reticulum (ER) (Riscal *et al.*, 2019). The concentration of intracellular FC regulate cholesterol synthesis via a feedback mechanism to SREBP2 (Fig 5) (Wen *et al.*, 2018). At low intracellular FC levels, SREBP2 is translocated from the ER to the golgi apparatus by SREBP cleavage activating protein (SCAP), where its cleavage and subsequent activation occurs (Riscal *et al.*, 2019). The activated SREBP2 will locate to the nucleus and target Sterol Regulatory Elements (SREs) which leads to the activation of MP genes (Cruz *et al.*, 2013; Karlic and Varga, 2019; Riscal *et al.*, 2019).

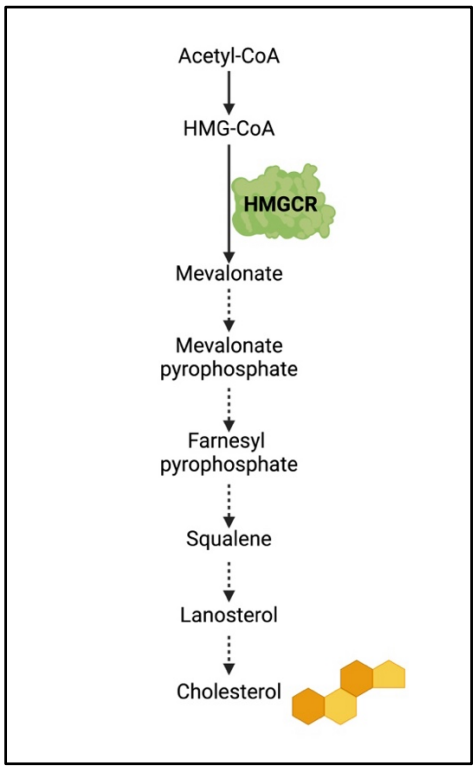


Figure 4: Simplistic overview of enzyme catalysed reactions of the Mevalonate Pathway

ATP Citrate Lyase (ACLY) provides Acetyl-CoA as precursor for *de novo* cholesterol synthesis (Carrer *et al.*, 2019). Three Acetyl-CoA molecules are converted into 3-hydroxy-3-

methylglutaryl-CoA (HMG-CoA). HMG-CoA reductase (HMGCR) reduces HMG-CoA into mevalonate which is the rate limiting step. Since HMGCR catalyses the rate limiting reaction, it can be inhibited (statins) to reduce the synthesis of cholesterol. Mevalonate is then converted into mevalonate pyrophosphate by phospho-mevalonate kinase. Subsequently, activated isoprenoids are generated (not depicted), which serve as precursors for farnesyl pyrophosphate. The process then continues with the transformation of this substance into squalene, followed by lanosterol, and finally resulting in the formation of cholesterol (*dashed arrows* indicate multiple steps; adapted from Gu *et al*., 2019; Created in Biorender.com).

Cancer cells activate the MP to increase their intracellular cholesterol amount (Fig 5) (Cruz *et al.*, 2013). Mutant KRAS in PDAC cells maintain a continuous supply of Acetyl-CoA which feeds into the MP (Carrer *et al.*, 2019). It is important to note that the production of Acetyl-CoA is also increased as a result of the upregulated glycolytic pathway in cancer cells (Warburg effect) (Cruz *et al.*, 2013). It has been found that interrupting the feed of Acetyl-CoA by *ACLY* gene knockdown, hinders the formation of PanINs, thus compromising PDAC tumour formation (Carrer *et al.*, 2019). Furthermore, HMGCR is upregulated in PDAC patients, ensuring the continued synthesis of cholesterol (Tsuchiya *et al.*, 2010; Cruz *et al.*, 2013; Guillaumond *et al.*, 2015; Yunkuo Li *et al.*, 2023). In PDAC cells, SREBP2 is overactivated through the KRAS-activated PI3K pathway, along with mutant TP53 to establish a continuous increase in cholesterol synthesis via upregulation of HMGCR expression (Fig 5) (Wen *et al.*, 2018; Yi *et al.*, 2020; Laka *et al.*, 2022; Duan *et al.*, 2024). In addition to cholesterol synthesis, the MP has several extra functions in PDAC such as the activation of proteins and maintenance of cancer stem cells. The MP pyrophosphate intermediates (such as farnesyl pyrophosphate) aid in the prenylation of small GTPases, leading to the activation of Rho-GTPases, including KRAS and its mutant form, thus, maintaining the viability of PC stem cells (Di Carlo *et al.*, 2018; Karlic and Varga, 2019; Göbel *et al.*, 2020). The MP is inarguably overactivated in PDAC cells, however, it is not the only means of increasing intracellular FC levels. In addition to synthesis, cholesterol can also be taken-up into the cell.

1.5.1.1 Uptake of cholesterol

The uptake of cholesterol represents a more energy-efficient mechanism for increasing intracellular FC levels (Mayengbam *et al.*, 2021b). Cholesterol can be taken up from the extracellular environment, in the form of cholesteryl esters (CEs) (Cruz *et al.*, 2013). Since CEs are insoluble, they rely on lipoproteins for transport between the liver and peripheral tissues (Cruz *et al.*, 2013). Low density lipoprotein (LDL) serves as the primary vehicle for CEs in the bloodstream, facilitating its transport away from the liver to outlying tissues

(Tsuchiya *et al.*, 2010). LDL binds to the LDL-receptor (LDLR) on the cell surface, which mediates the endocytosis of CEs, which are then hydrolysed into FC (Fig 5) (Tsuchiya *et al.*, 2010; Li and Pfeffer, 2016). LDLR is regulated by proprotein convertase subtilisin/kexin type 9 (PCSK9), a glycoprotein that binds to LDLR and targets it for lysosomal degradation, downregulating LDL-cholesterol uptake (Fig 5) (Mahboobnia *et al.*, 2021). Similar to synthesis, the uptake of cholesterol is also transcriptionally regulated by SREBP2. Both LDLR and PCSK9 expression is regulated by SREBP2 to increase intracellular FC (Hyun *et al.*, 2008; Kuzu *et al.*, 2016).

Cancer cells show upregulated cholesterol uptake to satisfy their dependence on intracellular FC (Cruz *et al.*, 2013). In PDAC, KRAS-activated SREBP2 also stimulates the transcription of LDLR to increase the influx of cholesterol (Fig 5) (Kuzu *et al.*, 2016; Wen *et al.*, 2018; Yi *et al.*, 2020). This is supported by the increased LDLR expression seen in PDAC patients, which facilitates chemoresistance, increases the risk of recurrence and lowers patient survival rates (Abdulla *et al.*, 2021; Yin *et al.*, 2022). The silencing of LDLR in PDAC cells disrupts the intracellular distribution of cholesterol, retarding proliferative signalling pathways, making cells more sensitive to chemotherapeutics (Guillaumond *et al.*, 2015). This dependence of cancer cells on cholesterol uptake can be attributed to the fact that they utilize less energy than *de novo* cholesterol synthesis (Mayengbam *et al.*, 2021). Interestingly, in PDAC, SREBP2 is seen to upregulate *PCSK9* gene expression (Hyun *et al.*, 2008; Mahboobnia *et al.*, 2021). However, the upregulated PCSK9 protein expression does not decrease the uptake of cholesterol but rather inhibits apoptosis, aiding in tumour growth, as seen in liver and colon cancer (SZ Zhang *et al.*, 2021; Wang *et al.*, 2022). There is still much uncertainty behind the mechanism of PCSK9 in PDAC and its downstream effects. Therefore, further research is warranted for better understanding of the mechanisms involved. Similar to cholesterol import, the export of cholesterol is also an important mechanism that should be tightly regulated.

1.5.1.2 Efflux of cholesterol

Cholesterol efflux is essential for cells to maintain a balance of intracellular FC, since high levels of FC can induce ER stress, resulting in apoptosis (Sozen and Ozer, 2017). The efflux of cholesterol is mediated by cholesterol exporters, such as ATP-binding Cassette Subfamily A member 1 (ABCA1) and Subfamily G member 1 (ABCG1), which are transcriptionally regulated by Nuclear Liver X Receptors (LXRs) that are activated upon ligand-binding (Fig 5)

(Gu *et al.*, 2019; Abdulla *et al.*, 2021). ABCG-family transporters are half transporters that form homodimers or heterodimers in order to function (Duvivier *et al.*, 2024). Along with exporting cholesterol, ABCA1 will inhibit the maturation of SREBP2, downregulating the MP, leading to less cholesterol being synthesized, allowing the cell to maintain FC homeostasis (Moon *et al.*, 2019).

Cancer cells will downregulate the efflux of cholesterol to satisfy their cholesterol requirements (Cruz *et al.*, 2013; Kuzu *et al.*, 2016). Cancer cells achieve this by decreasing the expression of ABCA1 and ABCG1 (King *et al.*, 2022). Furthermore, mTOR, activated via PI3K, inhibits ABCA1-mediated cholesterol efflux (Kuzu *et al.*, 2016). The decreased efflux of cholesterol is not only related to increased cancer cell proliferation but also in immune system suppression (King *et al.*, 2022). ABCG1 has been proposed as a potential oncogene due to its involvement in several cancer related processes, which include tumour immunity, tumourigenesis and resistance to cell death (Sag *et al.*, 2015; Namba *et al.*, 2018; Sharma and Agnihotri, 2019; Xu *et al.*, 2022; Duvivier *et al.*, 2024). Elevated ABCG1 protein expression has been correlated with increased expression of CSC markers in lung cancer cells (Duvivier *et al.*, 2024). The role of ABCG1 in PDAC has not been extensively investigated and necessitates further research to elucidate its contribution to PDAC. Another means to maintain a homeostatic balance of FC, besides export, is the storage and transport of cholesterol in the form of CEs.

1.5.1.3 Storage and transport of cholesterol

Cholesterol can be transported via intracellular and extracellular mechanisms. Intracellularly, FC, produced from biosynthesis or uptake, will be utilized by the cell to produce hormones, bile acids and to synthesise membranes (Gu *et al.*, 2019). The excess FC, not utilized by the cell, is esterified by Acetyl-CoA Cholesterol Acetyl Transferase 1 (ACAT1), and the resulting CEs are transported via cholesteryl ester transfer protein (CETP) to lipid droplets for storage (Fig 5) (Gu *et al.*, 2019). Extracellularly, CEs can be transported by lipoproteins throughout the body. As noted earlier, LDL serves as the primary vehicle for cholesterol in the bloodstream, facilitating its transport from the liver to outlying tissues. In contrast, high density lipoproteins (HDLs) will facilitate reverse transport of cholesterol from the peripheral tissues to the liver (Cruz *et al.*, 2013; T Liu *et al.*, 2021). When HDL arrives at the liver, it can either target cholesterol for excretion, or cholesterol (CEs) can be shuttled by CETP from HDL to LDL to be recycled back to the peripheral tissues (Mabuchi, Nohara and Inazu, 2014).

Cholesterol is usually transported in the form of CEs, however it has been noted in literature that lipoproteins can carry both FC (on their surface) and CEs (within their hydrophobic core) (Smith *et al.*, 1978).

Drug resistant PDAC cells lines can contain up to 20 times more lipid droplets than normal cells (Li *et al.*, 2016). A high ACAT1 expression is usually accompanied with the high CE content in PDAC (Xu *et al.*, 2020). The increased CE production from ACAT1 provides a necessary mechanism for PDAC cells to avoid toxicity induced from excess FC, thus, keeping the cell metabolically active at a high rate (Li *et al.*, 2016). Lowering the levels of FC also activates the negative feedback loop to SREBP2 to mediate the synthesis and uptake of more cholesterol (Fig 5) (Li *et al.*, 2016, 2018). Thus the high ACAT1 expression in PDAC promotes cell dependence on cholesterol synthesis and uptake. This is evident in PANC-1 cells, where inhibition of ACAT1 protein reduces cell proliferation and migration in cells exhibiting drug resistance (Li *et al.*, 2016, 2018; Yuchuan Li *et al.*, 2023). Furthermore, patients with high *ACAT1* expression levels also have a shorter survival rate (Rebelo *et al.*, 2023). Another study reports that the increase in CEs results in the upregulation of the PI3K pathway, further promoting cell growth and survival (Yue *et al.*, 2014; Giacomini *et al.*, 2021). On the extracellular level, PDAC patients show increased levels of cholesterol transport in the bloodstream. In PDAC, LDL-cholesterol is seen to promote cell proliferation, migration and invasiveness (Yin *et al.*, 2022).

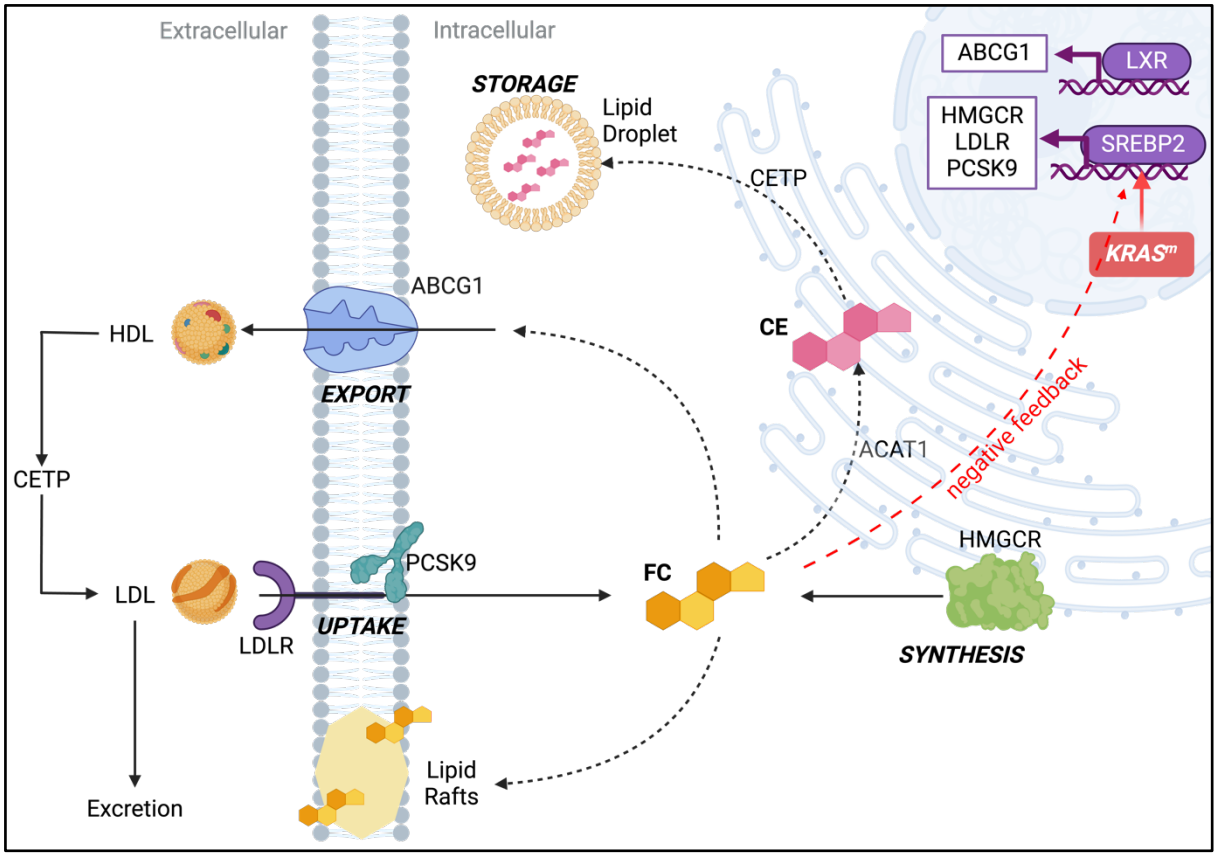


Figure 5: Cholesterol homeostasis in PDAC

Intracellular FC can be increased by either synthesis or uptake. HMGCR controls the rate limiting step in the MP to synthesize cholesterol. Cholesterol is taken up into the cell through receptor mediated endocytosis of LDLR once bound to LDL. PCSK9 is a negative regulator of LDLR and targets it for degradation. Cholesterol has several fates inside the cell. It can be shuttled to the plasma membrane, where it can be directly incorporated into the phospholipid bilayer or as part of lipid rafts. FC can also be converted into CEs by ACAT1, which are then targeted for storage in lipid droplets by CETP. Lastly, cholesterol can be exported from the cell via ABCG1, where it is loaded onto HDL and transported back to the liver. In the liver CEs are transferred from HDL to LDL via CETP, where it is either transported back to the peripheral tissues or excreted. When the intracellular FC is too high, it activates LXR, which will facilitate the export of cholesterol. Conversely, when the FC level is too low, it activates a negative feedback loop to SREBP2, which will replenish FC via synthesis and uptake. The KRAS mutant is a key player in initiating PDAC and it also reprogrammes cholesterol metabolism by activating SREBP2 via the PI3K pathway (Created in Biorender.com).

1.6 Targeting cholesterol for anticancer therapy

Cholesterol metabolism is inarguably central to PDAC progression and drug resistance. Therefore, targeting cholesterol may be a potential anticancer strategy. There are two means by which intracellular cholesterol can be targeted: inhibitors of cholesterol synthesis and cholesterol depleting agents (Gu *et al.*, 2019). There are key differences in the two approaches,

where one utilises statins to inhibit cholesterol synthesis and the other uses cyclodextrins to deplete excess cholesterol. Both approaches have been seen to have anticancer potential.

1.6.1 Statins

Statins are well known for their use in treating hypercholesterolemia and received approval from the Federal Drug Administration, USA in the 1980s (Longo *et al.*, 2020). Statins are competitive inhibitors of HMGCR, and thereby target the rate-limiting step of the MP (Longo *et al.*, 2020). The competition for the active site on HMGCR halts the production of mevalonic acid, subsequently ceasing cholesterol synthesis, lowering intracellular cholesterol concentrations (Longo *et al.*, 2020). This essentially lowers serum LDL levels due to increased cholesterol uptake through the activation of the restorative SREBP2/LDLR feedback loop of the MP (Göbel *et al.*, 2020). Additionally, the statin-induced halt of the MP decreases its metabolic intermediates, including isoprenoid intermediates required for protein prenylation (Li *et al.*, 2016). Prenylation is essential for the activity of RAS proteins such as KRAS and affect the PI3K pathway, downregulating proliferative signalling (Cruz *et al.*, 2013; Gu *et al.*, 2019). This effect resulted in the latter use of statins as a possible adjuvant cancer therapy for their anti-proliferative effects (Kumar and Mandal, 2021). There is much controversy surrounding the anticancer effect of statins and a direct link between statin-use and improved cancer treatment is yet to be reported (Osmak, 2012; Gu *et al.*, 2019). Statins have been explored for PDAC treatment, however clinical trial data show that they do not result in a reduction of PDAC-risk (Li *et al.*, 2016; Vona *et al.*, 2021). The combination of statins with GEM and 5-FU decreased PDAC cell survival, however, no effect was observed on the metastatic potential and invasiveness of PDAC tumours (Göbel *et al.*, 2020). Moreover, cancer cells exhibit alternative HMGCR splicing, reducing their sensitivity to statins (Göbel *et al.*, 2020). In addition, the increase in cholesterol uptake via the SREBP2/LDLR feedback loop, promotes tumourigenesis (Göbel *et al.*, 2020). Statin-resistant cells contain elevated levels of lipid rafts, indicating that the cancer cell is able to reverse the effects of HMGCR-inhibition (Göbel *et al.*, 2020). Statins also produce non-specific toxicity in non-malignant cells, especially at high doses (Matusewicz *et al.*, 2020). This could possibly be linked to the inhibition of protein prenylation by statins (Li *et al.*, 2016). These off-target effects limit the success of statins for cancer treatment (Li *et al.*, 2016). Furthermore, statin intolerance has been observed in 9.1% of the global population, with African patients demonstrating an elevated risk of statin intolerance (Bytyçi *et al.*, 2022). Thus, the use of statins as an anticancer agent

should be further studied for their potential benefits in the treatment of PDAC. In light of the studies highlighting the potential benefit of using statins as an anticancer agent, the use of cholesterol depleting agents has emerged as a possible anticancer therapy.

1.6.2 Cyclodextrins

The high dependence of cancer cells on cholesterol make them sensitive to cholesterol depleting agents (Göbel *et al.*, 2020). Cyclodextrins (CDs) , such as methyl-β-cyclodextrin (MβCD), and 2-hydroxypropyl-β-cyclodextrin (HPβCD), are agents that sequester and deplete cholesterol. MβCD and HPβCD are derivates of β-cyclodextrin (Yamaguchi and Perkins, 2017). CDs are hydrophilic, water-soluble, cyclic carbohydrates with a hollowed truncated cone-like structure (Fig 6) (Sandilya *et al.*, 2020). Their hydrophobic cavity allows them to form inclusion complexes with hydrophobic substances, such as cholesterol (Qiu *et al.*, 2017; Ganjali Koli and Fogolari, 2023).

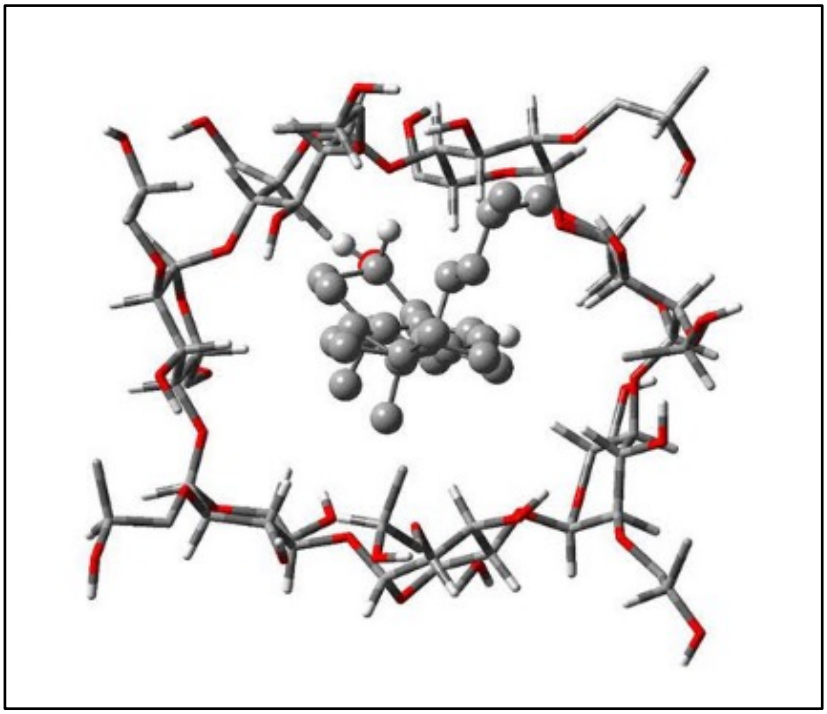


Figure 6: Computational configuration of HPβCD with cholesterol

Molecular dynamics simulation used to produce the computational configuration of HPβCD (spherical structure) and cholesterol in its hydrophobic cavity. (Image adapted from Ganjali, Koli and Fogolari, 2023).

Both *in vitro* and *in vivo* studies reported the potential anticancer effects of CDs (Qiu *et al.*, 2017). Tumour growth and invasion can be disrupted with cholesterol depletion and inhibition

of cholesterol trafficking (Huang *et al.*, 2020). Furthermore, CDs are readily available, easy to produce and cost effective (Niculescu *et al.*, 2022). MβCD, specifically, sequesters membrane-associated cholesterol, inducing apoptosis and blocking PI3K pathway activation (Onodera *et al.*, 2013; Qiu *et al.*, 2017). Unfortunately, MβCD exhibits toxic effects to normal cells (Saha *et al.*, 2023). On the other hand, HPβCD, successfully solubilizes cholesterol and reduces the intracellular cholesterol concentration (Houben *et al.*, 2021). Furthermore, HPβCD is less toxic to normal cells compared to MβCD (Saha *et al.*, 2023), and it does not cross the blood-brain barrier (Calias, 2017). HPβCD enters the cell via endocytosis, where it sequesters cholesterol (Rosenbaum *et al.*, 2010; Plazzo *et al.*, 2012; El-Darzi *et al.*, 2021). HPβCD also has a higher cholesterol complexation compacity compared to other MβCD (Jingang He *et al.*, 2024), making it the better option as cholesterol depleting agent (Yancey *et al.*, 1996). HPβCD has shown success in the treatment of Niemann-Pick disease Type C, where it is currently in phase III clinical trials and have been approved for clinical use (Megías-Vericat *et al.*, 2017; Sitarska *et al.*, 2021; Hastings *et al.*, 2022). Other studies also mention its potential in treatment of atherosclerosis and leukaemia (Yokoo *et al.*, 2015; Zimmer *et al.*, 2016). Furthermore, more recent studies have investigated HPβCD for its anticancer effects in triple negative breast cancer (Saha *et al.*, 2023; Zhu *et al.*, 2023). It is important to note that the precise mechanism of action of HPβCD is not yet completely understood (Váradi *et al.*, 2019). It is understood that HPβCD can target cholesterol-loaded cells, where it sequesters cholesterol, shifting cholesterol equilibrium away from the cancer cell, disrupting their altered cholesterol homeostasis (Gaspar *et al.*, 2017; Saha *et al.*, 2023). Thus, HPβCD is a promising avenue to explore in the treatment of PDAC through a reduction in cholesterol.

1.7 Rationale for the present study

Intrinsic and acquired drug resistance in PDAC result in poor prognosis and renders the current chemotherapeutic treatments ineffective. Literature reports cholesterol metabolism to be upregulated in PDAC and central to its drug resistance mechanisms. However, the mechanistic correlation between key proteins, involved in cholesterol metabolism, and PDAC has not yet been fully elucidated. Therapeutic strategies, such as the use of cyclodextrins to target cholesterol, provide a promising opportunity for overcoming drug resistance in PDAC. *In vitro* studies conducted by a PhD candidate (Tasvi Daya) in our lab have demonstrated promising results utilizing HPβCD in combination with GEM and 5-FU to overcome drug resistance in PDAC cells. This study provides mechanistic insights into the effect of cholesterol depletion,

in vivo, on the relative expression of key proteins, involved in cholesterol metabolism, and PDAC treatment response.

2 AIMS AND OBJECTIVES

2.1 Aim

To assess the effect of chemotherapeutic agents, with and without cholesterol depletion, on the relative expression levels of essential proteins involved in cholesterol metabolism in PDAC xenograft tumour tissue.

2.2 Objectives

1) To help with a PDAC mouse xenograft model and carry out single and combination treatments with first-line chemotherapeutic agents (5-FU and GEM) and a cholesterol-depleting agent (HPβCD).
2) To extract protein from cryopreserved mice tumour tissues utilizing both chemical and mechanical tissue lysis methods.
3) To identify and quantify the relative expression of key proteins involved in cholesterol metabolism using BCA assay and Western blotting.

2.3 Workflow

The methodology employed in this study is illustrated in figure 7 below. The PC cell line (PANC-1) was utilized for the mice xenograft study. The tumour volume and weight were analysed to assess the overall effectiveness of the treatment. To better understand the role of cholesterol homeostasis in response to treatment, key proteins in cholesterol-related pathways were evaluated with Western blotting.

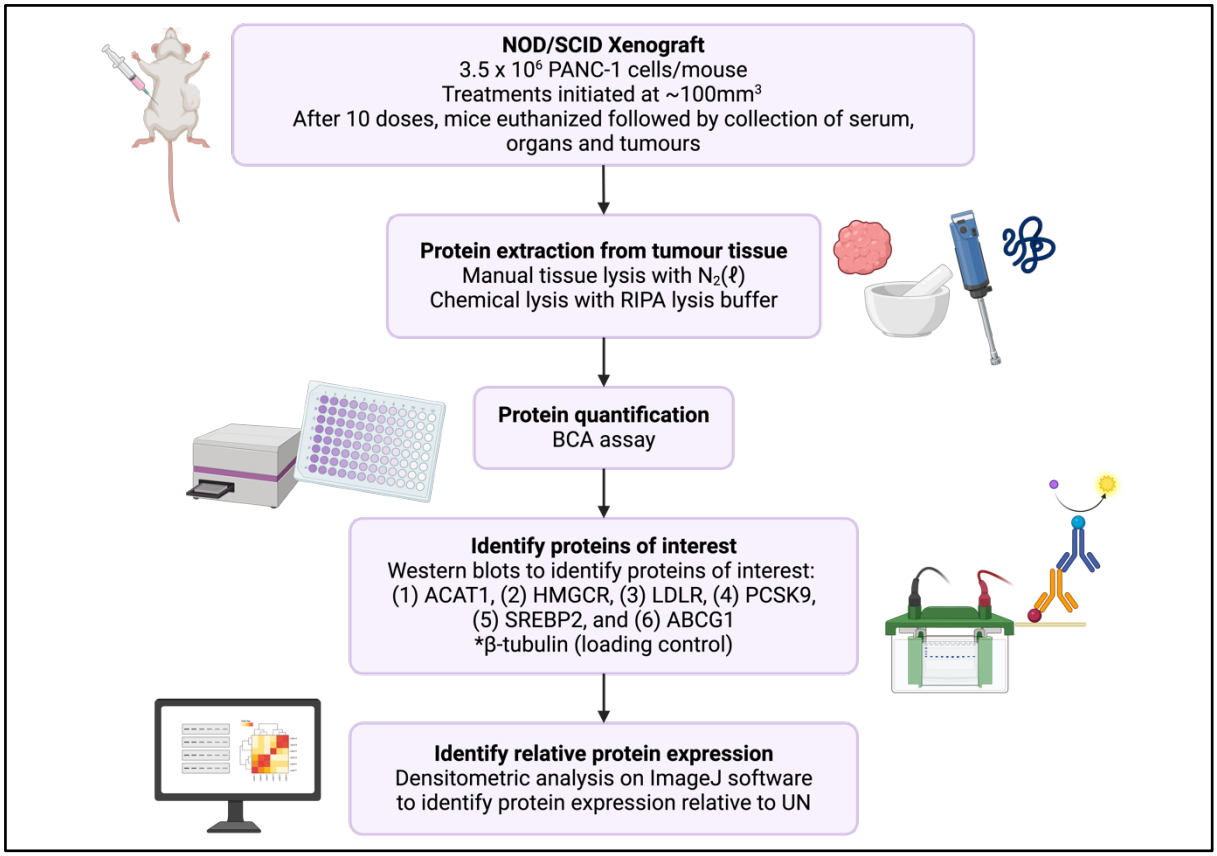


Figure 7: Workflow used in the present study

Briefly, NOD/SCID mice were acclimatised and subcutaneously inoculated with 3.5 x 10^6 PANC-1 cells per mouse in the left flank. Treatments were initiated once tumours were palpable at 100 mm^3 and administered via intraperitoneal (IP) injections. After completion of single and combination treatment regimens, mice were euthanized, and samples collected. Tumour volume was measured after excision. Protein was extracted from snap-frozen tumour tissue using manual and chemical lysis techniques. Protein was quantified using the BCA assay. Lastly, the expression of key proteins relative to the untreated (UN) was detected by Western blots and densitometric analysis (Created in Biorender.com).

3 METHODS

3.1 Pancreatic Cancer Mice Xenograft Model

This research was an extension of the mice xenograft study from a PhD candidate (Tasvi Daya) in the lab, where I assisted in the handling and monitoring of the mice throughout the study. This *in vivo* study was approved by the Wits Animal Ethics Screening Committee (AESC number: 2019/09/52/D). NOD/SCID mice were subcutaneously inoculated with PANC-1 cells (100 µL of 3.5 ×10^6 cells/mouse) in the left flank. Once tumours reached an approximate volume of 100 mm^3, treatments were initiated. The treatment regimens comprised three monotherapies, including 5-FU (30 mg/kg), GEM (30 mg/kg), and HPβCD (3000 mg/kg), as well as two combination therapies consisting of 5-FU & HPβCD (30 mg/kg and 3000 mg/kg

respectively), and GEM & HPβCD (30 mg/kg and 3000 mg/kg respectively) (Table 1). Detailed methodology regarding PANC-1 cell culture and mice xenograft study can be found in the appendix (Appendix, section 8.1).

Table 1: Cell-derived Xenograft Treatment Regimens

Treatment Group	**Mouse ID**	**Mouse Gender**	**Number of mice per treatment group**	**Treatment Regimen**	**Number of treatment doses**
Untreated (UN)	2	Male	4	UN	not applicable
	3				
	5				
	10				
HPβCD	18	Female	4	HPβCD (3000 mg/kg)	10 (twice a week)
	20				
	25				
	28				
5-FU	1	Male	4	5-FU (30 mg/kg)	10 (twice a week)
	6				
	9				
	13				
5-FU & HPβCD	4	Male	4	5-FU (30 mg/kg) and HPβCD (3000 mg/kg)	10 (twice a week)
	7				
	12				
	14				
GEM	23	Female	1	GEM (30 mg/kg)	6 (weekly)
GEM & HPβCD	21	Female	3	GEM (30 mg/kg) and HPβCD (3000 mg/kg)	3 (weekly)
	29				4 (weekly)
	30				
DMSO	8	Male	2	4% DMSO	10 (twice a week)
	15				

3.2 Protein Extraction from Cryopreserved PDAC Xenograft Tissue

3.2.1 Protein Extraction Protocol

Extraction of proteins from the xenograft tumour tissue provided the foundation to investigate the relative expression of proteins involved in cholesterol homeostasis. The protein extraction protocol was adapted from Börner *etl al.* 2009. The snap-frozen tumour tissue was slightly thawed on ice. A 30 mg piece was dissected from the tumour, and submerged in liquid nitrogen, followed by mechanical lysis by using a mortar and pestle to grind the tissue into a powder. The grinding of frozen tissue exposed cells to chemical lysis detergents (Börner *et al.*, 2009). The powdered tissue was suspended in 1 X radio-immunoprecipitation assay (RIPA) lysis buffer (600 µL) (Table 2) and homogenized on ice for 5 minutes at 3000 rpm. RIPA lysis buffer is commonly used to extract nuclear, cytosolic and membrane proteins. RIPA buffer contains sodium deoxycholate and sodium dodecyl sulphate, which will solubilize the plasma membrane and organelle membranes, exposing cytosolic- and organelle proteins (Keane *et al.*, 2016). The buffering agents in the RIPA lysis buffer consist of Tris-HCl and NaCl, ensuring a stable pH during lysis (Stuart *et al.*, 1977; Islam *et al.*, 2017). Cellular debris were pelleted at 13000 rpm for 15 minutes at 4°C. The supernatant (protein lysate) was transferred to a clean 1.5 mL Eppendorf tube and stored at −20°C for downstream analysis.

Table 2: RIPA lysis buffer components

1 X RIPA lysis Buffer		
Component	**Amount**	**Supplier**
50 mM Tris-HCl (pH 7.4)	1.21 g	Sigma-Aldrich, UK
300 mM NaCl	0.876 g	
1% Triton X-100	1 mL	
1% Sodium deoxycholate	1 g	
0.1% Sodium dodecyl sulphate	1 mL of 10% Sodium dodecyl sulphate	
10 mM EDTA	1 mL	
dH_2O	100 mL	

3.3 Protein Identification and Quantification with Western Blotting

Western blotting provided a means to discern alterations in the relative expression of proteins related to cholesterol homeostasis.

3.3.1 Protein Quantification: BCA Assay

The Bicinchoninic Acid (BCA) assay was performed to quantify the total protein concentration in each protein lysate. It is a colorimetric assay that measures the reduction of Copper Sulphate (Cu^{2+}) to Cu^{+} in the presence of proteins (Otieno *et al.*, 2016). Two Cu^{+} will interact with BCA to form a chromophore complex with a purple colour (Rogatsky, 2021). The protein concentration was quantified by measuring the absorption spectra at 562 nm and compared to a standard curve made from a known bovine serum albumin (BSA) (Sigma Aldrich, UK) protein concentration (Cortés-Ríos *et al.*, 2020; Rogatsky, 2021). Quantifying protein concentration was essential to ensure equal loading of samples during Sodium Dodecyl Sulphate Polyacrylamide Gel Electrophoresis (SDS-PAGE) in Western blotting. BSA (Sigma Aldrich, UK) was dissolved in the 1 X RIPA lysis buffer (Table 2) and stored at −20°C until required. The standard concentrations ranged between 0-2 mg/mL in increments of 0.2 mg/mL and were used to construct a standard curve (Fig 8). In a 96-well plate, 25 µL of each BSA standard was loaded in triplicate. Thereafter, 5 µL of each protein lysate and 20 µL of RIPA

lysis buffer was loaded in triplicate. The protein lysate samples were diluted in RIPA lysis buffer to decrease their concentration, allowing higher accuracy since the BCA assay is more sensitive at lower concentrations. To each well, 200 µL of BCA working solution (196 µL BCA and 4 µL Cu^{2+}) was added. The plate was placed on a shaker (IKA®, Germany) for 30 seconds at 500 rpm, to ensure proper mixing of components, thereafter the plate was incubated for 45 minutes at 37°C in the dark. The absorbance of each well was measured at 562 nm in the Multiskan™ GO Microplate Reader (Thermo Fisher Scientific, USA, SkanIt™ software). The concentration of each protein lysate was determined using the straight-line formula from the standard curve generated in Microsoft Office Excel© (Equation 1).

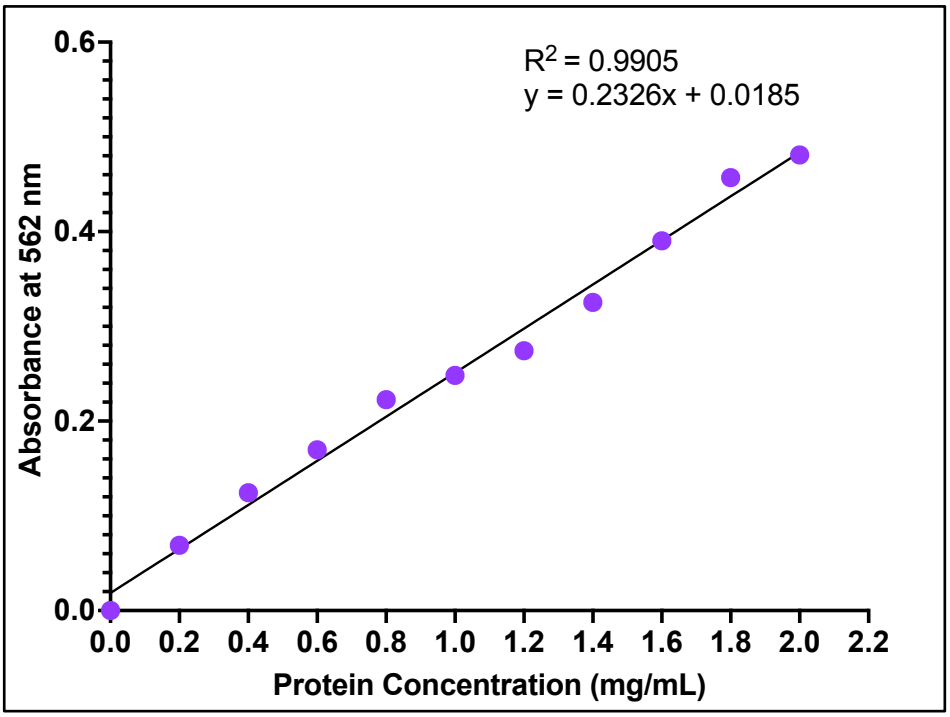


Figure 8: A prototypical standard curve used in a BCA assay

The straight-line formula used to determine protein concentration from the standard curve in BCA assay, where y is the average corrected absorbance and x is the protein concentration (mg/mL) multiplied by a factor of 5 to account for dilution.

$$Sample\ average - Blank\ average = (a)$$
$$(a) = mx + c$$
$$solve\ for\ x$$
$$Concentration\ of\ protein\ lysate\ \left(\frac{mg}{mL}\right) = x\ \times\ 5\ (dilution\ factor)$$

Equation 1: Calculation for concentration of protein lysate

The triplicate absorbance values for each sample is averaged and normalized by subtracting the blank. This value (a) was then substituted into the straight line equation and the x-value was solved. To account for the dilution factor, the answer was duplicated by five to obtain the final concentration of protein in the lysate (mg/mL).

3.3.2 Protein separation: SDS-PAGE

SDS-PAGE was utilized to separate proteins according to their molecular weight, since this technique is based on their ability to migrate under the influence of an electric field (Roy and Kumar, 2014; Reed *et al.*, 2016). Working concentrations (2 mg/mL) of protein lysates were prepared by mixing the relevant amounts of lysate and 2 X Laemmli sample buffer (Sigma-Aldrich, UK). Laemmli contains β-mercaptoethanol, SDS, bromophenol blue and glycerol. SDS is an anionic detergent (negative charge) and was used to denature the disulfide links in tertiary protein structures and denature secondary structures (Manns, 2011). Along with SDS, β-mercaptoethanol ensures breaking of disulfide bonds. In addition, SDS removes the native charge from amino acids and coats the primary structure in a uniform negative charge with a magnitude directly proportional to the molecular weight of the protein (Nowakowski *et al.*, 2014). This universal net charge induced by SDS allow proteins to separate according to size with a high resolution (Nowakowski *et al.*, 2014). Bromophenol blue allows for a visual indication of the sample location in the SDS-PAGE gel. The glycerol component allows for the sample to sink into the wells, since glycerol is denser than the water in which the Running buffer components are dissolved (Laemmli, 1970).

A 10%, 1 mm, 10-lane polyacrylamide gel was prepared according to Table 3. This thickness allowed to separate the proteins over a broad range for of molecular weights (20-250 kDa). Tetramethyl ethylenediamine (TEMED) allowed for the cross-linking of acrylamide monomers (Manns, 2011; Reed *et al.*, 2016). All components for the resolving gel were thoroughly mixed in a 20 mL beaker and poured into the glass casting frame (Bio-Rad, USA), leaving sufficient

space for the stacking gel. To prevent air pockets and an even polymerised surface, 100% isopropanol was overlayed over the resolving gel. The resolving gel was allowed to polymerise for 20 minutes, afterwards the isopropanol layer was removed. The stacking gel solution was prepared in a similar manner. The stacking gel solution was poured over the resolving gel in the gel casting frame. A 10-lane comb was inserted, and the stacking gel was allowed to polymerise for another 15 minutes. The polymerized gel was assembled in clamping frame and placed in the electrophoresis tank. The clamping frame was filled with 1 X Running buffer (Table 4) and the comb was removed. Air bubbles and any gel-webs were removed by flushing the wells with running buffer using a pipette.

The Precision Plus Protein™ ladder (Bio-Rad, USA) was used as the molecular weight marker and 2 µL was loaded in the first lane. Samples were loaded in duplicate, with a normalized concentration of 10 µg/5 µL protein per well. The electrophoresis tank was filled with 1 X Running buffer and the SDS-PAGE was subject to a current of 80 V for 120 min using the PowerPac™ basic power supply (Bio-Rad, USA).

Table 3: SDS-PAGE resolving and stacking gel components

Component	Ingredients	Volume required	
		Resolving gel	Stacking gel
Resolving gel buffer	• 36.2 g Trizma Base (Sigma Aldrich, UK) • 0.8 g SDS (Sigma Aldrich, UK) • pH 8.9 (adjust with HCl/NaOH) • Make up to final volume of 200 mL with dH_2O • Stored 4°C	3 mL	–
Stacking gel buffer	• 5.9 g Trizma Base (Sigma Aldrich, UK) • 0.4 g SDS (Sigma Aldrich, UK) • pH 6.8 (adjust with HCl/NaOH) • Make up to final volume of 100 mL with dH_2O • Stored 4°C	–	750 µL
30% Bis-Acrylamide	• 30 g Acrylamide (Sigma Aldrich, UK) • 0.8 g Bis-Acrylamide (Sigma Aldrich, UK) • 0.1 g SDS (Sigma Aldrich, UK) • Make up to final volume of 100 mL with dH_2O • Stored 4°C	3 mL	500 µL
dH_2O	NA	3 mL	1.75 mL
10% Ammonium Persulfate (APS) (1 mL)	• 100 mg/mL APS (Thermo Fisher Scientific, USA) • Make up to final volume of 1 mL with dH_2O • Stored 4°C	100 µL	30 µL
TEMED (Thermo Fisher Scientific, USA)	NA	10 µL	3 µL

Where, NA = Not Applicable

Table 4: Running buffer components

Running Buffer	Components for 1 L
10 X stock	• 30.2 g Tris • 144 g Glycine • 10 g SDS • 1 L dH_2O • (all reagents from Sigma-Aldrich, UK)
1 X working solution	• 100 mL 10 X stock • 900 mL dH_2O

3.3.3 Protein identification: Western Blotting

Western blotting is a protocol that allows for the immuno-detection of proteins and was established in 1981 . This technique can detect the size of the protein of interest and its relative protein expression can be determined through densitometry. The resolved proteins were transferred from the SDS-PAGE gel onto a 0.22 μM polyvinylidene fluoride (PVDF) membrane (Thermo Fisher Scientific, USA) using the semi-dry Trans-Blot®Turbo™ Transfer System (Bio-Rad, South Africa) at 25 V for 30 minutes in 1 X transfer buffer (Table 5). The utilization of PVDF membrane instead of nitrocellulose membrane was due to its greater strength, which is typically used for high molecular weight proteins (>20 kDa) and has a higher adsorption capacity, making it suitable for detecting lowly expressed proteins and re-probing. Prior to transfer, the PVDF membrane was immersed in 100% methanol for 1 minute, followed by an equilibration step in 1 X transfer buffer, which served to activate the membrane and enhance the transfer process and protein binding. The SDS-PAGE gel and filter papers were also immersed in 1 X transfer buffer to equilibrate before transfer. After proteins were successfully transferred, the membrane was incubated for an hour in a 3 % BSA blocking solution (Table 5) at room temperature on the Orbit™ LS low speed laboratory shaker (Labnet, USA). BSA was used to lower background signal, by binding to the unoccupied sites on the PVDF membrane. Tris buffered saline prevented a high background signal and possible protein interference. Maintaining a low background signal was important to perform more accurate densitometric analysis on the blots.

Table 5: Ingredients for blocking and transfer buffers and their components

Blotting Buffer	Ingredients
Tris Buffered Saline (TBS) (10×) in dH_2O	– 60.5 g Trizma base (Sigma Aldrich, UK) – 87.6 g NaCl (Sigma Aldrich, UK) – pH 7.5 (1× TBS) – Final volume of 1 L
TBS-Tween (TBST) in dH_2O	– 100 mL of 10× TBS – 1 mL Tween-20 (Sigma Aldrich, UK) – Final volume of 1 L
Blocking Buffer	– 3% BSA (Sigma Aldrich, UK) – 1× TBST
Transfer buffer (10×) in dH_2O	– 144 g Glycine (Sigma Aldrich, UK) – 38 g Trizma base (Sigma Aldrich, UK) – Final volume of 1 L
Transfer buffer (1×) in dH_2O	– 100 mL of 10× Transfer buffer – 700 mL dH2O – 200 mL methanol/isopropanol (Sigma Aldrich, UK) – Final volume of 1 L

After blocking, the membrane was probed with the primary antibody of interest (Table 6) at the manufacturer's recommended dilution ratio (in 10 mL of 3 % BSA blocking solution) at 4°C overnight on a shaking platform. The membrane was washed in 1 X TBST at room temperature five times for 5 minutes each on a shaking platform. This step ensured that any unbound primary antibody was adequately removed. Thereafter, the membrane was probed with the relevant secondary antibody (Table 7) conjugated with horse-radish peroxidase (HRP) at a 1:5000 dilution (in 10 mL of 3 % BSA blocking solution) for one hour in the dark on a shaking platform at room temperature. Subsequently, five washes of 1 X TBST for 5 minutes each was performed on a shaking platform to ensure removal of unbound secondary antibody.

Table 6: Primary antibodies

Primary Antibody	Host	Clonality	Dilution ratio	Supplier
Anti-β-tubulin	Rabbit	Monoclonal	1:2000	Cape Biologix Technologies, SA
Anti-ACAT1	Goat	Polyclonal	1:2000	Thermo Fisher Scientific, USA
Anti-HMGCR	Rabbit	Monoclonal	1:2000	Novus Biologicals
Anti-LDLR	Mouse	Monoclonal	1:500	Santa Cruz Biotechnology, USA
Anti-PCSK9	Goat	Polyclonal	1:1000	Novus Biologicals
Anti-SREBP2	Rabbit	Polyclonal	1:1000	Novus Biologicals
Anti-ABCG1	Rabbit	Polyclonal	1:2000	Novus Biologicals

Table 7: Secondary antibodies

Secondary Antibody	Host	Dilution ratio	Supplier
Anti-mouse IgG (H+L)-HRP conjugate	Goat	1:2000	Bio-Rad, USA
Anti-rabbit IgG (H+L)-HRP conjugate	Goat	1:2000	Bio-Rad, USA
Anti-goat IgG-HRP conjugate	Mouse	1:2000	Sigma-Aldrich, UK

Chemiluminescent detection was performed on the ChemiDoc MP system (Bio-Rad, USA) post membrane incubation in Clarity™ Western Enhanced Chemiluminescent (ECL) substrate (Bio-Rad, USA). The ECL substrate is comprised of a peroxide solution and a luminol solution, which were added in a 1:1 v/v (1 mL each) to cover the membrane and was incubated for 1 minute before viewing. This substrate is well-suited for detecting proteins bound to membranes using HRP conjugates, as it provides high sensitivity and low background, resulting in long-lasting signals with high intensity. The oxidation of luminol, catalysed by HRP (on the secondary antibody) and facilitated by hydrogen peroxide (H_2O_2), results in the formation of an excited chemiluminescent molecule (Karatani, 2022). As the oxidized luminol returns to its base state, it emits energy as light which is detected by the ChemiDoc MP system (Bio-Rad, USA) (Karatani, 2022).

A monoclonal antibody against β-tubulin served as a loading control in the study, given that this protein is continuously expressed in cells and is widely recognized as a standard loading control in Western blots (Dittmer and Dittmer, 2006; Liu and Xu, 2006; Nie *et al.*, 2017). The expression levels of this protein were utilized to normalize the results acquired from the protein expression levels of all other proteins examined in the study. Furthermore, the use of this loading control confirmed that the primary antibodies used were specifically targeting the desired proteins (ACAT1, HMGCR, LDLR, PCSK9, SREBP2, ABCG1). Subsequent densitometry analysis was performed on ImageJ software (Schneider *et al.*, 2012) to calculate the relative protein expression in all treatment groups.

3.4 Statistical Analysis

Densitometry analysis was performed on ImageJ software (version 13.0.6) (Schneider *et al.*, 2012). All Western blot experiments were performed with two biological replicates, each with two technical repeats. All statistical analyses were performed on GraphPad Prism (version 10.2.3). A Brown-Forsythe analysis of variance (ANOVA) test was performed to compare the means of three or more treatment groups for statistical significance (Brown and Forsythe, 1974). This was followed by a Dunnett's multiple comparison test to identify which treatment groups showed significant differences compared to the Untreated (UN) control (Dunnett, 1955). The GEM single treatment group was omitted when performing these analyses since the sample size was too small, however, this data point is still included in the visual and graphical data for reference. Additionally, to compare the DMSO vehicle control to the UN control, a Mann-Whitney U test was performed (Mann and Whitney, 1947). Non-parametric analysis were used in this study, as they do not depend on assumptions related to sample size and account for the unequal sample sizes across treatment groups. The samples sizes were as follows: UN: n=4, HPβCD: n=4, 5-FU: n=4, 5-FU & HPβCD: n=4, GEM: n=1, GEM& HPβCD: n=3 and DMSO: n=2. Values were considered significant at $p<0.05$.

4 RESULTS

4.1 Tumour volume

The assessment of tumour volumes for each treatment group provided a crucial metric for evaluating PDAC response to therapy post cholesterol depletion. Xenograft models were established by subcutaneously injecting PANC-1 cells into the left flank of NOD/SCID mice. Treatments were administered, once tumours were palpable at 100 mm^3 (Table 1). Due to the adverse effects observed in the treatment groups receiving the initial toxic concentration of GEM (100 mg/kg), new treatment groups were established with mice that exceeded the desired age. Despite the reduction in GEM concentration (30 mg/kg), these mice (number 21, 23, 29 and 30) were euthanized prior to the completion of ten doses due to strict following of humane endpoints. At the end of the experimental phase, tumours were removed, and their volume and weight were measured. The images of the excised tumours (Fig 9A) exhibit signs of metastasis for the HPβCD single, GEM single, and GEM & HPβCD combination treatments. All mice in these treatment groups were female. The tumour volume data (Fig 9B) revealed that the 5-FU single (-41%) and 5-FU & HPβCD combination (-46%) treatments resulted in decreased tumour volumes compared to all other treatments. The tumours exhibited GEM resistance, as evidenced by the increased tumour volume (+42%) observed following GEM monotherapy. This resistance was mitigated by HPβCD, as the GEM & HPβCD combination treatment resulted in a smaller increase (+4%). Nevertheless, HPβCD did not affect tumour volume when used alone (+3%). The tumour weights (Fig 9C) followed a similar trend as that of tumour volume. Overall, the combination treatments with HPβCD demonstrated improved treatment response compared to the corresponding single treatments, with the 5-FU & HPβCD combination treatment being most effective in reducing tumour volume.

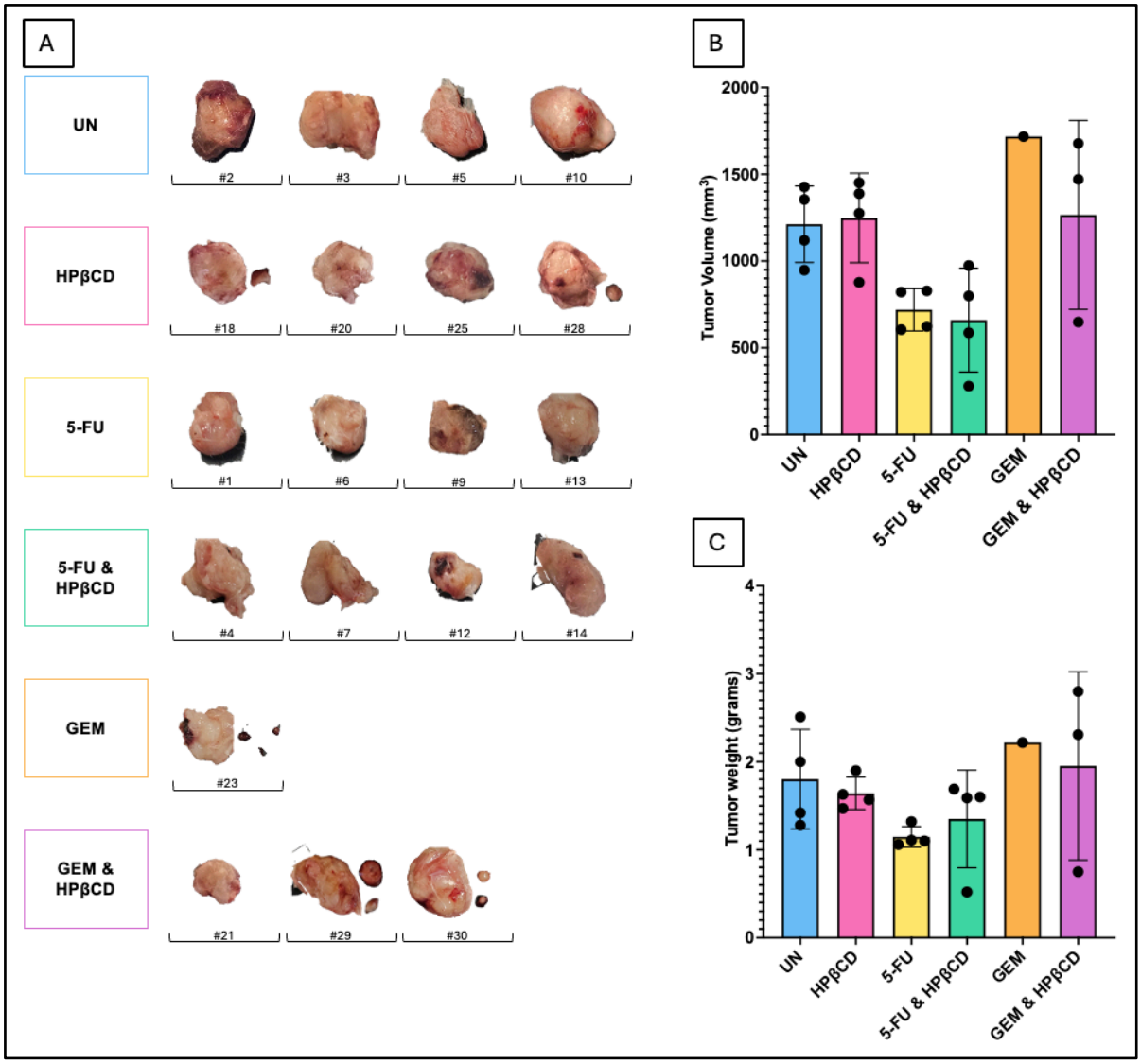


Figure 9: PDAC tumours from xenograft mice

(A) Images of excised subcutaneous tumours. Metastasized tumours were excised from: mouse 18 and 28 (HPβCD); mouse 23 (GEM); mouse 29 and 30 (GEM & HPβCD). (B) Average tumour volume for each treatment group. The tumour volume of each treatment group was compared to the average UN control volume (1212 mm^3). HPβCD showed a 3% increase in tumour volume (1249 mm^3, +3%). 5-FU single treatment showed a 41% decrease in tumour volume (720 mm^3, –41%). 5-FU & HPβCD combination treatment showed the largest decrease in tumour volume of 46% (660 mm^3, –46%). GEM single treatment showed the largest increase in tumour volume of 42% (1718 mm^3, +42%). Lastly, GEM & HPβCD combination treatment showed a 4% increase in tumour volume (1266 mm^3, +4%). Statistically, there were no significant differences in tumour volume. (C) Average tumour weight for each treatment group. The tumour weight of each treatment group was compared to the average UN control weight (1.80 g) . HPβCD showed a 9% decrease in tumor weight (1.64 g, –9%). 5-FU single treatment showed the largest decrease in tumour weight of 36% (1.15 g, –36%). 5-FU & HPβCD combination treatment showed a 25% decrease in tumour weight (1.35 g, –25%). GEM single treatment showed the largest increase in tumour weight of 23% (2.22 g, +23%) Lastly, GEM & HPβCD combination treatment showed a 8% increase in tumour weight (1.95 g, +8%). Statistical analysis found no significant differences in tumour weight. Data shown as mean ±

SD. The data was analysed using a Brown-Forsythe ANOVA test followed by a Dunnett's multiple comparisons test to compare individual differences to the UN control.

4.2 Relative protein expression in xenograft tumour tissue

Considering the effects the different treatments had on tumour volume, it was important to discern the possible molecular mechanisms behind cholesterol homeostasis and drug response in PDAC tumours. The relative expression of key proteins from each of the four cholesterol homeostasis pathways (synthesis, uptake, storage, and export) were analysed with Western blotting. Snap-frozen tissues were processed for Western blotting as described in section 3.

4.2.1 β-tubulin normalization

β-tubulin was used as the loading control for all Western blots. The loading of samples was normalized to match the UN control, as evidenced by the equal bands seen in the blots (Fig 10). For ease of reference, the normalized bands are shown in figure 10 for all samples, however, due to the large sample size, normalized bands will not be shown in subsequent figures.

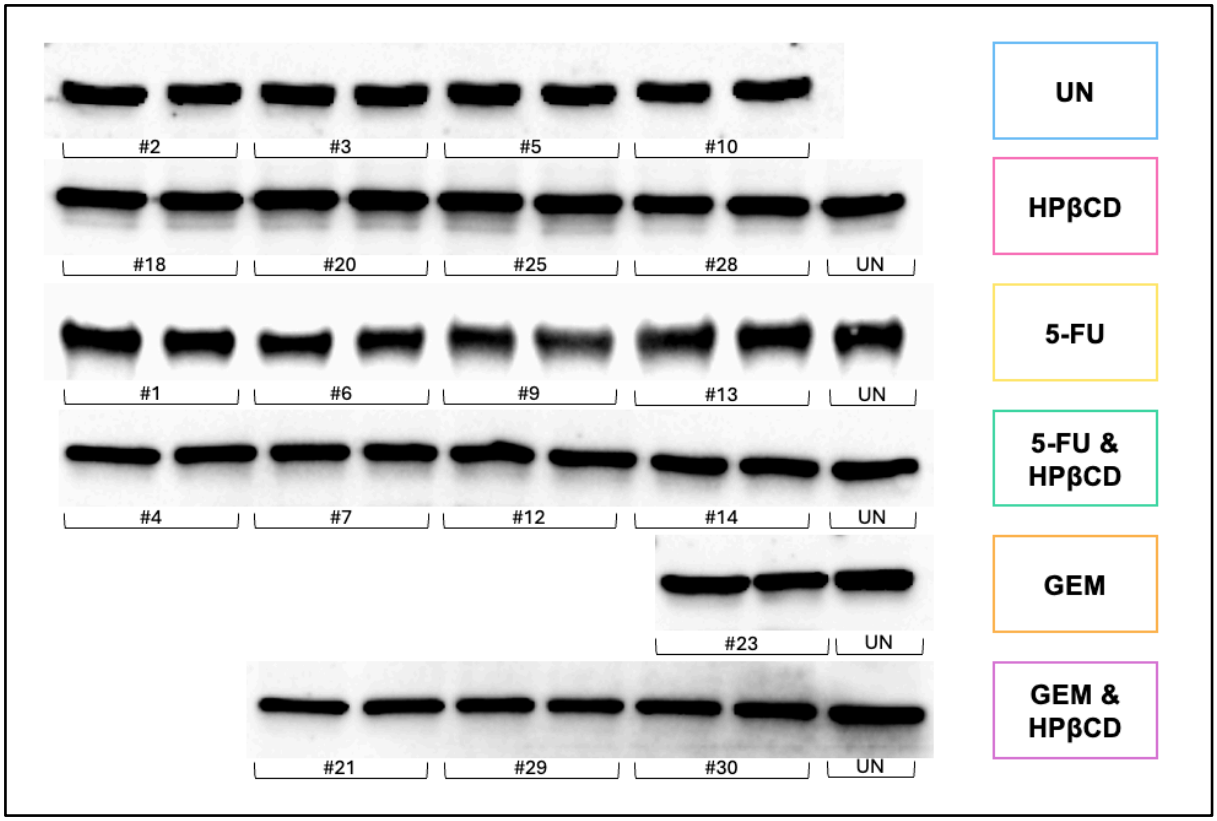


Figure 10: Normalization of loading with β-tubulin

Representative Western blots showing the normalized expression of β-tubulin (55 kDa) with 10 µg/5 µL protein loaded per well. Each mouse sample was loaded in duplicate, with the corresponding sample number labelled for each band-pair. The treatment groups were normalized against the UN, which is shown in the far-right lane. Band size/density correlates to protein expression.

4.2.2 Cholesterol storage: ACAT1

ACAT1 converts FC into CEs, which are then stored in lipid droplets. ACAT1 is crucial in maintaining a homeostatic balance of FC within the cell, as high FC concentrations can cause ER stress, which is toxic to the cell. Furthermore, a high CE concentration provides the cell with on-demand cholesterol to incorporate into the membrane and lipid rafts, contributing to rapid proliferation and drug resistance. Given that ACAT1 expression is influenced by the cellular concentration of FC, it can provide insight into the amount of FC being converted to CEs within tumour cells. Upon comparing each treatment group to the UN control group, no statistical significant differences were observed in ACAT1 expression from densitometric analysis (Fig 11B). However, it is important to note that ACAT1 expression in the group receiving GEM single treatment was visibly higher than that of the untreated tumours in the Western blots (Fig 11A). Although this difference was not statistically significant due to the limited sample size, it is still worth addressing the observed variation. This result suggests that

GEM treatment resulted in increased intracellular CE conversion. Interestingly, the combination of HPβCD with GEM resulted in lower expression (–4%) of ACAT1 than GEM alone (+31%). This indicates that the cholesterol sequestering capability of HPβCD leads to a decrease in CE conversion from FC induced by GEM. ACAT1 expression after treatment with 5-FU (+3%) and the combination of 5-FU with HPβCD (+6%) was relatively similar, indicating that 5-FU does not significantly influence CE levels to the extent that GEM does. HPβCD monotherapy increased ACAT1 expression in two mice (mouse 25 and 28), whereas it slightly decreased for the other two mice (mouse 18 and 20). This observation suggests that individual differences in FC homeostasis may influence the response to HPβCD. Notably, the mice from both combination treatments with HPβCD exhibited less variation in ACAT1 expression. The overall increase in ACAT1 expression for HPβCD (+16%) might suggest a resistance mechanism used by the tumour cells to counteract FC sequestering by HPβCD.

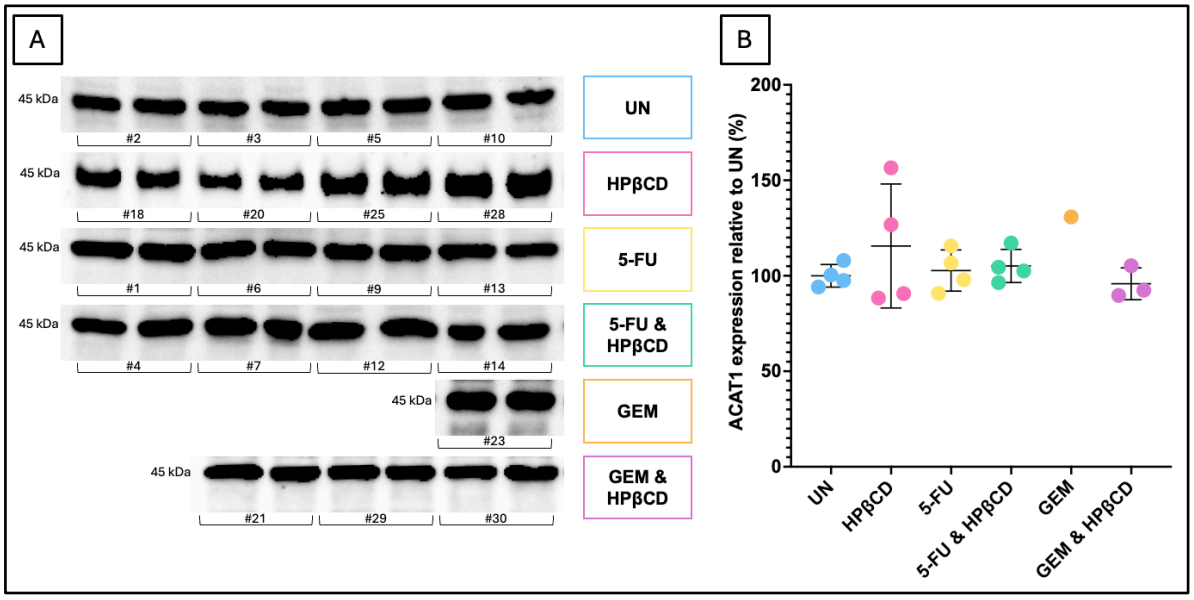


Figure 11: Relative protein expression levels of ACAT1

(A) Representative Western blots for ACAT1 (45 kDa) expression for each treatment group. Varied band sizes are observed for the HPβCD treatment group. There was no visible difference in band size when comparing 5-FU treatment and 5-FU & HPβCD to the UN control. A visible difference was noted when comparing GEM treatment to the UN control, with GEM treatment showing larger bands. The GEM & HPβCD combination treatment is similar to the UN, but has visibly thinner bands compared to the GEM treatment. Band size/density correlates to protein expression. (B) Average densitometry for two experimental repeats of ACAT1 for each treatment group relative to the UN control, expressed as a percentage: HPβCD (+16%), 5-FU (+3%), 5-FU & HPβCD (+6%), GEM (+31%) and GEM & HPβCD (–4%). No significant differences were observed in mean ACAT1 expression compared to the UN control. Data shown as mean ± SD. The data was analysed using a Brown-Forsythe ANOVA test followed by a Dunnett's multiple comparisons test to compare individual differences.

4.2.3 Cholesterol Synthesis: HMGCR

Drug resistance in PDAC is substantially influenced by cellular cholesterol content, which is shaped by cholesterol synthesis through the MP. Therefore, it is crucial to evaluate the impact of chemotherapeutic treatments, as well as in combination with a cholesterol depleting agent on the cholesterol synthesis pathway. Densitometric analysis revealed notable differences in the mean HMGCR expression levels among the treatments (Fig 12B). Western blot images (Fig 12A) demonstrate that GEM monotherapy (+35%) increased cholesterol synthesis, whilst 5-FU monotherapy (±0%) had no effect. Surprisingly, the HPβCD single treatment (–2%) did not have a comparable effect on cholesterol synthesis compared to the combined treatment with chemotherapeutic agents. Both 5-FU & HPβCD (–18%) and GEM & HPβCD (–24%) combination treatments decreased HMGCR expression, with 5-FU & HPβCD exhibiting a significant decrease in cholesterol synthesis.

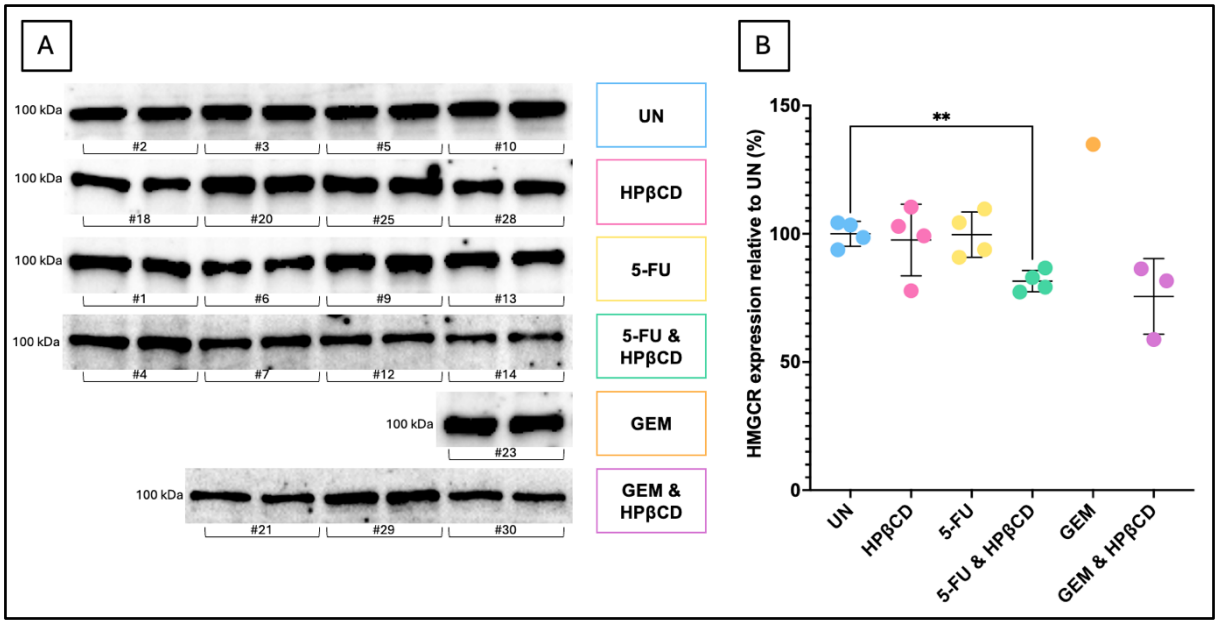


Figure 12: Relative protein expression levels of HMGCR

(A) Representative Western blots for HMGCR (100 kDa) expression for each treatment group. Band sizes for HPβCD treatment group are relatively similar to UN control, with the exception of mouse 18 showing slightly smaller bands. The bands for 5-FU & HPβCD combination treatment are thinner compared to 5-FU single treatment and UN control. GEM single treatment bands are larger than UN control. The combination of GEM & HPβCD show a reduction in bands size compared to GEM single treatment and UN control. Band size/density correlates to protein expression. (B) Average densitometry for two experimental repeats of HMGCR for each treatment group relative to the UN control, expressed as a percentage: HPβCD (–2%), 5-FU (±0%), 5-FU & HPβCD (–18%), GEM (+35%) and GEM & HPβCD

(–24%). A significant difference in mean HMGCR expression was observed for 5-FU & HPβCD compared to the UN. Data shown as mean ± SD. The data was analysed using a Brown-Forsythe ANOVA test followed by a Dunnett's multiple comparisons test to compare individual differences, where *=p<0.05, **=p<0.01 and ***=p<0.001 indicates a significant difference.

4.2.4 Cholesterol Uptake: LDLR & PCSK9

Another means of increasing the cellular FC content to contribute to drug resistance, besides synthesis, is the uptake of cholesterol from blood plasma by LDLR. Difficulties were encountered for LDLR immunodetection, and 100 μg protein had to be loaded per well to produce interpretable results. The densitometric analysis showed no statistically significant differences in the mean LDLR expression (Fig 13B). However, Western blots (Fig 13A) showed noticeable visual differences. Multiple bands were observed, however, the 120 kDa band was quantified using densitometry. This common phenomenon in tissue samples is possibly attributed to non-specific binding of the primary antibody to other proteins, as the primary antibody used was produced in mice (Zhu *et al.*, 2018; Zhao *et al.*, 2020). Although the target is for human species, the xenograft tissue contains trace amounts of the mouse host tissue and proteins. HPβCD (-11%) monotherapy did not exhibit a significant effect on LDLR expression. The GEM monotherapy (+141%) elicited the highest LDLR expression among all treatments, thereby demonstrating increased cholesterol uptake, while the combination treatment of GEM & HPβCD resulted in reduced cholesterol uptake (+22%), albeit still higher than UN. In contrast, 5-FU monotherapy (-2%) did not demonstrate increased cholesterol uptake to the extent of GEM, however, the combination treatment of 5-FU & HPβCD (-40%) led to a substantial decrease in LDLR expression. These findings suggest that the combination of chemotherapy with HPβCD reduces cholesterol uptake.

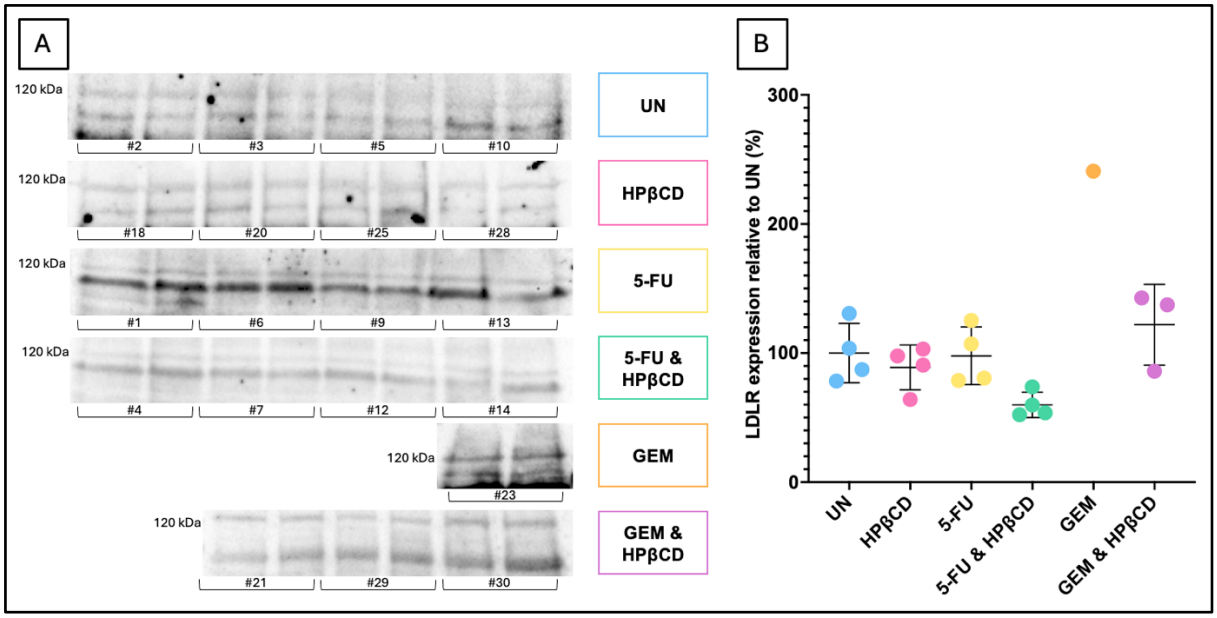


Figure 13: Relative protein expression levels of LDLR

(A) Representative Western blots for LDLR (120 kDa top band) expression for each treatment group. HPβCD single and 5-FU single treatments have similar band densities to the UN control. The 5-FU & HPβCD combination treatment have visually less dense bands than the 5-FU single treatment. The GEM single treatment has the most dense bands out of all treatment groups. The GEM & HPβCD combination treatment has less dense bands compared to the GEM single treatment. Band size/density correlates to protein expression. (B) Average densitometry for two experimental repeats of LDLR for each treatment group relative to the UN control, expressed as a percentage: HPβCD (–11%), 5-FU (–2%), 5-FU & HPβCD (–40%), GEM (+141%) and GEM & HPβCD (+22%). No significant differences were observed in mean LDLR expression compared to the UN control. Data shown as mean ± SD. The data was analysed using a Brown-Forsythe ANOVA test followed by a Dunnett's multiple comparisons test to compare individual differences.

Negative regulation of cholesterol uptake is primarily mediated by PCSK9, which targets LDLR for degradation. Due to the high non-specificity observed on LDLR blots, it was crucial to investigate PCSK9 expression to further confirm the expression levels of LDLR. Densitometric analysis failed to reveal any statistical significant differences in mean PCSK9 expression (Fig 14B). However, visual differences in PCSK9 expression were observed in Western blots (Fig 14A). Once again, multiple bands were detected (Xu *et al.*, 2021). It is known that PCSK9 has a precursor and mature form. The mature form (bottom band at 60 kDa) was quantified in densitometry. Notably, treatment with HPβCD (+37%) resulted in the highest expression of PCSK9 among all treatments, which corresponds to its decrease in LDLR, demonstrating the inverse relationship between PCSK9 and LDLR. Interestingly, GEM monotherapy demonstrated an increase (+13%) in PCSK9, whereas the GEM & HPβCD combination treatment decreased (-20%) PCSK9, both of which do not inversely correspond

to their LDLR expression profiles. A similar phenomenon is observed for 5-FU & HPβCD combination treatment, showing the largest reduction (-36%) in PCSK9 expression, whereas 5-FU monotherapy (-19%) did not affect PCSK9 levels to as great an extent. The reduction in PCSK9 expression, observed for 5-FU & HPβCD combination treatment, was significantly reduced from HPβCD monotherapy. These findings suggest that PCSK9 might not be targeting LDLR, due to the absence of a consistent inverse relationship across all treatments containing GEM and 5-FU, indicating that PCSK9 may exert its effects elsewhere due to chemotherapeutic intervention.

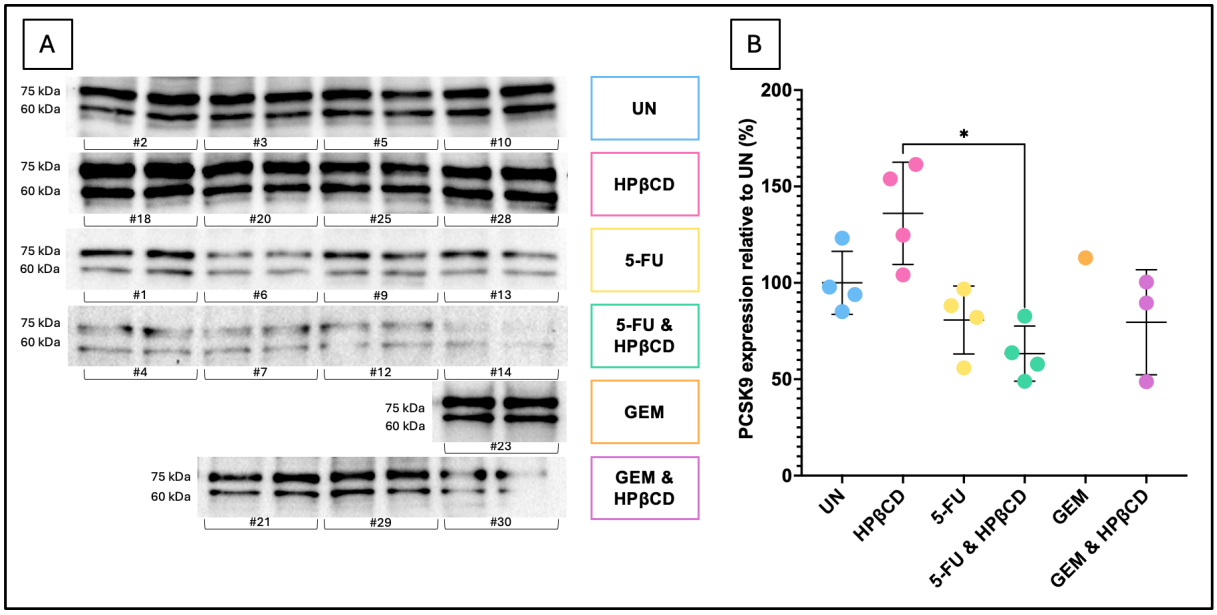


Figure 14: Relative protein expression levels of PCSK9

(A) Representative Western blots for mature PCSK9 (60 kDa bottom band) expression for each treatment group. Bands for HPβCD are larger compared to UN control. GEM single treatment shows more dense bands compared to UN, where GEM & HPβCD combination treatment show less dense bands. Both 5-FU single and 5-FU & HPβCD combination treatments have less dense bands compared to UN control. Band size/density correlates to protein expression. (B) Average densitometry for two experimental repeats of PCSK9 for each treatment group relative to the UN control, expressed as a percentage: HPβCD (+37%), 5-FU (–19%), 5-FU & HPβCD (–36%), GEM (+13%) and GEM & HPβCD (–20%). A significant difference was observed in mean PCSK9 expression for 5-FU & HPβCD combination treatment compared to HPβCD. Data shown as mean ± SD. The data was analysed using a Brown-Forsythe ANOVA test followed by a Dunnett's multiple comparisons test to compare individual differences, where *=$p<0.05$, **=$p<0.01$ and ***=$p<0.001$ indicates a significant difference.

4.2.5 Regulation of cholesterol synthesis and uptake: SREBP2

To gain a deeper understanding of the proteins involved in the uptake and synthesis processes, the expression of SREBP2, the master transcriptional regulator of these processes, was

examined. Both the precursor and active forms of the protein were detected using Western blots (Fig 15A). Multiple bands were detected for both precursor and active forms, however, this phenomenon is a common issue encountered in tissue samples (Howell et al., 2020; Quiroz-Figueroa et al., 2021). Densitometric analysis was performed on both bands at the active 60 kDa size range (Fig 15B). The HPβCD single treatment demonstrated a statistically significant increase in SREBP2 expression compared to the UN control, exhibiting the highest expression among all treatments. The single treatments of GEM and 5-FU also exhibited elevated expression of SREBP2 relative to the UN, and the combination treatments with HPβCD further enhanced this expression, with the 5-FU & HPβCD combination treatment also reaching statistical significance.

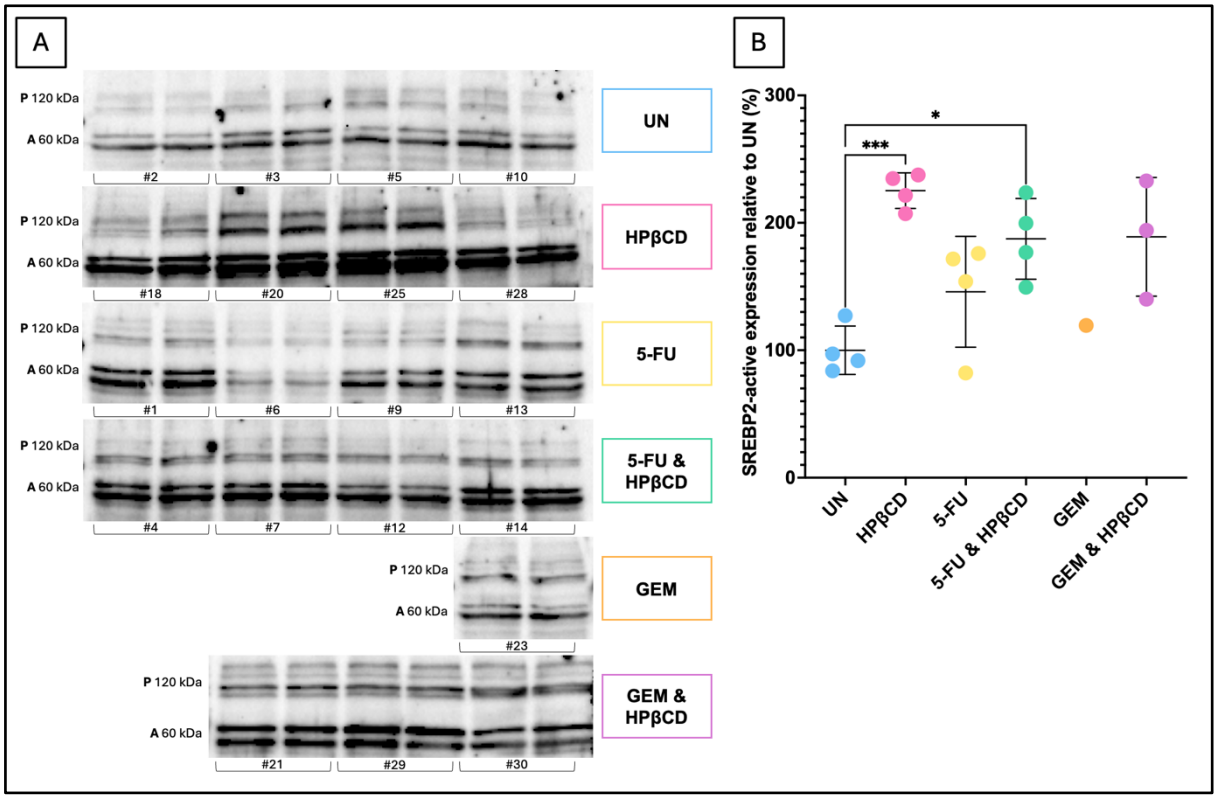


Figure 15: Relative protein expression level of SREBP2 active and precursor form

(A) Representative Western blots for SREBP2-active (60 kDa both bottom bands) expression for each treatment group. HPβCD single treatment shows the most dense bands for SREBP2-active compared to all other treatments. The GEM and 5-FU single treatments show slightly thicker bands compared to UN control. Both combination treatments (GEM & HPβCD and 5-FU & HPβCD) show more dense bands compared to their corresponding single treatments. Band size/density correlates to protein expression (B) Average densitometric analysis for two experimental repeats of SREBP2-active bands for each treatment group relative to the UN control, expressed as a percentage: HPβCD (+126%), 5-FU (+46%), 5-FU & HPβCD (+88%), GEM (+20%) and GEM & HPβCD (+90%). Significant differences were observed for HPβCD single and 5-FU & HPβCD combination treatments compared to the UN. Data shown as mean

± SD. The data was analysed using a Brown-Forsythe ANOVA test followed by a Dunnett's multiple comparisons test to compare individual differences, where *=p<0.05, **=p<0.01 and ***=p<0.001 indicates a significant difference.

4.2.6 Cholesterol Efflux: ABCG1

Cholesterol efflux is crucial for maintaining a homeostatic balance of intracellular free cholesterol, which is influenced by both uptake and synthesis mechanisms. To gain insight into the process of cholesterol efflux in tumour cells, the expression of ABCG1 was examined. Densitometry results showed no statistically significant difference in mean ABCG1 expression (Fig 16B). However, Western blot analysis revealed notable differences (Fig 16A). Similar double-band patterns have been reported in literature for this antibody product (Beer *et al.*, 2013).HPβCD single treatment displayed the highest (+32%) ABCG1 expression, while GEM single treatment showed the lowest (–57%). Additionally, both combination treatments indicated higher ABCG1 expression compared to their respective single treatments. The reduction in ABCG1 expression, observed for 5-FU monotherapy, was significantly reduced from HPβCD monotherapy. The data suggest that in addition to sequestering cholesterol, HPβCD may further promote its export from the cell.

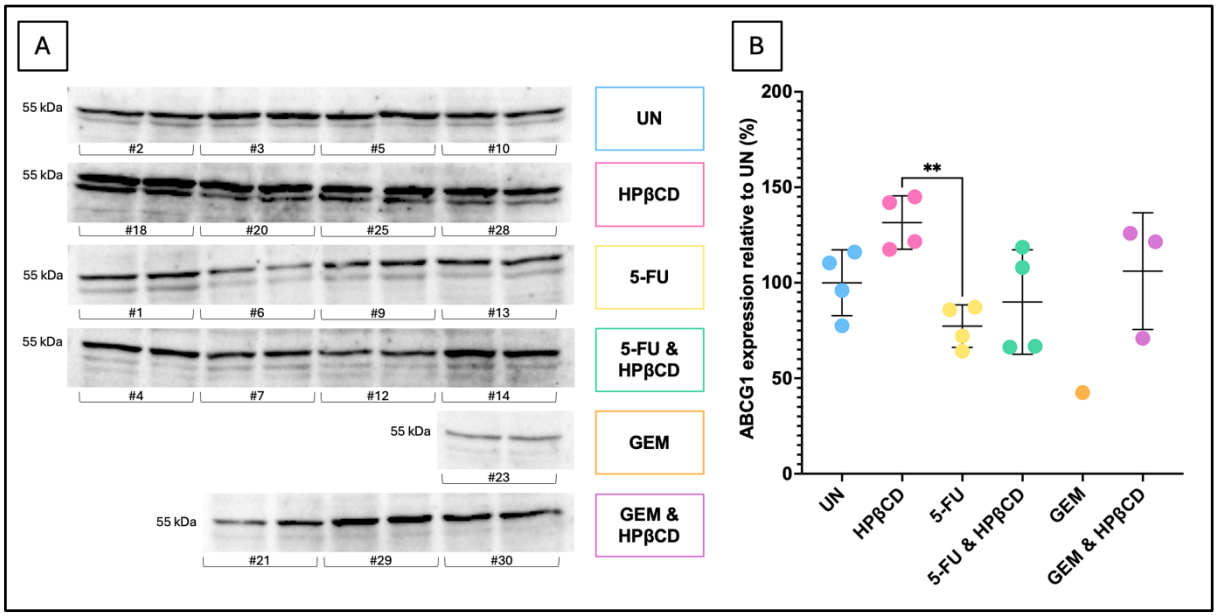


Figure 16: Relative protein expression level of ABCG1

(A) Representative Western blots for ABCG1 (55 kDa top band) expression for each treatment group. HPβCD single treatment shows the densest bands compared to all treatment groups. The 5-FU single treatment show less dense bands compared to the untreated control. The combination treatment of 5-FU & HPβCD show slightly more dense bands compared to the 5-FU single treatment. GEM treatment has the least dense bands out of all treatment groups. The

combination treatment of GEM & HPβCD show increased band density compared to the GEM single treatment. Band size/density correlates to protein expression (B) Average densitometry for two experimental repeats of ABCG1 for each treatment group relative to the UN control, expressed as a percentage: HPβCD (+32%), 5-FU (–22%), 5-FU & HPβCD (–10%), GEM (–57%) and GEM & HPβCD (+7%). A significant difference was observed in mean ABCG1 expression for 5-FU monotherapy compared to HPβCD. Data shown as mean ± SD. The data was analysed using a Brown-Forsythe ANOVA test followed by a Dunnett's multiple comparisons test to compare individual differences, where *=$p<0.05$, **=$p<0.01$ and ***=$p<0.001$ indicates a significant difference.

5 DISCUSSION

The metabolic heterogeneity of PDAC poses a significant challenge in clinical settings, mainly due to its tendency to metastasize and its highly chemo-resistant nature, particularly to GEM and 5-FU. As PDAC is highly dependent on its altered cholesterol homeostasis, it is important to consider the potential impact of cholesterol-lowering medications on PDAC drug resistance. Previous studies in Kaur lab presented a positive correlation between HPβCD concentration and viability inhibition in breast cancer (Saha *et al.,* 2023), colorectal cancer (Pillay, 2024) and PC (Daya, 2024). Therefore, this study focused on evaluating the impact of cholesterol-depleting agent, HPβCD, on PDAC drug response in mice tumurs and identifying potential strategies to overcome drug resistance. Using PANC-1 cells, a xenograft mice model was established and subject to various treatment strategies using GEM and 5-FU alone and in combination with HPβCD. Using this approach, this study aimed to gain a mechanistic understanding of cholesterol depletion effects on treatment response.

5.1 Tumour volume and metastasis

Tumour volume provides an important measure of treatment response, particularly in the preclinical setting. The data from this study provided a quantifiable metric that reflects the physiological behaviour of PANC-1 cell-derived tumours in response to treatment. Calliper measurements were used to assess tumour volume. There was no statistical significant difference amongst tumour volumes due to the large standard deviation, which is to be expected from manual calliper measurements and individual mouse variability (Fig 9). Nonetheless, a notable difference occurred between GEM monotherapy (+42%) and its combination with HPβCD (+4%) compared to the UN. Furthermore, the combination of 5-FU with HPβCD (–46%) produced the greatest reduction in tumour volume, although it did not differ much from the 5-FU monotherapy (–41%). Suggesting that cholesterol depletion might only be beneficial in improving treatment response to GEM and not as much for 5-FU.

5.1.1 HPβCD was not effective as monotherapy and possibly induced epithelial-mesenchymal transition (EMT)

HPβCD has been effective in inducing breast cancer cell death and tumour reduction, as shown in *in vitro* and *in vivo* studies (Saha *et al.*, 2023; Zhu *et al.*, 2023). Similarly, unpublished data from Prof Kaur's lab have also proven that HPβCD is effective in reducing colorectal cancer tumours (Pillay, 2024). This is not in line with results of this study, where, unexpectedly, no significant change in tumour volume was observed with HPβCD treatment (+3%) (Fig 9). The results propose that HPβCD exhibits a distinct mode of action in PDAC, where its monotherapy did not yield a favourable result. Moreover, two mice in the group receiving HPβCD, had secondary tumours excised from the liver, an indication of metastasis (Fig 9). A key driver in the metastasis of PDAC is EMT, as it promotes the migration of tumour cells from the primary site to distant organs (Xu *et al.*, 2015; S Wang *et al.*, 2017; Lai *et al.*, 2020; Ma *et al.*, 2022). EMT entails the loss of epithelial characteristics and the acquisition of mesenchymal traits, which increases the motility and invasive capabilities of tumour cells (Maier *et al.*, 2010; S Wang *et al.*, 2017). Literature shows that low concentrations (such as 290 μg/mL and 467 μg/mL) of HPβCD has no cytotoxic effect on PANC-1 cells and does not induce apoptosis (Iacobazzi *et al.*, 2020; Kano *et al.*, 2023). Furthermore, it has been found that in breast cancer cells, HPβCD, administered at low concentrations (900 – 1440 μg/mL), induced EMT (Zhao *et al.*, 2021). However, these are cell-based studies and the concentrations to be used in animals are very different. In our lab, it was found that lower than 3000 mg/Kg dosage was not effective in animals and the higher dosage was not well tolerable by animals. Literature has not yet reported on the use of HPβCD on EMT in PDAC, however, studies indicate that the use of statins (to target cholesterol synthesis) induces EMT in PDAC (Gabitova-Cornell *et al.*, 2020; Rebelo *et al.*, 2023). It is possible that in both cases, for HPβCD and statins, manipulating the homeostatic balance of cholesterol further aggravates PDAC, and is discussed in more depth in subsequent sections.

5.1.2 Combination with HPβCD did not significantly improve 5-FU efficacy

The most effective treatments in reducing tumour volume were 5-FU single (–41%) and 5-FU & HPβCD combination (–46%) treatments (Fig 9). 5-FU is reported to induce apoptosis in PANC-1 cells (Zhao *et al.*, 2022), and reduces the size of PANC-1 cell-derived tumours (Wang

et al., 2020; H Liu *et al.*, 2021). In colorectal cancer, combining 5-FU with HPβCD significantly decreased tumour volume as found by Pillay, 2024. However, in PDAC it did not significantly decrease tumour volume as was expected, but it did result in the smallest average tumour volume. It has been reported that combining 5-FU with agents targeting cholesterol synthesis, such as statins, sensitizes PANC-1 cells to 5-FU induced apoptosis (Mistafa and Stenius, 2009). Furthermore, the combination of β-cyclodextrin with 5-FU increased the efficacy of 5-FU in inhibiting colon cancer cell growth (Di Donato *et al.*, 2016). Additionally, HPβCD is often used as a drug excipient to form an inclusion complex with 5-FU to increase the efficiency of drug transport and uptake in colon-rectal cancer (LL Wang *et al.*, 2016). Therefore, HPβCD may potentially re-sensitize PDAC tumour cells to 5-FU, either through the sequestration of FC or by enhancing 5-FU drug delivery.

5.1.3 Single and combination treatments of GEM and HPβCD potentially induced metastasis in PDAC

GEM remains the standard first-line chemotherapy for PDAC, despite its widespread use, patients develop GEM resistance within weeks of initiating treatment (De Sousa Cavalcante and Monteiro, 2014; Amrutkar and Gladhaug, 2017; Sarvepalli *et al.*, 2019; Miller *et al.*, 2020). Similar to HPβCD monotherapy, secondary tumours were observed in the mouse that received only GEM treatment. This mouse also had the largest increase in tumour volume (+42%) (Fig 9), which is consistent with findings in the literature. Despite various studies demonstrating that GEM can reduce tumour volume in PANC-1 cell-derived xenografts (Liu *et al.*, 2014; Kang *et al.*, 2021; Kim *et al.*, 2024), the PANC-1 cell line is well documented to exhibit resistance to GEM, and consequently, a suboptimal treatment response was expected (Maier *et al.*, 2010; Hu *et al.*, 2014; Sweeney *et al.*, 2017; Kong *et al.*, 2022; Ji He *et al.*, 2024). It is well reported that GEM often induces metastasis via activating EMT. The KRAS-induced PI3K pathway aids in bypassing apoptosis and induces EMT (Binenbaum *et al.*, 2015; Xu *et al.*, 2015). EMT contributes to GEM resistance by decreasing the expression of nucleoside transporters which are responsible for the uptake of these drugs (Grant *et al.*, 2016; Di Carlo *et al.*, 2018; Zeng *et al.*, 2019). Immunohistochemical studies on human PDAC specimens and organoids showed that there is an elevated expression of EMT markers, which was associated with an increase in tumour budding after exposure to chemotherapeutic agents, indicating the role of EMT in acquired drug resistance (Xu *et al.*, 2015; Palamaris *et al.*, 2021).

One way to overcome GEM resistance is to combine it with other therapeutic strategies. In this study, it was evident that the GEM & HPβCD combination (+4%) therapy resulted in a lower tumour volume compared to that of GEM monotherapy (+42%) (Fig 9). Similar positive effects were observed when GEM was combined with statins, where it re-sensitized PANC-1 cells to GEM-induced apoptosis (Mistafa and Stenius, 2009). It is possible that HPβCD induces a similar effect, where cells are re-sensitized to GEM upon cholesterol depletion. Another possibility is that HPβCD improved the targeting of GEM to cancer cells. When GEM is encapsulated in positively charged β-cyclodextrin, drug delivery into cancer cells is improved (Rodriguez-Ruiz *et al.*, 2017). Unfortunately, the combination of GEM & HPβCD did not reduce the risk of metastasis, since two mice in this treatment group had secondary tumours. However, it is interesting to note that the mice showing metastasis were all from treatment groups consisting of female mice.

The impact of mouse gender on treatment response is a multifaceted issue, with studies indicating that biological sex can influence both the progression of cancer and the efficacy of treatments. In the preclinical and clinical setting, there is a lack of gender-specific investigations within the field of cancer therapeutics (Becher and Oertelt-Prigione, 2023). Limited literature shows contradicting findings when it comes to the impact of gender in cancer treatment response. A PC study indicated that male mice responded better to treatment and had smaller tumours in comparison to female mice (Schulz *et al.*, 2024). Female mice with PC exhibit lower heart rates and heightened heart rate variability, indicative of a suboptimal response to treatment (Gams *et al.*, 2023). When analysing PDAC tumour tissues from human patients, differences were noted in the immune response of males and females (Ahmed *et al.*, 2023). These sex-based differences highlight the importance of including both male and female mice in treatment groups for preclinical studies to better understand treatment response. Undoubtedly, when considering the results of this study, gender might influence treatment response, as all exhibiting metastasis were female.

5.2 Effects on cholesterol homeostasis using HPβCD monotherapy and in combination with first-line chemotherapies: 5-FU and GEM

The current standard treatment for advanced PDAC involves the use of 5-FU or GEM, either alone or in combination with other traditional therapies. However, this approach has demonstrated minimal success in improving overall survival rates and has shown limited

effectiveness, particularly in late-stage PDAC cases. Cyclodextrins are commonly used to encapsulate drugs to improve drug delivery. However, the present study sought to explore whether depleting cholesterol using HPβCD, to alter cholesterol homeostasis, could potentially enhance the effectiveness of GEM and 5-FU in treating PDAC. The expression of key proteins involved in cholesterol homeostatic pathways (storage, synthesis, uptake, regulation, and efflux) (Fig 17) was investigated to elucidate a potential mechanism by which cholesterol may influence the response to 5-FU and GEM.

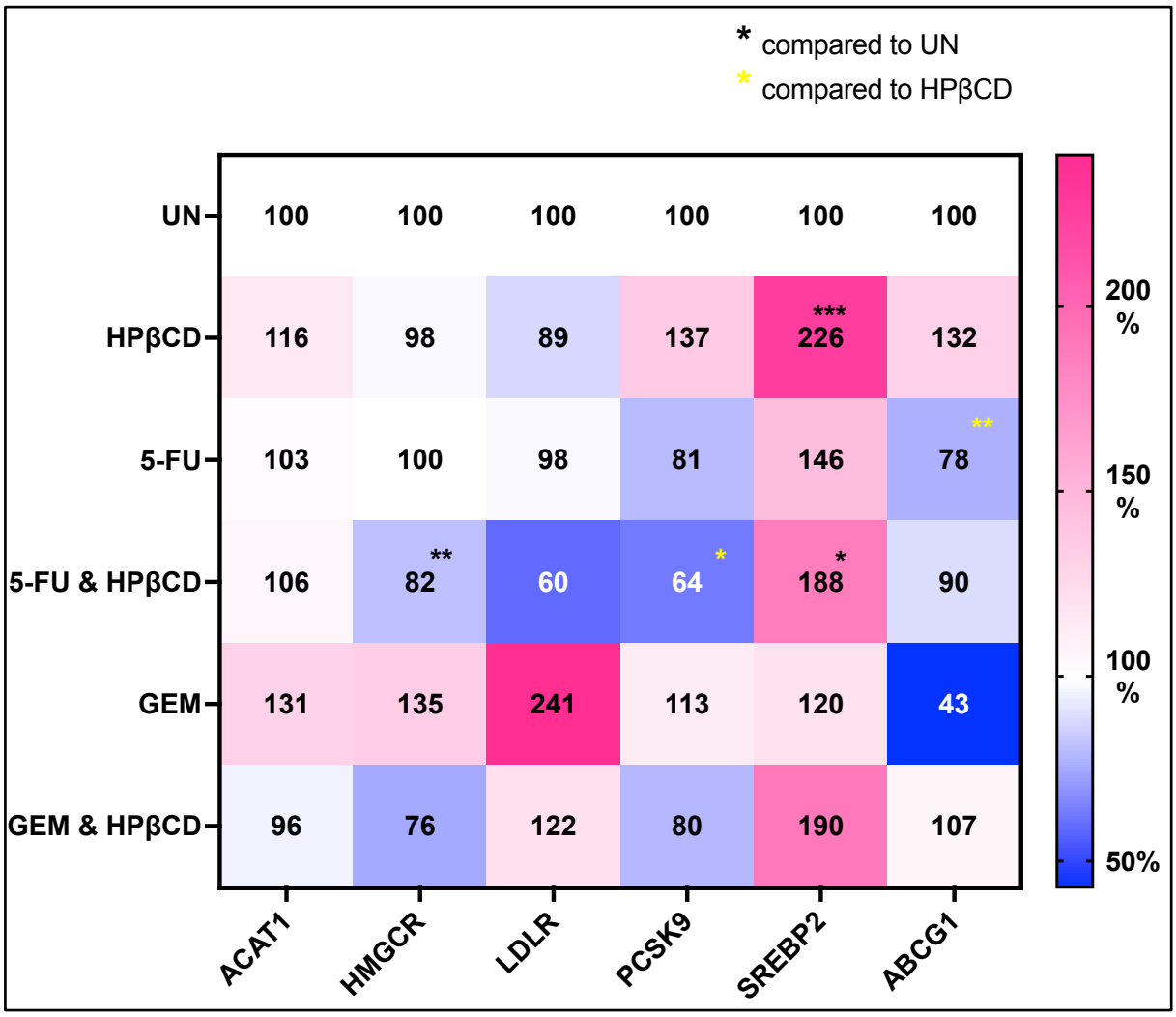


Figure 17: A heat map summarising the protein expression profiles (%) of key proteins involved in cholesterol homeostasis

Heat map showing the percentage (%) protein expression profile for each treatment relative to the UN (100%). Compared to the UN, HPβCD monotherapy increases ACAT1, PCSK9, SREBP2 and ABCG1, whereas it decreases HMGCR and LDLR. 5-FU monotherapy, compared to the UN, increases ACAT1 and SREBP2, whereas it decreases LDLR, PCSK9 and ABCG1, and HMGCR remains unchanged. The combination treatment of 5-FU & HPβCD, compared to the UN, increases ACAT1 and SREBP2, whereas it decreases HMGCR, LDLR, PCSK9 and ABCG1. Upon comparing the 5-FU & HPβCD combination treatment to 5-FU

monotherapy, ACAT1, SREBP2 and ABCG1 is increased, whereas HMGCR, LDLR and PCSK9 is decreased. GEM monotherapy, compared to the UN, shows an increase in ACAT1, HMGCR, LDLR, PCSK9 and SREBP2, whereas it shows a decrease in ABCG1. The combination treatment of GEM & HPβCD, compared to the UN, increases LDLR, SREBP2 and ABCG1, whereas it decreases ACAT1, HMGCR and PCSK9. Upon comparing the GEM & HPβCD combination treatment to GEM monotherapy, SREBP2 and ABCG1 is increased, whereas ACAT1, HMGCR, LDLR and PCSK9 is decreased. (Black asterisks indicate significant differences compared to UN, and yellow asterisks indicate significant differences compared to HPβCD).

5.2.1 Cholesterol storage

HPβCD is renowned for its capacity to sequester cholesterol (Mitrofanova *et al.*, 2018; Kanagaki *et al.*, 2021). It has been proposed to act as a mediator to target cholesterol for esterification by ACAT1 or hydroxylation by other cytochrome P450 enzymes (Liza *et al.*, 1996; El-Darzi *et al.*, 2023). In hyperlipidaemic mice, HPβCD treatment increases cellular levels of CEs, and in turn, lowers intracellular FC (Walenbergh *et al.*, 2015), supporting the proposed mechanism whereby HPβCD may target FC for esterification by ACAT1. The results from the present study show that HPβCD single treatment resulted in a slight increase of ACAT1 expression (+16%) (Fig 17), which corroborates with previous studies on Niemann-Pick disease Type C, indicating that HPβCD has the capacity to liberate FC, which exhibits cytotoxicity, thereby prompting the cell to counteract this effect by increasing ACAT1 to upregulate cholesterol esterification (Peake and Vance, 2012; Vance and Karten, 2014; Ramirez *et al.*, 2020). Consequently, the cholesterol-sequestering action of HPβCD may induce a similar compensatory mechanism in PDAC tumour cells, whereby they upregulate ACAT1 to increase the storage of cholesterol. This increase in ACAT1 expression is unfavourable, since a high ACAT1 expression is strongly correlated with increased cell proliferation, tumour metastasis and poor prognosis (Rebelo *et al.*, 2023; Tu *et al.*, 2023). On the contrary, in nasopharyngeal carcinoma, inactivation of ACAT1 promoted metastasis (Lu *et al.*, 2021). The role of cholesterol esterification in metastasis remains unclear. Specifically, there is ongoing debate about why and under what circumstances the mobilization of stored CE's from lipid droplets would be necessary to induce a metastatic phenotype (Cruz *et al.*, 2020). Interestingly, the two mice with metastasis had different levels of ACAT1 expression, suggesting that ACAT1 might not be the cause of metastasis in the present study.

Neither treatment with 5-FU (+3%) nor 5-FU & HPβCD (+6%) exhibited significant changes in expression levels of ACAT1 (Fig 17). Limited research has been conducted on the interplay

between ACAT1 and 5-FU resistance. The results from this study indicate that ACAT1 possibly does not promote 5-FU resistance, hence combining HPβCD with 5-FU shows no benefit in the context of ACAT1 and cholesterol esterification. These findings suggest that ACAT1 may not play a significant role in conferring resistance to 5-FU treatment. Further investigation into alternative pathways or targets could be necessary to improve the efficacy of 5-FU-based therapies. The lack of synergistic effect between HPβCD and 5-FU in relation to ACAT1 expression highlights the need to explore other molecular targets for enhancing 5-FU efficacy in cancer treatment. GEM monotherapy (+31%) resulted in the highest ACAT1 expression conferring to high resistance (Fig 17). However, the combination with HPβCD reduced this expression (–4%). GEM-resistant PDAC cells have an increased level of CE accumulation, indicative of a high ACAT1 expression (Li *et al.*, 2018). In more complex PDAC models, such as metastatic PDAC organoids, similar patterns of high ACAT1 expression and high CE levels are observed (Rebelo *et al.*, 2023). Suggesting that ACAT1 plays a key role in GEM resistance, and combination with HPβCD may reduce this resistance. Since decreased ACAT1 expression is associated with reduced PDAC cell proliferation *in vivo* (Li *et al.*, 2016), this explains the reduction in tumour volume seen when HPβCD was combined with GEM.

5.2.2 Cholesterol synthesis

The MP is overexpressed in human PDAC, as well as in PDAC mouse models (Oni *et al.*, 2020; Rebelo *et al.*, 2023). Targeting the MP as a novel treatment strategy in PDAC has shown conflicting results. The most common means to downregulate cholesterol biosynthesis is by HMGCR inhibition using statins. In PANC-1 cells, when HMGCR is inhibited by statins, it reduces proliferation and migration (Yuchuan Li *et al.*, 2023). The use of statins, to target HMGCR expression in PDAC, have only been beneficial to early stages of cancer in inhibiting cancer development (Rebelo *et al.*, 2023), but does not prove useful in the current clinical setting where patients already present with advanced stages of PDAC. The use of statins should be focused more on reducing the risk of PC instead of treating it (Rebelo *et al.*, 2023). Interestingly, exposure to statins induces a compensatory mechanism, whereby *HMGCR* gene expression is increased to counteract the inhibitory effect of statins on HMGCR. This mechanism, which upregulates *HMGCR* gene expression to re-balance cholesterol levels, also activates EMT pathways, thus, the use of statins has been linked to EMT activation (Rebelo *et al.*, 2023). Targeting HMGCR with statins also did not result in reduced tumour volume in PDAC xenografts established from patient derived cell line (Kubota *et al.*, 2024). However,

despite the overexpression of *HMGCR* observed in PDAC patients, it is not associated with a shorter survival (Rebelo *et al.*, 2023). HPβCD does not directly inhibit HMGCR, such as statins, therefore no significant change in HMGCR expression was observed with the HPβCD single treatment group (-2%) (Fig 12). Since FC is being depleted in the tumour cells by HPβCD, the expression of HMGCR is unchanged to compensate for the loss of FC by keeping the cholesterol synthesis pathway active. Although HPβCD alone did not largely affect HMGCR expression, when combined with 5-FU or GEM, it decreased HMGCR expression.

Interestingly, 5-FU monotherapy had no effect on cholesterol synthesis (±0%), but, the 5-FU & HPβCD combination treatment (-18%) reduced cholesterol synthesis (Fig 12), suggesting that the tumour cells have become less dependent on cholesterol synthesis due to the combination treatment. The cholesterol synthesis pathway enzymes, such as HMGCR and squalene epoxidase (SQLE), have been linked to 5-FU resistance in colorectal cancer (Liu *et al.*, 2024). However, there is limited evidence supporting this link in PDAC. One study showed that the combination of statins with 5-FU ultimately reversed 5-FU resistance in PANC-1 cells (Mistafa and Stenius, 2009). In this study, HPβCD might exert a similar effect, as seen from the decrease in HMGCR expression when combined with 5-FU, resensitizing the PANC-1 cells, as evidenced from the small tumour volume observed for 5-FU & HPβCD combination therapy (Fig 9).

GEM monotherapy (+35%) showed the highest HMGCR expression (Fig 17). It is evident in literature that HMGCR imparts GEM resistance by increasing its expression to enhance Tumour growth and metastasis, inducing a more aggressive phenotype (Qiu *et al.*, 2016; Göbel *et al.*, 2020). Targeting the cholesterol synthesis pathway has shown to decrease GEM resistance (X Wang *et al.*, 2017). When statins are combined with GEM, it reverses GEM resistance in PANC-1 cells (Mistafa and Stenius, 2009). However, in a clinical setting, the combination of statin with GEM did not improve patient outcome (Hong *et al.*, 2014). Although the combination with HPβCD did not reduce the risk of metastasis, HMGCR expression was decreased which is favourable in the context of PDAC to improve sensitivity to GEM, as evident in the reduced tumour volume exhibited by GEM & HPβCD combination treatment (Fig 9).

5.2.3 Cholesterol uptake

The uptake of cholesterol via LDLRs is favoured over cholesterol biosynthesis in PDAC since it requires less energy (Guillaumond *et al.*, 2015; Vasseur and Guillaumond, 2016). HPβCD increased the expression of PCSK9 (+37%) (Fig 17), and as a result, lowered LDLR expression (-11%) (Fig 17) due to its degradation in a PCSK9 dependent manner. It has been reported that HPβCD can increase PCSK9 levels as seen in intestinal epithelial cells (Leblond *et al.*, 2009). The increased PCSK9 expression is beneficial in this case since it targets LDLR for degradation (Rebelo *et al.*, 2023). It has been reported that HPβCD can reduce *LDLR* gene expression in human fibroblast cells (Gaspar *et al.*, 2017), and downregulates LDLR-related protein 1B in mice (Becktel *et al.*, 2022). Furthermore, it was shown that LDLR degradation results in the death of PC cells (Zhang *et al.*, 2022). Another reason for the decrease in LDLR levels observed in this study, could be that HPβCD has depleted the cholesterol available in the surrounding tissue of the tumour, as well as in serum (Appendix, Table A2). On the downside, PCSK9 is also involved in several other cancer related processes, such as invasion, growth, radiation resistance and tumour immunity (Liu *et al.*, 2020; Suh *et al.*, 2021; Alannan *et al.*, 2022; Wang *et al.*, 2024). PCSK9 has been identified as a biomarker for PC, since an increase in PCSK9 mRNA was directly correlated to shorter survival (Liu *et al.*, 2022). In pancreatic neuroendocrine tumours, siRNA knockdown of PCSK9 induced apoptosis, as well as inhibited invasion (Mahboobnia *et al.*, 2021). This indicates that the increase in PCSK9 expression caused by HPβCD is not necessarily favourable, since HPβCD monotherapy slightly increased tumour volume (+3%) and exhibited metastasis (Fig 9). In colorectal cancer mice models, an increase in PCSK9 proteins levels was associated with shorter survival (Rebelo *et al.*, 2023). Furthermore, other studies suggest that the function PCSK9 plays in cancer progression is more related to tumour immunity instead of its cholesterol regulating function (Liu *et al.*, 2020; Suh *et al.*, 2021; Alannan *et al.*, 2022; Wang *et al.*, 2024). To add another layer of complexity, PCSK9 can modulate the cholesterol supply in the TME through regulating LDLR expression, indirectly affecting tumour immunity, as a cholesterol rich TME negatively impacts immune surveillance (Xu *et al.*, 2021). The evidence on PCSK9 within literature and results from this study highlights a gap in the understanding of PCSK9 and its role in PDAC. Moreover, the inverse correlation between PCSK9 and LDLR, as observed for HPβCD, was not evident for 5-FU or GEM in either monotherapies or combination treatments.

Although LDLR has been implicated in 5-FU resistance, as evidenced in colorectal cancer cells that exhibit upregulated LDLR levels (Ortega Duran *et al.*, 2024), the 5-FU monotherapy

(–2%) (Fig 17) did not affect LDLR expression to a great extent. Interestingly, the combination therapy of 5-FU & HPβCD (–40%) (Fig 17) exhibits a substantial decrease in cholesterol uptake. This combination therapy approach, with HPβCD, may enhance the efficacy of 5-FU treatment in resistant PDAC, since this combination treatment resulted in the greatest tumour volume reduction (Fig 9). The downregulation of LDLR could potentially resensitize the cancer cells to 5-FU, offering a promising strategy to improve 5-FU response. No inverse relationship was observed between LDLR and PCSK9 expression, as PCSK9 expression was also decreased for 5-FU monotherapy (–19%) as well as the combination therapy of 5-FU & HPβCD (–36%) (Fig 17). This finding aligns with the hypothesis that PCSK9 may function beyond the cholesterol pathway, potentially targeting tumour immunity, as previously mentioned (Liu *et al.*, 2020; Suh *et al.*, 2021; Alannan *et al.*, 2022; Wang *et al.*, 2024). This observation supports the rationale for the improved response of PDAC tumours to 5-FU treatment. Similar findings were observed for GEM single and combination treatments.

Out of all treatment groups, GEM monotherapy showed the highest LDLR expression (+141%), which was reduced when combined with HPβCD (+22%) (Fig 17). Interference with LDLR endocytosis in PDAC results in changes to the balance between FC and CEs. This is amplified *in vivo* when treatment with GEM is introduced, where inhibition of LDLR increases GEM sensitivity (Guillaumond *et al.*, 2015). Suggesting that PDAC cells increase cholesterol uptake via LDLR as mechanism to gain resistance to GEM. Thus, HPβCD in the combination treatment may re-sensitize cells to GEM, since a decrease in LDLR reduces GEM resistance (Vasseur and Guillaumond, 2016). Likewise, PCSK9 expression was reduced when combining GEM with HPβCD (–20%) compared to GEM monotherapy (+13%) which showed an increase (Fig 17). Also aligning with the hypothesis regarding PCSK9's involvement in supressing the immune system, adding the tumour to evade immune response (Liu *et al.*, 2020; Suh *et al.*, 2021; Alannan *et al.*, 2022; Wang *et al.*, 2024). Analogous to the combination of HPβCD with 5-FU, its association with GEM may potentially reduce the tumour's ability to evade the immune system, consequently leading to an improved tumour response to GEM treatment. However, the role of HPβCD on PCSK9 in relation to tumour immunity remains unexplored, indicating a significant gap in the current research literature. Furthermore, there might be additional proteins involved in LDLR degradation and stability, which function independently of PCSK9. In addition to the unexpected results observed for PCSK9, the findings for SREBP2,

which governs the regulation of cholesterol synthesis and uptake processes, were also unanticipated.

5.2.4 SREBP2 mediated transcriptional regulation of cholesterol synthesis and uptake

SREBP2 has been linked to PC progression (Yu *et al.*, 2019). Given the observed decrease in cholesterol synthesis and uptake proteins (HMGCR and LDLR) for HPβCD, it was anticipated that SREBP2 would exhibit a corresponding decrease, as SREBP2 typically activates HMGCR and LDLR under normal conditions. Contrastingly, HPβCD did not decrease, but rather led to a significant increase in SREBP2 expression (+126%) (Fig 17). Research has shown that the FC pool inside the cell acts as a negative regulator of SREBP2 (Rebelo *et al.*, 2023). HPβCD's cholesterol-depleting action results in a decreased FC pool, activating the negative feedback loop and increasing SREBP2 expression. This suggests that the high SREBP2 expression observed is a compensatory mechanism to HPβCD's action. This effect has been observed in intestinal epithelial cells, where SREBP2 was upregulated as a result of HPβCD treatment (Leblond *et al.*, 2009), as well as in a mouse model of Niemann-pick-disease type C1 (Ebner *et al.*, 2018). Insufficient research has been conducted on the influence of alternative cyclodextrins on SREBP2 expression, and consequently, no definitive conclusions can be drawn. In addition to the negative feedback loop that activates SREBP2, the KRAS-induced PI3K pathway is also responsible for activating SREBP2 via mTORC1 (Wen *et al.*, 2018; Xiao *et al.*, 2023). Therefore, the significant increase in SREBP2 may be a combined result of both HPβCD and KRAS, possibly promoting cancer aggressiveness as evidenced from the presence of metastasis (Fig 9). Novel target genes of SREBP2 have recently been uncovered that extend beyond its known role in lipid biosynthesis regulation (Wen *et al.*, 2018), suggesting that SREBP2 is acting beyond the cholesterol pathway. Two mice in the HPβCD treatment group showed metastasis, which is a consequence of EMT (Fig 9). In lung and prostate cancer, SREBP2 has been shown to promote EMT by activating downstream transcription factors (Lethongsavarn *et al.*, 2021; F Zhang *et al.*, 2023). It has previously been shown that disrupting the cholesterol pathway upregulates TGF-β, a key EMT transcription factor, in an SREBP1 related manner (Gabitova-Cornell *et al.*, 2020). The data from this study might indicate that SREBP2 may also activate EMT transcription factors in PDAC. This was confirmed in the gene expression analysis data (Daya, 2024), where an increase in expression of *Snail* (one of several EMT transcription factors) upon treatment with HPβCD was observed (Appendix, Fig A1). SREBP2's potential role in activating EMT in PDAC could have significant implications

for understanding the progression and metastasis of this aggressive cancer type. Further investigation into the specific mechanisms by which SREBP2 might influence EMT in PDAC cells could reveal new therapeutic targets or prognostic markers. This finding may also suggest a broader involvement of cholesterol metabolism in PC development and progression, warranting additional research into the interplay between lipid homeostasis and cancer biology in PDAC. An example of an additional pathway that may be affected by SREBP2 is drug metabolism, as seen for 5-FU.

Monotherapy with 5-FU increased SREBP2 expression (+46%), and 5-FU & HPβCD combination treatment demonstrated a significant increase (+88%) (Fig 17), which also did not correspond to an increase in expression of synthesis nor uptake proteins. This observation suggests that similar to HPβCD monotherapy, SREBP2 is activating pathways beyond cholesterol metabolism. Interestingly, SREBP2 did not activate EMT to the same extent as in HPβCD monotherapy, since no metastasis was observed for these treatment groups (Fig 9). However, the gene expression studies indicate an increase in *Snail* expression when 5-FU was combined with HPβCD (Appendix, Fig A1), thus it might be due to gender that no metastasis was observed (as previously discussed). It is suggested that SREBP2 may be influencing alternative pathways in both 5-FU mono- and combination therapies. One such alternative pathway might be drug metabolism. The levels of enzymes crucial for 5-FU metabolism, particularly DPD and TS (Fig 3), play a vital role in determining how patients respond to treatment. SREBP2 might impact the expression of these enzymes, thus influencing 5-FU's pharmacodynamics. For example, high TS expression has been linked to unfavourable outcomes and 5-FU resistance in several cancer types, including urothelial carcinoma (Ide *et al.*, 2012; Narimatsu *et al.*, 2019). Thus, there might be an underlying mechanism by which SREBP2 influences drug metabolism to affect 5-FU treatment response. Furthermore, 5-FU might be counteracting the EMT-related effects induced by HPβCD. 5-FU influences the cell's translational machinery, affecting the processing of ribosomal and transfer RNA (Bash-Imam *et al.*, 2017). As a result, 5-FU may decrease the likelihood of HPβCD inducing an EMT phenotype, thereby not enhancing metastasis. However, additional research is needed to fully understand these anomalous results. In contrast to 5-FU, HPβCD might be inducing EMT when combined with GEM in an SREBP2-dependent manner.

The combined treatment of GEM & HPβCD (+90%) resulted in a notable upregulation of SREBP2 expression as compared to GEM monotherapy (+20%) (Fig 17). Again, this increase

did not correlate to enhanced HMGCR nor LDLR expression, indicating that SREBP2 might also trigger pathways that extend beyond cholesterol metabolism when exposed to GEM treatment. It is highly likely that SREBP2 is activating EMT related pathways, since metastasis was present for both GEM monotherapy and combination therapy with HPβCD (Fig 9). Although the low gene expression of *Snail* (Appendix, Fig A1) does not fully support this hypothesis, other transcription factors of EMT should also be considered, which was not addressed in this study. The network between SREBP2, EMT and GEM resistance is an emerging topic in PDAC. Cancer cells that exhibit resistance to GEM, upregulate their expression of EMT markers, which might also be influenced by SREBP2 (Lou *et al.*, 2012; Jin *et al.*, 2018). It is also important to take note of the connection between SREBP2 and cancer stem cells, of which, typically exhibit EMT characteristics. Research shows that SREBP2 takes part in sustaining cancer stem cell-like characteristics, potentially contributing to GEM-resistance (Yin *et al.*, 2011; Wei *et al.*, 2022). Lastly, to gain a comprehensive perspective of cholesterol homeostasis, the cholesterol efflux protein, ABCG1, was investigated.

5.2.5 Cholesterol efflux

HPβCD monotherapy increased cholesterol efflux via upregulating ABCG1 expression (+32%) and has the highest relative expression out of all treatment groups (Fig 17). It is well reported in literature that HPβCD increases cholesterol efflux via increasing the expression of ABCA1 and ABCG1 (Mitrofanova *et al.*, 2018; Mahjoubin-Tehran *et al.*, 2020; Becktel *et al.*, 2022; Zhu *et al.*, 2023). Similarly, other cyclodextrins, such as MβCD, also increase expression of ABCA1 and ABCG1 (Mahjoubin-Tehran *et al.*, 2020). Different effects, beneficial and non-beneficial, have been reported regarding the role that HPβCD plays in cholesterol efflux. HPβCD has been reported in literature to both increase and decrease ABCG1 expression, and it is suggested that this is dependent on HPβCD concentration. In breast cancer cells, HPβCD decreases cholesterol efflux via decreasing the expression of ABCG1 and ABCA1 (Zhao *et al.*, 2021; Saha *et al.*, 2023). This downregulation of ABCG1 observed was associated with a decrease in EMT (Zhao *et al.*, 2021). This suggests that HPβCD can contribute to EMT in a cholesterol efflux dependent manner. However, this effect was dependent on HPβCD concentration, with high concentrations (10 mmol/L) exerting a suppressive effect on EMT, and low concentrations (2 mmol/L) promoting EMT (Zhao *et al.*, 2021). Similar effects were observed in colon tumouroids, where cholesterol efflux promoted metastasis (Namba *et al.*, 2018). Contrasting to this, Saha *et al.* (2023) showed that the HPβCD-induced efflux of

cholesterol is favourable and resulted in reduced tumour volume in breast cancer (Saha *et al.*, 2023). Although there is a strong argument for the benefits of HPβCD-induced efflux of cholesterol, the majority of literature suggests that ABCG1-mediated cholesterol efflux is inversely related to cancer cell survival, and depleting ABCG1 results in tumour regression (Namba *et al.*, 2018; Zhao *et al.*, 2021; Yin *et al.*, 2022). This could suggest that the increase in ABCG1 observed in this study may be associated with an increase in EMT and could possibly explain why two mice in the HPβCD monotherapy treatment group had metastasis (Fig 9). In addition to cholesterol efflux, ABCG1 is also known to export drugs from cells and thus possibly contributes toward drug resistance (Yin *et al.*, 2022). To add another layer of complexity, increased ABCG1 expression is also known to upregulate SREBP2 expression, which was evident from our results (Tarling and Edwards, 2011). ABCG1 and its role in drug resistance is poorly studied and highlights a gap in PC research. The contradictory findings regarding ABCG1-mediated cholesterol efflux and its impact on cancer progression warrant further investigation. Examining the potential dual role of ABCG1 in both cholesterol efflux and drug export could provide valuable insights into developing targeted therapies for PC patients. For both 5-FU and GEM, the combination with HPβCD also exhibited increased cholesterol efflux.

ABCG1 expression was higher for the combination treatment of 5-FU & HPβCD (−10%) compared to 5-FU monotherapy (−22%), but still lower than that of HPβCD monotherapy (+32%) (Fig 17). Thus, the resulting increase may be attributed to HPβCD, and not 5-FU, since 5-FU decreased cholesterol efflux compared to the UN control (Fig 17). High intracellular cholesterol levels have been implicated in 5-FU resistance, since they can increase the expression of cholesterol efflux pumps, which can also contribute to drug efflux, thereby facilitating drug resistance (Wu *et al.*, 2015; Wang *et al.*, 2023). Surprisingly, the expression of ABCG1 expression for 5-FU monotherapy was lower than that of the untreated, whereas the combination of 5-FU with HPβCD resultingly increased (Fig 17). Research findings indicate that increased ABCG1 expression correlates with reduced responsiveness to 5-FU in colorectal cancer (Blondy *et al.*, 2020). This correlates with the findings for the tumour volumes (Fig 9), which did not exhibit significant reduction when 5-FU was combined with HPβCD. This lack of reduction may be attributed to the increased ABCG1 potentially effluxing the 5-FU drug itself rather than cholesterol (Yin *et al.*, 2022). Furthermore, it has also been reported that ABCG1 is elevated in glioblastoma cancer stem cells, further complicating 5-FU treatment

response (Chockalingam and Ghosh, 2013). In addition to the efflux of drugs, when ABCG1 increases cholesterol efflux, it promotes a cholesterol rich TME, which can contribute to resistance in the case of GEM.

It was hypothesized that a high intracellular FC level is favoured for GEM resistance, and thus the decreased expression of ABCG1 was expected for GEM monotherapy (−57%) (Fig 17). Indeed, this low expression is increased when GEM is combined with HPβCD (+7%). The upregulation of ABCG1 has been reported in several drug resistant cancers (Liao *et al.*, 2020; Po *et al.*, 2020). The elevation in cholesterol efflux from the tumour cells result in a cholesterol-rich TME, enhancing tumour immunity (Yin *et al.*, 2023), potentially further promoting GEM resistance in conjunction with possible increased drug efflux. This observation may contribute to the explanation for the occurrence of metastasis in both GEM monotherapy and combination therapy (Fig 9). From the results in this study, it is confirmed that cholesterol efflux plays an important role in conferring GEM resistance. However, cholesterol homeostasis in its entirety must be considered when deciphering the cause of drug resistance.

5.3 Conclusion

Cholesterol can be considered both a causative factor and a consequence of cancer. GEM monotherapy promoted the synthesis, uptake, and storage of cholesterol while suppressing the efflux of cholesterol (Fig 17), ultimately maintaining a high level of intracellular cholesterol and promoting oncogenesis. 5-FU monotherapy did not affect cholesterol storage, synthesis and uptake to the same extent as GEM (Fig 17), suggesting that cholesterol homeostatic pathways might contribute more towards GEM resistance than to 5-FU resistance. Using cholesterol depletion as monotherapy to treat PDAC, promoted a more metastatic phenotype. This is evidenced by the secondary tumours excised from mice in the HPβCD treatment group (Fig 9), as well as the increase in ABCG1 expression and significant upregulation of SREBP2 (Fig 17), potentially activating non-cholesterol-related pathways, and promoting invasiveness (Fig 18). Combining cholesterol depleting agent, HPβCD, with current first-line chemotherapeutic agents, 5-FU and GEM, yielded contrasting results. Firstly, when combined with GEM, HPβCD reduced tumour volume, but it did not mitigate the risk for metastasis (Fig 9), which may be attributed to the observed increase in SREBP2 and ABCG1 expression (Fig 17). Although it was thought that the resulting decrease in ACAT1, HMGCR and LDLR expression was favorable in GEM & HPβCD combination therapy (Fig 17), the presence of

metastasis (Fig 9) suggest that the tumour cells are channeling their energy away from cholesterol storage, uptake and synthesis and towards processes involved in metastasis. In contrast to GEM, when HPβCD was combined with 5-FU, it neither reduced tumour volume nor significantly enhanced the response to 5-FU. Interestingly, ABCG1 and SREBP2 expression was also upregulated due to HPβCD combination with 5-FU (Fig 17). In addition to promoting aggressiveness, literature suggest that SREBP2 and ABCG1 might be involved in decreased drug metabolism of 5-FU as well. Nonetheless, it can be concluded that GEM & 5-FU in combination with HPβCD does not significantly improve treatment response and combining it with strategies to target SREBP2 and ABCG1 may provide novel insights into drug resistance mechanisms in PDAC. It is evident that PDAC tumour cells appear to sense the targeting of their FC pool, activating the negative feedback loop to SREBP2 (Fig 18). Subsequently, PDAC tumour cells employ SREBP2 and ABCG1 to reallocate resources toward metastasis and drug efflux, rather than reestablishing cholesterol homeostasis (Fig 18). Taken together, the relationship between cholesterol homeostasis and drug resistance in PDAC is still an emerging area in cancer research. The findings from this study highlight the complex interplay between cholesterol balance and chemotherapy efficiency.

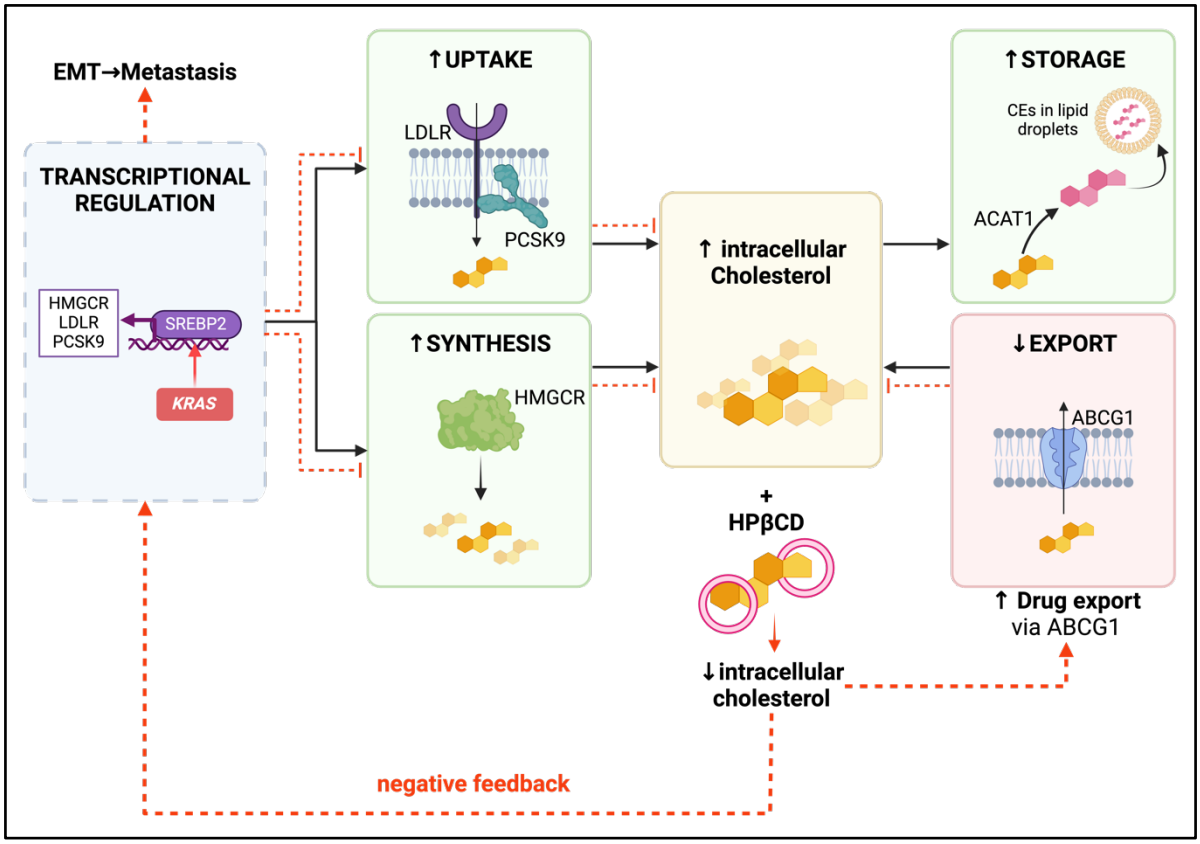


Figure 18: Visual summary on cholesterol depletion and PDAC tumour response

PDAC tumours maintain a high level of intracellular cholesterol. They achieve this through the *KRAS* oncogene, which increases synthesis (HMGCR) and uptake (LDLR and PCSK9) of cholesterol by upregulating their transcriptional regulation via SREBP2. The export of cholesterol via ABCG1 is decreased and the additional intracellular cholesterol is targeted for storage by ACAT1. When HPβCD is used as monotherapy, or in combination with 5-FU and GEM, the intracellular cholesterol pool is depleted. This activates a negative feedback loop to SREBP2. Rather than replenishing intracellular cholesterol levels, the PDAC tumour cells employ SREBP2 to activate metastatic pathways and utilize ABCG1 for drug export.

5.4 Limitations and future work

Xenograft study

It has been elucidated that mouse gender may have influenced treatment response, which imposed a limitation in this study since treatment groups were composed entirely of one gender, either male or female. In future animal studies, it is recommended that treatment groups should comprise of both male and female mice. This approach will mitigate any sex-based discrepancies and provide insight into the potential role of gender in treatment response. Additionally, a larger sample size is advised to minimize error due to individual mouse

variability. Given that the xenografts were derived from the PANC-1 cell line, the resultant tumours do not exhibit the same degree of heterogeneity as would be observed in human specimens. Mice also exhibit shorter lifespans and accelerated metabolic rates, presenting challenges in investigating the long-term effects of treatments and cancer progression.

Relative protein and gene expression

Given the hypothesis that SREBP2 may influence EMT pathways, it is recommended to investigate more proteins and genes involved in EMT, such as Vimentin, E-cadherin, Snail, and SMAD, utilizing Western blot analysis and RT-qPCR techniques. Furthermore, due to limited number of proteins that were investigated in this study, additional proteins and genes involved in cholesterol metabolism should be included for future studies, particularly ABCA1, LXR, SREBP1, SQLE, and CETP. In addition to protein expression studies in tissue, mouse serum samples can be further analysed for CETP, LDL and HDL as well as PCSK9 expression. This comprehensive approach will provide a more holistic insight into the mechanisms governing cholesterol metabolism and drug resistance.

5-FU solubility in DMSO

5-FU has limited aqueous solubility, thus vehicles are used to address this challenge (Abdrakhimova *et al.*, 2014). DMSO is used to improve 5-FU's dissolution rate and solubility, potentially enhancing absorption and therapeutic outcomes (Abdrakhimova *et al.*, 2014). Since DMSO is used to dissolve 5-FU, its possible influence on 5-FU function cannot be ignored. The DMSO vehicle control did not significantly reduce tumour volumes to that of the UN group (Appendix, Fig A2). However on average, it reduced by 13% as compared to UN, while 5-FU single treatment induced a 41% reduction (Appendix, Fig A2). DMSO's influence on 5-FU can be explained by its function as a solvent and its capacity to modify the drug's physicochemical characteristics, thus affecting its effectiveness. A key feature of DMSO's effect is its capacity to alter the solubility and stability of 5-FU. Enhanced dissolution in DMSO-based solutions can lead to improved body absorption and potentially more effective treatment outcomes for 5-FU. Furthermore, studies indicate that DMSO-water mixtures significantly impact the self-organization properties of 5-FU, potentially influencing its interactions with cell membranes and its uptake by cancerous cells (Ghosh *et al.*, 2022). The interaction between DMSO and 5-FU may also affect drug pharmacokinetics. Studies have shown that DMSO can influence the permeability of cellular membranes, potentially enhancing the cellular absorption of 5-FU (Sum and De Pablo, 2003). In addition to improving 5-FU

action, DMSO may also exert its own response on protein expression as seen from this study (Appendix Fig A4). The efficacy of DMSO as a cancer therapy remains controversial. While its primary use is as a solvent, DMSO exhibits various biological functions that could potentially contribute to anticancer effects. Several pharmaceutical properties of DMSO have been utilized in pre-clinical settings and include: anti-viral, anti-fungal, anti-bacterial, anti-inflammatory, local and systemic analgesia, as well as membrane permeability properties (Hoang *et al.*, 2022). Furthermore, DMSO can induce differentiation in cancer cells, which allows them to adopt a behaviour similar to normal cells with slow growth and reduced invasiveness (Hoang *et al.*, 2022). This corresponds with the data from this study where genes involved in multi-drug resistance and tumour suppression are upregulated and genes involved in metastasis are downregulated (Appendix, Fig A1). Confirming this, DMSO has demonstrated to induce the upregulation of tumour suppressors and reversing the effects of overactivated cell proliferative pathways in cancer, such as KRAS-activated PI3K pathways (Hoang *et al.*, 2022). Another study has suggested that DMSO can be implemented as an adjuvant in immunotherapy as it downregulated tumour immune evasion *in vivo* (Jiang *et al.*, 2016). This is further complemented by the reduced expression in PCSK9 exerted by DMSO in this study, which would result in reduced tumour immunity as discussed earlier (Appendix, Fig A3). Although DMSO possesses certain characteristics that could potentially aid in cancer treatment, its effectiveness as a standalone therapy is becoming a subject of debate. Additional research is necessary to elucidate its potential in cancer therapy and to develop appropriate protocols for its application.

6 TROUBLESHOOTING

6.1 Protein Extraction

Manual tissue lysis utilizing $N_2(\ell)$ was optimized to two iterations prior to proceeding with chemical lysis employing RIPA lysis buffer. Tissue sections from different regions of the tumour were combined and utilized to account for tissue structure and tumour heterogeneity. Tumour tissues exhibit spatial heterogeneity. The outer regions (periphery or invasive front) show aggressive growth, active proliferation, and increased angiogenesis due to better oxygenation and nutrient access. In contrast, the inner core is hypoxic and nutrient-deprived, leading to necrosis and slower cell proliferation. Furthermore, protein extraction was performed in a temperature controlled room (4°C) and samples were kept on ice during chemical lysis. This was to avoid degradation of tissue and preserve protein integrity.

6.2 Western Blots

The normalization step is the most critical in Western blots. The BCA assay was repeated several times to ensure accurate total protein quantification (where $R^2 > 0.9$ was accepted) before proceeding to the normalization step. The UN control group was normalized first, since the protein expression of other treatment groups would be expressed relative to the UN. Hereafter, the loading of all other treatment groups were normalized to that of the UN. Once samples were normalized, the relative expression of proteins were determined. Upon performing densitometry, band intensities were normalized to the loading control before relative expression compared to the UN was calculated. The transfer step in Western blots is often troublesome, which is why it was performed at 4°C to ensure consistent environmental conditions for each transfer. This approach helps maintain protein stability and reduces variability between experiments. This was necessary to ensure reliability of Western blots, since it was not feasible to perform a loading control with every experimental repeat once sample loading was normalized. In the cases where multiple bands were detected on blots, the SDS-PAGE gel was run for longer, to ensure better bands separation. However, when gels were run for too long, this caused smearing of bands, thus, the SDS-PAGE run time for each protein had to be optimized individually to achieve a balance between optimal band separation and band density. Multiple bands are frequently observed on Western blots when analysing xenograft tissues. This phenomenon is not uncommon and can be attributed to several factors inherent to the complexity of tissue samples. Xenograft tissues, being heterogeneous in nature, often contain a mixture of cell types and proteins at various stages of post-translational modification. This heterogeneity can lead to the detection of multiple bands representing different isoforms, splice variants, or modified versions of the target protein. Additionally, the presence of proteases in tissue samples may result in partial protein degradation, contributing to the appearance of multiple bands. While this can complicate interpretation, it is a well-recognized occurrence in Western blot analysis of tissue samples, particularly those derived from xenografts. Due to sample heterogeneity, some proteins proved more difficult to detect. To overcome this, a higher concentration was loaded for ABCG1 (50 μg/10 μL), SREBP2 (50 μg/10 μL) and LDLR (100 μg/10 μL).

7 REFERENCES

Abdrakhimova, G. S., Ovchinnikov, M. Y., Lobov, A. N., Spirikhin, L. V., Ivanov, S. P. and Khursan, S. L. (2014). '5-Fluorouracil solutions: NMR study of acid–base equilibrium in water and DMSO', *Journal of Physical Organic Chemistry*. John Wiley & Sons, Ltd, 27(11), pp. 876–883. doi: 10.1002/POC.3350.

Abdulla, N., Vincent, C. T. and Kaur, M. (2021). 'Mechanistic Insights Delineating the Role of Cholesterol in Epithelial Mesenchymal Transition and Drug Resistance in Cancer', *Frontiers in Cell and Developmental Biology*. Frontiers Media SA, 9. doi: 10.3389/FCELL.2021.728325.

Adamska, A. and Falasca, M. (2018). 'ATP-binding cassette transporters in progression and clinical outcome of pancreatic cancer: What is the way forward?', *World Journal of Gastroenterology*. Baishideng Publishing Group Inc, 24(29), p. 3222. doi: 10.3748/WJG.V24.I29.3222.

Aghevlian, S., Cai, Z., Hedley, D., Winnik, M. A. and Reilly, R. M. (2020). 'Radioimmunotherapy of PANC-1 human pancreatic cancer xenografts in NOD/SCID or NRG mice with Panitumumab labeled with Auger electron emitting, 111In or β-particle emitting, 177Lu', *EJNMMI Radiopharmacy and Chemistry*. Springer, 5(1). doi: 10.1186/S41181-020-00111-Y.

Ahmed, A., Köhler, S., Klotz, R., Giese, N., Hackert, T., Springfeld, C., Jäger, D. and Halama, N. (2023). 'Sex Differences in the Systemic and Local Immune Response of Pancreatic Cancer Patients', *Cancers*. Multidisciplinary Digital Publishing Institute (MDPI), 15(6). doi: 10.3390/cancers15061815.

Alannan, M., Fatrouni, H., Trézéguet, V., Dittrich-Domergue, F., Moreau, P., Siegfried, G., Liet, B., Khatib, A. M., Grosset, C. F., Badran, B., Fayyad-Kazan, H. and Merched, A. J. (2022). 'Targeting PCSK9 in Liver Cancer Cells Triggers Metabolic Exhaustion and Cell Death by Ferroptosis', *Cells 2023, Vol. 12, Page 62*. Multidisciplinary Digital Publishing Institute, 12(1), p. 62. doi: 10.3390/CELLS12010062.

Alshememry, A. K., Alsaleh, N. B., Alkhudair, N., Alzhrani, R. and Alshamsan, A. (2022). 'Recent nanotechnology advancements to treat multidrug-resistance pancreatic cancer: Pre-clinical and clinical overview', *Frontiers in Pharmacology*. Frontiers Media S.A., 13, p. 3329. doi: 10.3389/FPHAR.2022.933457/BIBTEX.

Amrutkar, M. and Gladhaug, I. P. (2017). 'Pancreatic cancer chemoresistance to gemcitabine', *Cancers*. MDPI AG. doi: 10.3390/cancers9110157.

Bash-Imam, Z., Thérizols, G., Vincent, A., Lafôrets, F., Espinoza, M. P., Pion, N., Macari, F., Pannequin, J., David, A., Saurin, J. C., Mertani, H. C., Textoris, J., Auboeuf, D., Catez, F., Venezia, N. D., Dutertre, M., Marcel, V. and Diaz, J. J. (2017). 'Translational reprogramming of colorectal cancer cells induced by 5-fluorouracil through a miRNA-dependent mechanism', *Oncotarget*. Oncotarget, 8(28), pp. 46219–46233. doi: 10.18632/ONCOTARGET.17597.

Becher, E. and Oertelt-Prigione, S. (2023). 'The Impact of Sex and Gender in Medicine and Pharmacology.', *Handbook of experimental pharmacology*, 282, pp. 3–23. doi: 10.1007/164_2023_688.

Becktel, D. A., Zbesko, J. C., Frye, J. B., Chung, A. G., Hayes, M., Calderon, K., Grover, J. W., Li, A., Garcia, F. G., Tavera-Garcia, M. A., Schnellmann, R. G., Wu, H. J. J., Nguyen, T. V. V. and Doyle, K. P. (2022). 'Repeated Administration of 2-Hydroxypropyl-b-Cyclodextrin (HPbCD) Attenuates the Chronic Inflammatory Response to Experimental Stroke', *Journal of Neuroscience*. Society for Neuroscience, 42(2), pp. 325–348. doi: 10.1523/JNEUROSCI.0933-21.2021.

Beer, M. C. de, Wroblewski, J. M., Noffsinger, V. P., Ji, A., Meyer, J. M., Westhuyzen, D. R. van der, Beer, F. C. de and Webb, N. R. (2013). 'The Impairment of Macrophage-to-Feces Reverse Cholesterol Transport during Inflammation Does Not Depend on Serum Amyloid A', *Journal of Lipids*. Wiley, 2013, pp. 1–11. doi: 10.1155/2013/283486.

Binenbaum, Y., Na'Ara, S. and Gil, Z. (2015). 'Gemcitabine resistance in pancreatic ductal adenocarcinoma', *Drug Resistance Updates*. Churchill Livingstone, 23, pp. 55–68. doi: 10.1016/J.DRUP.2015.10.002.

Bjånes, T. K., Jordheim, L. P., Schjøtt, J., Kamceva, T., Cros-Perrial, E., Langer, A., de Garibay, G. R., Kotopoulis, S., McCormack, E. and Riedel, B. (2020). 'Intracellular cytidine deaminase regulates gemcitabine metabolism in pancreatic cancer cell lines', *Drug Metabolism and Disposition*. American Society for Pharmacology and Experimental Therapy, 48(3), pp. 153–158. doi: 10.1124/DMD.119.089334/-/DC1.

Blondy, S., David, V., Verdier, M., Mathonnet, M., Perraud, A. and Christou, N. (2020). '5-Fluorouracil resistance mechanisms in colorectal cancer: From classical pathways to promising processes', *Cancer Science*. John Wiley & Sons, Ltd, 111(9), pp. 3142–3154. doi: 10.1111/CAS.14532.

Börner, A., Warnken, U., Schnölzer, M., Von Hagen, J., Giese, N., Bauer, A. and Hoheisel, J. D. (2009). 'Subcellular protein extraction from human pancreatic cancer tissues', *BioTechniques*, 46(4), pp. 297–304. doi: 10.2144/000113090.

Brown, M. B. and Forsythe, A. B. (1974). 'Robust Tests for the Equality of Variances', *Journal of the American Statistical Association*. JSTOR, 69(346), p. 364. doi: 10.2307/2285659.

Bytyçi, I., Penson, P. E., Mikhailidis, D. P., Wong, N. D., Hernandez, A. V., Sahebkar, A., Thompson, P. D., Mazidi, M., Rysz, J., Pella, D., Reiner, Ž., Toth, P. P. and Banach, M. (2022). 'Prevalence of statin intolerance: a meta-analysis', *European Heart Journal*. Oxford Academic, 43(34), pp. 3213–3223. doi: 10.1093/EURHEARTJ/EHAC015.

Calias, P. (2017). '2-Hydroxypropyl-β-cyclodextrins and the Blood-Brain Barrier: Considerations for Niemann-Pick Disease Type C1', *Current Pharmaceutical Design*. Bentham Science Publishers, 23(40), p. 6231. doi: 10.2174/1381612823666171019164220.

Di Carlo, C., Brandi, J. and Cecconi, D. (2018). 'Pancreatic cancer stem cells: Perspectives on potential therapeutic approaches of pancreatic ductal adenocarcinoma', *World Journal of Stem Cells*. Baishideng Publishing Group Inc, 10(11), p. 172. doi: 10.4252/WJSC.V10.I11.172.

Carrer, A., Trefely, S., Zhao, S., Campbell, S. L., Norgard, R. J., Schultz, K. C., Sidoli, S., Parris, J. L. D., Affronti, H. C., Sivanand, S., Egolf, S., Sela, Y., Trizzino, M., Gardini, A., Garcia, B. A., Snyder, N. W., Stanger, B. Z. and Wellen, K. E. (2019). 'Acetyl-CoA

Metabolism Supports Multistep Pancreatic Tumorigenesis', *Cancer discovery*. Cancer Discov, 9(3), pp. 416–435. doi: 10.1158/2159-8290.CD-18-0567.

Chockalingam, S. and Ghosh, S. S. (2013). 'Amelioration of Cancer Stem Cells in Macrophage Colony Stimulating Factor-Expressing U87MG-Human Glioblastoma upon 5-Fluorouracil Therapy', *PLOS ONE*. Public Library of Science, 8(12), p. e83877. doi: 10.1371/JOURNAL.PONE.0083877.

Ciccolini, J., Serdjebi, C., Peters, G. J. and Giovannetti, E. (2016). 'Pharmacokinetics and pharmacogenetics of Gemcitabine as a mainstay in adult and pediatric oncology: an EORTC-PAMM perspective', *Cancer Chemotherapy and Pharmacology*. Springer Verlag. doi: 10.1007/s00280-016-3003-0.

Cortés-Ríos, J., Zárate, A. M., Figueroa, J. D., Medina, J., Fuentes-Lemus, E., Rodríguez-Fernández, M., Aliaga, M. and López-Alarcón, C. (2020). 'Protein quantification by bicinchoninic acid (BCA) assay follows complex kinetics and can be performed at short incubation times', *Analytical Biochemistry*. Academic Press, 608, p. 113904. doi: 10.1016/J.AB.2020.113904.

Cros, J., Raffenne, J., Couvelard, A. and Poté, N. (2018). 'Tumor Heterogeneity in Pancreatic Adenocarcinoma', *Pathobiology : journal of immunopathology, molecular and cellular biology*. Pathobiology, 85(1–2), pp. 64–71. doi: 10.1159/000477773.

Cruz, A. L. S., Barreto, E. de A., Fazolini, N. P. B., Viola, J. P. B. and Bozza, P. T. (2020). 'Lipid droplets: platforms with multiple functions in cancer hallmarks', *Cell Death & Disease 2020 11:2*. Nature Publishing Group, 11(2), pp. 1–16. doi: 10.1038/s41419-020-2297-3.

Cruz, P. M. R., Mo, H., McConathy, W. J., Sabnis, N. and Lacko, A. G. (2013). 'The role of cholesterol metabolism and cholesterol transport in carcinogenesis: A review of scientific findings, relevant to future cancer therapeutics', *Frontiers in Pharmacology*. Frontiers, 4 SEP, p. 119. doi: 10.3389/FPHAR.2013.00119/BIBTEX.

Dagogo-Jack, I. and Shaw, A. T. (2017). 'Tumour heterogeneity and resistance to cancer therapies', *Nature Reviews Clinical Oncology 2017 15:2*. Nature Publishing Group, 15(2), pp. 81–94. doi: 10.1038/nrclinonc.2017.166.

Daya, T. (2024). *Investigating the effects of cholesterol-depletory agent, 2-hydroxypropyl-beta-cyclodextrin, on Pancreatic Cancer and drug resistance in vitro and in vivo.* PhD thesis. University of the Witwatersrand.

Deer, E. L., González-Hernández, J., Coursen, J. D., Shea, J. E., Ngatia, J., Scaife, C. L., Firpo, M. A. and Mulvihill, S. J. (2010). 'Phenotype and Genotype of Pancreatic Cancer Cell Lines', *Pancreas*. NIH Public Access, 39(4), p. 425. doi: 10.1097/MPA.0B013E3181C15963.

Dittmer, A. and Dittmer, J. (2006). 'Beta-actin is not a reliable loading control in Western blot analysis', *Electrophoresis*. Electrophoresis, 27(14), pp. 2844–2845. doi: 10.1002/ELPS.200500785.

Di Donato, C., Lavorgna, M., Fattorusso, R., Isernia, C., Isidori, M., Malgieri, G., Piscitelli, C., Russo, C., Russo, L. and Iacovino, R. (2016). 'Alpha- and beta-cyclodextrin inclusion complexes with 5-fluorouracil: Characterization and cytotoxic activity evaluation', *Molecules*. MDPI AG, 21(12). doi: 10.3390/molecules21121644.

Duan, X., Zhang, T., Feng, L., de Silva, N., Greenspun, B., Wang, X., Moyer, J., Martin, M. L., Chandwani, R., Elemento, O., Leach, S. D., Evans, T., Chen, S. and Pan, F. C. (2024). 'A pancreatic cancer organoid platform identifies an inhibitor specific to mutant KRAS', *Cell Stem Cell*. Cell Press, 31(1), pp. 71-88.e8. doi: 10.1016/J.STEM.2023.11.011.

Dunnett, C. W. (1955). 'A Multiple Comparison Procedure for Comparing Several Treatments with a Control', *Journal of the American Statistical Association*. JSTOR, 50(272), p. 1096. doi: 10.2307/2281208.

Duvivier, L., Gerard, L., Diaz, A. and Gillet, J. P. (2024). 'Linking ABC transporters to the hallmarks of cancer', *Trends in Cancer*. Cell Press, pp. 124–134. doi: 10.1016/j.trecan.2023.09.013.

Ebner, L., Gläser, A., Bräuer, A., Witt, M., Wree, A., Rolfs, A., Frank, M., Vollmar, B. and Kuhla, A. (2018). 'Evaluation of two liver treatment strategies in a mouse model of niemann–pick-disease type C1', *International Journal of Molecular Sciences*. MDPI AG, 19(4). doi: 10.3390/ijms19040972.

Elander, N. O., Aughton, K., Ghaneh, P., Neoptolemos, J. P., Palmer, D. H., Cox, T. F., Campbell, F., Costello, E., Halloran, C. M., Mackey, J. R., Scarfe, A. G., Valle, J. W., McDonald, A. C., Carter, R., Tebbutt, N. C., Goldstein, D., Shannon, J., Dervenis, C., Glimelius, B., Deakin, M., Charnley, R. M., Anthoney, A., Lerch, M. M., Mayerle, J., Oláh, A., Büchler, M. W. and Greenhalf, W. (2018). 'Expression of dihydropyrimidine dehydrogenase (DPD) and hENT1 predicts survival in pancreatic cancer', *British Journal of Cancer*. Nature Publishing Group, 118(7), pp. 947–954. doi: 10.1038/s41416-018-0004-2.

El-Darzi, N., Mast, N., Hammer, S. S., Dorweiler, T. F., Busik, J. V. and Pikuleva, I. A. (2023). '2-Hydroxypropyl-β-cyclodextrin mitigates pathological changes in a mouse model of retinal cholesterol dyshomeostasis', *Journal of Lipid Research*. American Society for Biochemistry and Molecular Biology Inc., 64(2). doi: 10.1016/j.jlr.2022.100323.

El-Darzi, N., Mast, N., Petrov, A. M. and Pikuleva, I. A. (2021). '2-Hydroxypropyl-β-cyclodextrin reduces retinal cholesterol in wild-type and Cyp27a1−/−Cyp46a1−/− mice with deficiency in the oxysterol production', *British Journal of Pharmacology*. John Wiley & Sons, Ltd, 178(16), pp. 3220–3234. doi: 10.1111/BPH.15209.

Espiau-Romera, P., Courtois, S., Parejo-Alonso, B. and Sancho, P. (2020). 'Molecular and Metabolic Subtypes Correspondence for Pancreatic Ductal Adenocarcinoma Classification', *Journal of Clinical Medicine*. Multidisciplinary Digital Publishing Institute (MDPI), 9(12), pp. 1–21. doi: 10.3390/JCM9124128.

Feng, Z., Yang, C., Zhang, Y., Li, H., Fang, W., Wang, Junhua, Nie, Y., Wang, C.-Y., Liu, Z., Jiang, Z., Wang, Junjian and Wang, Y. (2023). 'Structure-Based Design and Characterization of the Highly Potent and Selective Covalent Inhibitors Targeting the Lysine Methyltransferases G9a/GLP.', *Journal of medicinal chemistry*, 66(12), pp. 8086–8102. doi: 10.1021/acs.jmedchem.3c00411.

Fidai, S. S., Sharma, A. E., Johnson, D. N., Segal, J. P. and Lastra, R. R. (2018). 'Dihydropyrimidine dehydrogenase deficiency as a cause of fatal 5-Fluorouracil toxicity', *Autopsy and Case Reports*. Editora Cubo Multimidia, 8(4). doi: 10.4322/acr.2018.049.

Gabitova-Cornell, L., Surumbayeva, A., Peri, S., Franco-Barraza, J., Restifo, D., Weitz, N., Ogier, C., Goldman, A. R., Hartman, T. R., Francescone, R., Tan, Y., Nicolas, E., Shah, N., Handorf, E. A., Cai, K. Q., O'Reilly, A. M., Sloma, I., Chiaverelli, R., Moffitt, R. A., Khazak, V., Fang, C. Y., Golemis, E. A., Cukierman, E. and Astsaturov, I. (2020). 'Cholesterol Pathway Inhibition Induces TGF-β Signaling to Promote Basal Differentiation in Pancreatic Cancer', *Cancer Cell*. Cell Press, 38(4), pp. 567-583.e11. doi: 10.1016/J.CCELL.2020.08.015.

Gams, A., Nevarez, A., Perkail, S., Venegas, A., George, S. A., Efimova, T. and Efimov, I. R. (2023). 'Evidence of sex differences in cancer-related cardiac complications in mouse models of pancreatic and liver cancer', *Physiological Reports*. American Physiological Society, 11(8). doi: 10.14814/phy2.15672.

Ganjali Koli, M. and Fogolari, F. (2023). 'Exploring the role of cyclodextrins as a cholesterol scavenger: a molecular dynamics investigation of conformational changes and thermodynamics', *Scientific Reports*. Nature Research, 13(1). doi: 10.1038/s41598-023-49217-8.

Gaspar, J., Mathieu, J. and Alvarez, P. (2017). '2-Hydroxypropyl-beta-cyclodextrin (HPβCD) reduces age-related lipofuscin accumulation through a cholesterol-associated pathway', *Scientific Reports*. Nature Publishing Group, 7(1). doi: 10.1038/s41598-017-02387-8.

Ghosh, M., Layek, S., Bera, N., Nandi, P. K., Hazra, R. and Sarkar, N. (2022). 'Modulation of the Photophysics of Nucleotide-Functionalized Copper Nanoclusters Using Aqueous Binary Mixtures', *Journal of Physical Chemistry C*. American Chemical Society, 126(50), pp. 21319–21327. doi: 10.1021/ACS.JPCC.2C07074/SUPPL_FILE/JP2C07074_SI_001.PDF.

Giacomini, I., Gianfanti, F., Desbats, M. A., Orso, G., Berretta, M., Prayer-Galetti, T., Ragazzi, E. and Cocetta, V. (2021). 'Cholesterol Metabolic Reprogramming in Cancer and Its Pharmacological Modulation as Therapeutic Strategy', *Frontiers in Oncology*. Frontiers Media S.A., 11, p. 1946. doi: 10.3389/FONC.2021.682911/BIBTEX.

Gillette, W. K., Esposito, D., Abreu Blanco, M., Alexander, P., Bindu, L., Bittner, C., Chertov, O., Frank, P. H., Grose, C., Jones, J. E., Meng, Z., Perkins, S., Van, Q., Ghirlando, R., Fivash, M., Nissley, D. V., McCormick, F., Holderfield, M. and Stephen, A. G. (2015). 'Farnesylated and methylated KRAS4b: high yield production of protein suitable for biophysical studies of prenylated protein-lipid interactions', *Scientific Reports 2015 5:1*. Nature Publishing Group, 5(1), pp. 1–13. doi: 10.1038/srep15916.

Göbel, A., Rauner, M., Hofbauer, L. C. and Rachner, T. D. (2020). 'Cholesterol and beyond - The role of the mevalonate pathway in cancer biology', *Biochimica et Biophysica Acta (BBA) - Reviews on Cancer*. Elsevier, 1873(2), p. 188351. doi: 10.1016/J.BBCAN.2020.188351.

Gould, S. E., Junttila, M. R. and De Sauvage, F. J. (2015). 'Translational value of mouse models in oncology drug development', *Nature Medicine 2015 21:5*. Nature Publishing Group, 21(5), pp. 431–439. doi: 10.1038/nm.3853.

Gradiz, R., Silva, H. C., Carvalho, L., Botelho, M. F. and Mota-Pinto, A. (2016). 'MIA PaCa-2 and PANC-1 – pancreas ductal adenocarcinoma cell lines with neuroendocrine differentiation and somatostatin receptors', *Scientific Reports*. Nature Publishing Group, 6. doi: 10.1038/SREP21648.

Grant, T. J., Hua, K. and Singh, A. (2016). 'Molecular Pathogenesis of Pancreatic Cancer', *Progress in molecular biology and translational science*. NIH Public Access, 144, p. 241. doi: 10.1016/BS.PMBTS.2016.09.008.

Grasso, C., Jansen, G. and Giovannetti, E. (2017). 'Drug resistance in pancreatic cancer: Impact of altered energy metabolism', *Critical Reviews in Oncology/Hematology*. Elsevier, 114, pp. 139–152. doi: 10.1016/J.CRITREVONC.2017.03.026.

Gu, L., Saha, S. T., Thomas, J. and Kaur, M. (2019). 'Targeting cellular cholesterol for anticancer therapy', *The FEBS Journal*. John Wiley & Sons, Ltd, 286(21), pp. 4192–4208. doi: 10.1111/FEBS.15018.

Guillaumond, F., Bidaut, G., Ouaissi, M., Servais, S., Gouirand, V., Olivares, O., Lac, S., Borge, L., Roques, J., Gayet, O., Pinault, M., Guimaraes, C., Nigri, J., Loncle, C., Lavaut, M. N., Garcia, S., Tailleux, A., Staels, B., Calvo, E., Tomasini, R., Iovanna, J. L. and Vasseur, S. (2015). 'Cholesterol uptake disruption, in association with chemotherapy, is a promising combined metabolic therapy for pancreatic adenocarcinoma', *Proceedings of the National Academy of Sciences of the United States of America*. National Academy of Sciences, 112(8), pp. 2473–2478. doi: 10.1073/PNAS.1421601112/-/DCSUPPLEMENTAL.

Hastings, C., Liu, B., Hurst, B., Cox, G. F. and Hrynkow, S. (2022). 'Intravenous 2-hydroxypropyl-β-cyclodextrin (Trappsol® CycloTM) demonstrates biological activity and impacts cholesterol metabolism in the central nervous system and peripheral tissues in adult subjects with Niemann-Pick Disease Type C1: Results of a phase 1 trial', *Molecular Genetics and Metabolism*. Academic Press, 137(4), pp. 309–319. doi: 10.1016/J.YMGME.2022.10.004.

He, Ji, Bugde, P., Li, J., Biswas, R., Li, S., Yang, X., Tian, F., Wu, Z. and Li, Y. (2024). 'Multidrug resistance protein 5 affects cell proliferation, migration and gemcitabine sensitivity in pancreatic cancer MIA Paca-2 and PANC-1 cells', *Oncology Reports*. Spandidos Publications, 51(1). doi: 10.3892/or.2023.8666.

He, Jingang, Dai, Y., Zhong, J., Liu, X. and Qin, X. (2024). 'Difference in the complexation of cholesterol with β-cyclodextrin derivatives: A combined theoretical and experimental study', *Food Chemistry*. Elsevier, 435, p. 137459. doi: 10.1016/J.FOODCHEM.2023.137459.

Hermann, P. C. and Sainz, B. (2018). 'Pancreatic cancer stem cells: A state or an entity?', *Seminars in Cancer Biology*. Academic Press, 53, pp. 223–231. doi: 10.1016/J.SEMCANCER.2018.08.007.

Hoang, B. X., Han, B., Fang, W. H., Tran, H. D., Hoang, C., Shaw, D. G. and Nguyen, T. Q. (2022). 'The Rationality of Implementation of Dimethyl Sulfoxide as Differentiation-inducing Agent in Cancer Therapy', *Cancer Diagnosis & Prognosis*. Anticancer Research USA Inc., 3(1), pp. 1–8. doi: 10.21873/cdp.10172.

Hong, J. Y., Nam, E. M., Lee, J., Park, J. O., Lee, S. C., Song, S. Y., Choi, S. H., Heo, J. S., Park, S. H., Lim, H. Y., Kang, W. K. and Park, Y. S. (2014). 'Randomized double-blinded,

placebo-controlled phase II trial of simvastatin and gemcitabine in advanced pancreatic cancer patients', *Cancer chemotherapy and pharmacology*. Cancer Chemother Pharmacol, 73(1), pp. 125–130. doi: 10.1007/S00280-013-2328-1.

Houben, T., Yadati, T., de Kruijf, R., Gijbels, M. J. J., Luiken, J. J. F. P., van Zandvoort, M., Kapsokalyvas, D., Lütjohann, D., Westerterp, M., Plat, J., Leake, D. and Shiri-Sverdlov, R. (2021). 'Pro-Inflammatory Implications of 2-Hydroxypropyl-β-cyclodextrin Treatment', *Frontiers in Immunology*. Frontiers Media S.A., 12, p. 3175. doi: 10.3389/FIMMU.2021.716357/BIBTEX.

Hu, H. feng, Ye, Z., Qin, Y., Xu, X. wu, Yu, X. jun, Zhuo, Q. feng and Ji, S. rong (2021). 'Mutations in key driver genes of pancreatic cancer: molecularly targeted therapies and other clinical implications', *Acta Pharmacologica Sinica 2021 42:11*. Nature Publishing Group, 42(11), pp. 1725–1741. doi: 10.1038/s41401-020-00584-2.

Hu, H., Gu, Y., Qian, Y., Hu, B., Zhu, C., Wang, G. and Li, J. (2014). 'DNA-PKcs is important for Akt activation and gemcitabine resistance in PANC-1 pancreatic cancer cells', *Biochemical and Biophysical Research Communications*. Academic Press, 452(1), pp. 106–111. doi: 10.1016/J.BBRC.2014.08.059.

Huang, B., Song, B. liang and Xu, C. (2020). 'Cholesterol metabolism in cancer: mechanisms and therapeutic opportunities', *Nature Metabolism 2020 2:2*. Nature Publishing Group, 2(2), pp. 132–141. doi: 10.1038/S42255-020-0174-0.

Hudson, W. A., Li, Q., Le, C. and Kersey, J. H. (1998). 'Xenotransplantation of human lymphoid malignancies is optimized in mice with multiple immunologic defects', *Leukemia 1998 12:12*. Nature Publishing Group, 12(12), pp. 2029–2033. doi: 10.1038/sj.leu.2401236.

Hyun, J. J., Lee, H. S., Kim, K. S., Kim, Y. K., Yoon, D. and Sahng, W. P. (2008). 'Sterol-dependent regulation of proprotein convertase subtilisin/kexin type 9 expression by sterol-regulatory element binding protein-2', *Journal of lipid research*. J Lipid Res, 49(2), pp. 399–409. doi: 10.1194/JLR.M700443-JLR200.

Iacobazzi, R. M., Cutrignelli, A., Stefanachi, A., Porcelli, L., Lopedota, A. A., Di Fonte, R., Lopalco, A., Serratì, S., Laquintana, V., Silvestris, N., Franco, M., Cellamare, S., Leonetti, F., Azzariti, A. and Denora, N. (2020). 'Hydroxy-propil-β-cyclodextrin inclusion complexes of two biphenylnicotinamide derivatives: Formulation and anti-proliferative activity evaluation in pancreatic cancer cell models', *International Journal of Molecular Sciences*. MDPI AG, 21(18), pp. 1–14. doi: 10.3390/ijms21186545.

Ide, H., Kikuchi, E., Hasegawa, M., Kozakai, N., Kosaka, T., Miyajima, A. and Oya, M. (2012). 'Prognostic significance of 5-fluorouracil metabolism-relating enzymes and enhanced chemosensitivity to 5-fluorouracil by 5-chloro 2,4-dihydroxy-pyridine in urothelial carcinoma', *BMC Cancer*, 12. doi: 10.1186/1471-2407-12-420.

Islam, M. S., Aryasomayajula, A. and Selvaganapathy, P. R. (2017). 'A Review on Macroscale and Microscale Cell Lysis Methods', *Micromachines*. Multidisciplinary Digital Publishing Institute (MDPI), 8(3). doi: 10.3390/MI8030083.

Jiang, Z., Zhang, H., Wang, Y., Yu, B., Wang, C., Liu, C., Lu, J., Chen, F., Wang, M., Yu, X., Lin, J., Pan, X., Wang, P. and Zhu, H. (2016). 'Altered Hepa1-6 cells by dimethyl sulfoxide (DMSO)-treatment induce anti-tumor immunity in vivo', *Oncotarget*. Impact Journals, LLC, 7(8), p. 9340. doi: 10.18632/ONCOTARGET.7009.

Jin, H., Zhao, Y., Zhang, S., Yang, J., Zhang, X. and Ma, S. (2018). 'Hyperthermia inhibits the motility of gemcitabine-resistant pancreatic cancer PANC-1 cells through the inhibition of epithelial-mesenchymal transition', *Molecular Medicine Reports*. Spandidos Publications, 17(5), pp. 7274–7280. doi: 10.3892/mmr.2018.8763.

Kamitani, N., Nakamae, I., Yoneda-Kato, N., Kato, J. ya and Sho, M. (2022). 'Preclinical evaluation of pentagamavunone-1 as monotherapy and combination therapy for pancreatic cancer in multiple xenograft models', *Scientific Reports 2022 12:1*. Nature Publishing Group, 12(1), pp. 1–16. doi: 10.1038/s41598-022-26863-y.

Kanagaki, S., Suezawa, T., Moriguchi, K., Nakao, K., Toyomoto, M., Yamamoto, Y., Murakami, K., Hagiwara, M. and Gotoh, S. (2021). 'Hydroxypropyl cyclodextrin improves amiodarone-induced aberrant lipid homeostasis of alveolar cells', *American Journal of*

Respiratory Cell and Molecular Biology. American Thoracic Society, 64(4), pp. 504–514. doi: 10.1165/rcmb.2020-0119OC.

Kang, G., Hu, M., Ren, H., Wang, J., Cheng, X., Li, R., Yuan, B., Balan, Y., Bai, Z. and Huang, H. (2021). 'VHH212 nanobody targeting the hypoxia-inducible factor 1α suppresses angiogenesis and potentiates gemcitabine therapy in pancreatic cancer in vivo', *Cancer Biology and Medicine*. Cancer Biology and Medicine, 18(3), pp. 772–787. doi: 10.20892/j.issn.2095-3941.2020.0568.

Kano, M. T., Kokuryo, T., Baba, T., Yamazaki, K., Yamaguchi, J., Sunagawa, M., Ogura, A., Watanabe, N., Onoe, S., Miyata, K., Mizuno, T., Uehara, K., Igami, T., Yokoyama, Y., Ebata, T. and Nagino, M. (2023). 'Cyclodextrin Conjugated α-Bisabolol Suppresses FAK Phosphorylation and Induces Apoptosis in Pancreatic Cancer', *Anticancer Research*. International Institute of Anticancer Research, 43(3), pp. 1009–1016. doi: 10.21873/anticanres.16245.

Kaoutari, A. El, Fraunhoffer, N. A., Hoare, O., Teyssedou, C., Soubeyran, P., Gayet, O., Roques, J., Lomberk, G., Urrutia, R., Dusetti, N. and Iovanna, J. (2021). 'Metabolomic profiling of pancreatic adenocarcinoma reveals key features driving clinical outcome and drug resistance', *EBioMedicine*. Elsevier, 66, p. 103332. doi: 10.1016/J.EBIOM.2021.103332.

Karatani, H. (2022). 'Luminol–hydrogen peroxide–horseradish peroxidase chemiluminescence intensification by kosmotrope ammonium sulfate', *Analytical Sciences*. Springer, 38(3), p. 613. doi: 10.1007/S44211-022-00069-8.

Karlic, H. and Varga, F. (2019). 'Mevalonate Pathway', *Encyclopedia of Cancer*. Academic Press, pp. 445–457. doi: 10.1016/B978-0-12-801238-3.65000-6.

Keane, T. J., Saldin, L. T. and Badylak, S. F. (2016). 'Decellularization of mammalian tissues: Preparing extracellular matrix bioscaffolds', *Characterisation and Design of Tissue Scaffolds*. Woodhead Publishing, pp. 75–103. doi: 10.1016/B978-1-78242-087-3.00004-3.

Kim, S., Lee, J. Y., Park, E. J., Ahn, Y. D., Cheon, Y., Sim, W. and Lee, H. J. (2024). 'Tumor suppression effect of ultrasound-sensitive nanoparticles with focused ultrasound in a pancreas

cancer xenograft model', *European Radiology Experimental*. Springer Science and Business Media Deutschland GmbH, 8(1). doi: 10.1186/s41747-024-00436-2.

Kimmelman, A. C. (2015). 'Metabolic Dependencies in RAS-Driven Cancers', *Clinical Cancer Research*. American Association for Cancer Research, 21(8), pp. 1828–1834. doi: 10.1158/1078-0432.CCR-14-2425.

King, R. J., Singh, P. K. and Mehla, K. (2022). 'The cholesterol pathway: impact on immunity and cancer', *Trends in Immunology*. Elsevier Current Trends, 43(1), pp. 78–92. doi: 10.1016/J.IT.2021.11.007.

Klein, A. P. (2021). 'Pancreatic cancer epidemiology: understanding the role of lifestyle and inherited risk factors', *Nature Reviews Gastroenterology and Hepatology*. Nature Research, pp. 493–502. doi: 10.1038/s41575-021-00457-x.

Kobayashi, Y., Ohshiro, N., Sakai, R., Ohbayashi, M., Kohyama, N. and Yamamoto, T. (2010). 'Transport mechanism and substrate specificity of human organic anion transporter 2 (hOat2 [SLC22A7])', *Journal of Pharmacy and Pharmacology*. Oxford Academic, 57(5), pp. 573–578. doi: 10.1211/0022357055966.

Koltai, T., Reshkin, S. J., Carvalho, T. M. A., Di Molfetta, D., Greco, M. R., Alfarouk, K. O. and Cardone, R. A. (2022). 'Resistance to Gemcitabine in Pancreatic Ductal Adenocarcinoma: A Physiopathologic and Pharmacologic Review', *Cancers*. Multidisciplinary Digital Publishing Institute (MDPI), 14(10). doi: 10.3390/CANCERS14102486.

Komori, S., Osada, S. and Yoshida, K. (2011). 'Novel Strategy with Gemcitabine for Advanced Pancreatic Cancer', *ISRN Oncology*. Wiley, 2011, pp. 1–5. doi: 10.5402/2011/936893.

Kong, K., Guo, M., Liu, Y. and Zheng, J. (2020). 'Progress in Animal Models of Pancreatic Ductal Adenocarcinoma', *Journal of Cancer*. Ivyspring International Publisher, 11(6), p. 1555. doi: 10.7150/JCA.37529.

Kong, R., Qian, X. and Ying, W. (2022). 'Pancreatic cancer cells spectral library by DIA-MS and the phenotype analysis of gemcitabine sensitivity', *Scientific Data*, 9(1), p. 283. doi: 10.1038/s41597-022-01407-1.

Kubota, C. S., Myers, S. L., Seppälä, T. T., Burkhart, R. A. and Espenshade, P. J. (2024). 'In vivo CRISPR screening identifies geranylgeranyl diphosphate as a pancreatic cancer tumor growth dependency', *Molecular Metabolism*, 85, p. 101964. doi: 10.1016/j.molmet.2024.101964.

Kumar, N. and Mandal, C. C. (2021). 'Cholesterol-Lowering Drugs on Akt Signaling for Prevention of Tumorigenesis', *Frontiers in Genetics*. Frontiers Media S.A., 12, p. 1706. doi: 10.3389/FGENE.2021.724149/BIBTEX.

Kurata, N., Fujita, H., Ohuchida, K., Mizumoto, K., Mahawithitwong, P., Sakai, H., Onimaru, M., Manabe, T., Ohtsuka, T. and Tanaka, M. (2011). 'Predicting the chemosensitivity of pancreatic cancer cells by quantifying the expression levels of genes associated with the metabolism of gemcitabine and 5-fluorouracil', *International Journal of Oncology*, 39(2), pp. 473–482. doi: 10.3892/ijo.2011.1058.

Kuzu, O. F., Noory, M. A. and Robertson, G. P. (2016). 'The role of cholesterol in cancer', *Cancer research*. NIH Public Access, 76(8), p. 2063. doi: 10.1158/0008-5472.CAN-15-2613.
Laemmli, U. K. (1970). 'Cleavage of structural proteins during the assembly of the head of bacteriophage T4', *Nature*. Nature, 227(5259), pp. 680–685. doi: 10.1038/227680A0.

Lai, X., Li, Q., Wu, F., Lin, J., Chen, J., Zheng, H. and Guo, L. (2020). 'Epithelial-Mesenchymal Transition and Metabolic Switching in Cancer: Lessons From Somatic Cell Reprogramming', *Frontiers in Cell and Developmental Biology*. Frontiers Media S.A., 8, p. 760. doi: 10.3389/FCELL.2020.00760/BIBTEX.

Laka, K., Makgoo, L. and Mbita, Z. (2022). 'Cholesterol-Lowering Phytochemicals: Targeting the Mevalonate Pathway for Anticancer Interventions', *Frontiers in Genetics*. Frontiers Media S.A., 13, p. 628. doi: 10.3389/FGENE.2022.841639/BIBTEX.

Leblond, F., Seidah, N. G., Précourt, L.-P., Delvin, E., Dominguez, M. and Levy, E. (2009). 'Regulation of the proprotein convertase subtilisin/kexin type 9 in intestinal epithelial cells', *Am J Physiol Gastrointest Liver Physiol*, 296, pp. 805–815. doi: 10.1152/ajpgi.90424.2008.-Proprotein.

Lethongsavarn, V., Pinault, M., Diedhiou, A., Guimaraes, C., Guibon, R., Bruyère, F., Mathieu, R., Rioux-Leclercq, N., Multigner, L., Brureau, L., Fournier, G., Doucet, L., Blanchet, P. and Fromont, G. (2021). 'Tissue cholesterol metabolism and prostate cancer aggressiveness: Ethno-geographic variations', *The Prostate*. Prostate, 81(16), pp. 1365–1373. doi: 10.1002/PROS.24234.

Li, J., Gu, D., Lee, S. S. Y., Song, B., Bandyopadhyay, S., Chen, S., Konieczny, S. F., Ratliff, T. L., Liu, X., Xie, J. and Cheng, J. X. (2016). 'Abrogating cholesterol esterification suppresses growth and metastasis of pancreatic cancer', *Oncogene 2016 35:50*. Nature Publishing Group, 35(50), pp. 6378–6388. doi: 10.1038/onc.2016.168.

Li, J., Li, Y., Chen, C., Guo, J., Qiao, M. and Lyu, J. (2022). 'Recent estimates and predictions of 5-year survival rate in patients with pancreatic cancer: A model-based period analysis', *Frontiers in Medicine*. Frontiers Media S.A., 9, p. 3568. doi: 10.3389/FMED.2022.1049136/BIBTEX.

Li, J. and Pfeffer, S. R. (2016). 'Lysosomal membrane glycoproteins bind cholesterol and contribute to lysosomal cholesterol export', *eLife*. eLife Sciences Publications, Ltd, 5(September2016). doi: 10.7554/ELIFE.21635.

Li, J., Qu, X., Tian, J., Zhang, J.-T. and Cheng, J.-X. (2018). 'Cholesterol esterification inhibition and gemcitabine synergistically suppress pancreatic ductal adenocarcinoma proliferation'. doi: 10.1371/journal.pone.0193318.

Li, Yuchuan, Amrutkar, M., Finstadsveen, A. V., Dalen, K. T., Verbeke, C. S. and Gladhaug, I. P. (2023). 'Fatty acids abrogate the growth-suppressive effects induced by inhibition of cholesterol flux in pancreatic cancer cells', *Cancer Cell International*. BioMed Central Ltd, 23(1). doi: 10.1186/s12935-023-03138-8.

Li, Yunkuo, Wu, S., Zhao, X., Hao, S., Li, F., Wang, Yuxiong, Liu, B., Zhang, D., Wang, Yishu and Zhou, H. (2023). 'Key events in cancer: Dysregulation of SREBPs', *Frontiers in Pharmacology*. Frontiers Media SA. doi: 10.3389/fphar.2023.1130747.

Liao, X., Song, G., Xu, Z., Bu, Y., Chang, F., Jia, F., Xiao, X., Ren, X., Zhang, M. and Jia, Q. (2020). 'Oxaliplatin resistance is enhanced by saracatinib via upregulation Wnt-ABCG1 signaling in hepatocellular carcinoma', *BMC Cancer*. BioMed Central Ltd., 20(1), pp. 1–12. doi: 10.1186/S12885-019-6480-9/FIGURES/5.

Lippi, G. and Mattiuzzi, C. (2020). 'The global burden of pancreatic cancer', *Archives of Medical Science : AMS*. Termedia Publishing, 16(4), p. 820. doi: 10.5114/AOMS.2020.94845.

Liu, C., Chen, J., Chen, H., Zhang, T., He, D., Luo, Q., Chi, J., Hong, Z., Liao, Y., Zhang, S., Wu, Q., Cen, H., Chen, G., Li, J. and Wang, L. (2022). 'PCSK9 Inhibition: From Current Advances to Evolving Future', *Cells*. MDPI. doi: 10.3390/cells11192972.

Liu, C., Li, C. and Liu, Y. (2023). 'The role of metabolic reprogramming in pancreatic cancer chemoresistance', *Frontiers in Pharmacology*. Frontiers Media SA, 13, p. 5584. doi: 10.3389/FPHAR.2022.1108776/BIBTEX.

Liu, H., Tao, H., Wang, H., Yang, Y., Yang, R., Dai, X., Ding, X., Wu, H., Chen, S. and Sun, T. (2021). 'Doxycycline Inhibits Cancer Stem Cell-Like Properties via PAR1/FAK/PI3K/AKT Pathway in Pancreatic Cancer', *Frontiers in Oncology*. Frontiers Media S.A., 10. doi: 10.3389/fonc.2020.619317.

Liu, J., Ma, J., Wu, Z., Li, W., Zhang, D., Han, L., Wang, F., Reindl, K. M., Wu, E. and Ma, Q. (2014). *Arginine deiminase augments the chemosensitivity of argininosuccinate synthetase-deficient pancreatic cancer cells to gemcitabine via inhibition of NF-κB signaling*. Available at: http://www.biomedcentral.com/1471-2407/14/686.

Liu, N. K. and Xu, X. M. (2006). 'β-Tubulin Is a More Suitable Internal Control than β-Actin in Western Blot Analysis of Spinal Cord Tissues after Traumatic Injury', *https://home.liebertpub.com/neu*. Mary Ann Liebert, Inc. 2 Madison Avenue Larchmont, NY 10538 USA , 23(12), pp. 1794–1801. doi: 10.1089/NEU.2006.23.1794.

Liu, Q., Zhang, Y., Li, H., Gao, H., Zhou, Y., Luo, D., Shan, Z., Yang, Y., Weng, J., Li, Q., Yang, W. and Li, X. (2024). 'Squalene epoxidase promotes the chemoresistance of colorectal cancer via (S)-2,3-epoxysqualene-activated NF-κB', *Cell Communication and Signaling*. Springer Science and Business Media LLC, 22(1). doi: 10.1186/s12964-024-01649-z.

Liu, T., Chen, J. M., Zhang, D., Zhang, Q., Peng, B., Xu, L. and Tang, H. (2021). 'ApoPred: Identification of Apolipoproteins and Their Subfamilies With Multifarious Features', *Frontiers in Cell and Developmental Biology*. Frontiers Media S.A., 8, p. 1583. doi: 10.3389/FCELL.2020.621144/BIBTEX.

Liu, X., Bao, X., Hu, M., Chang, H., Jiao, M., Cheng, J., Xie, L., Huang, Q., Li, F. and Li, C. Y. (2020). 'Inhibition of PCSK9 potentiates immune checkpoint therapy for cancer', *Nature*. Nature Research, 588(7839), pp. 693–698. doi: 10.1038/s41586-020-2911-7.

Liu, Y., Zhang, W., Zhou, H. and Chen, J. (2023). 'Steroidal saponins PPI/CCRIS/PSV induce cell death in pancreatic cancer cell through GSDME-dependent pyroptosis.', *Biochemical and biophysical research communications*, 673, pp. 51–58. doi: 10.1016/j.bbrc.2023.06.062.

Liza, M., Romero, J. R., Chico, Y., Fresnedo, O. and Ochoa, B. (1996). 'Application of 2-hydroxypropyl-beta-cyclodextrin in the assay of acyl-CoA:cholesterol acyltransferase and neutral and acid cholesterol ester hydrolases.', *Lipids*, 31(3), pp. 323–9. doi: 10.1007/BF02529879.

Longley, D. B., Harkin, D. P. and Johnston, P. G. (2003). '5-Fluorouracil: mechanisms of action and clinical strategies', *Nature Reviews Cancer 2003 3:5*. Nature Publishing Group, 3(5), pp. 330–338. doi: 10.1038/nrc1074.

Longo, J., van Leeuwen, J. E., Elbaz, M., Branchard, E. and Penn, L. Z. (2020). 'Statins as anticancer agents in the era of precision medicine', *Clinical Cancer Research*. American Association for Cancer Research Inc., 26(22), pp. 5791–5800. doi: 10.1158/1078-0432.CCR-20-1967/77556/AM/STATINS-AS-ANTI-CANCER-AGENTS-IN-THE-ERA-OF.

Lou, C., Zhang, F., Yang, M., Zhao, J., Zeng, W., Fang, X., Zhang, Y., Zhang, C. and Liang, W. (2012). 'Naringenin Decreases Invasiveness and Metastasis by Inhibiting TGF-β-Induced Epithelial to Mesenchymal Transition in Pancreatic Cancer Cells', *PLOS ONE*. Public Library of Science, 7(12), p. e50956. doi: 10.1371/JOURNAL.PONE.0050956.

Lu, H. and Martí, J. (2020). 'Influence of Cholesterol on the Orientation of the Farnesylated GTP-Bound KRas-4B Binding with Anionic Model Membranes', *Membranes 2020, Vol. 10, Page 364*. Multidisciplinary Digital Publishing Institute, 10(11), p. 364. doi: 10.3390/MEMBRANES10110364.

Lu, Y., Zhou, Xiaohui, Zhao, W., Liao, Z., Li, B., Han, P., Yang, Y., Zhong, X., Mo, Y., Li, P., Huang, G., Xiao, X., Zhang, Z. and Zhou, Xiaoying (2021). 'Epigenetic Inactivation of Acetyl-CoA Acetyltransferase 1 Promotes the Proliferation and Metastasis in Nasopharyngeal Carcinoma by Blocking Ketogenesis', *Frontiers in Oncology*. Frontiers Media S.A., 11, p. 1. doi: 10.3389/FONC.2021.667673/FULL.

Luo, J., Yang, H. and Song, B. L. (2020). 'Mechanisms and regulation of cholesterol homeostasis', *Nature reviews. Molecular cell biology*. Nat Rev Mol Cell Biol, 21(4), pp. 225–245. doi: 10.1038/S41580-019-0190-7.

Ma, Y., Di, Y., Li, Q., Zhan, Q., He, X., Liu, S., Zou, H., Corpe, C., Chen, L. and Wang, J. (2022). 'LncRNAs as epigenetic regulators of epithelial to mesenchymal transition in pancreatic cancer', *Discover Oncology*. Springer Science and Business Media B.V. doi: 10.1007/s12672-022-00522-0.

Mabuchi, H., Nohara, A. and Inazu, A. (2014). 'Cholesteryl Ester Transfer Protein (CETP) Deficiency and CETP Inhibitors', *Molecules and Cells*. Korean Society for Molecular and Cellular Biology, 37(11), p. 777. doi: 10.14348/MOLCELLS.2014.0265.

Mafi, A., Rezaee, M., Hedayati, N., Hogan, S. D., Reiter, R. J., Aarabi, M. H. and Asemi, Z. (2023). 'Melatonin and 5-fluorouracil combination chemotherapy: opportunities and efficacy in cancer therapy', *Cell Communication and Signaling*. BioMed Central Ltd. doi: 10.1186/s12964-023-01047-x.

Mahboobnia, K., Pirro, M., Marini, E., Grignani, F., Bezsonov, E. E., Jamialahmadi, T. and Sahebkar, A. (2021). 'PCSK9 and cancer: Rethinking the link', *Biomedicine & Pharmacotherapy*. Elsevier Masson, 140, p. 111758. doi: 10.1016/J.BIOPHA.2021.111758.

Mahjoubin-Tehran, M., Kovanen, P. T., Xu, S., Jamialahmadi, T. and Sahebkar, A. (2020). 'Cyclodextrins: Potential therapeutics against atherosclerosis', *Pharmacology and Therapeutics*. Elsevier Inc. doi: 10.1016/j.pharmthera.2020.107620.

Maier, H. J., Wirth, T. and Beug, H. (2010). 'Epithelial-Mesenchymal transition in Pancreatic Carcinoma', *Cancers*, pp. 2058–2083. doi: 10.3390/cancers2042058.

Mann, H. B. and Whitney, D. R. (1947). 'On a Test of Whether one of Two Random Variables is Stochastically Larger than the Other', *https://doi.org/10.1214/aoms/1177730491*. Institute of Mathematical Statistics, 18(1), pp. 50–60. doi: 10.1214/AOMS/1177730491.

Mann, K. M., Ying, H., Juan, J., Jenkins, N. A. and Copeland, N. G. (2016). 'KRAS-related proteins in pancreatic cancer', *Pharmacology & therapeutics*. Pharmacol Ther, 168, pp. 29–42. doi: 10.1016/J.PHARMTHERA.2016.09.003.

Manns, J. M. (2011). 'SDS-Polyacrylamide Gel Electrophoresis (SDS-PAGE) of Proteins', *Current Protocols in Microbiology*. John Wiley & Sons, Ltd, 22(1), p. A.3M.1-A.3M.13. doi: 10.1002/9780471729259.MCA03MS22.

Marin, J. J. G., Monte, M. J., Macias, R. I. R., Romero, M. R., Herraez, E., Asensio, M., Ortiz-Rivero, S., Cives-Losada, C., Di Giacomo, S., Gonzalez-Gallego, J., Mauriz, J. L., Efferth, T. and Briz, O. (2022). 'Expression of Chemoresistance-Associated ABC Proteins in Hepatobiliary, Pancreatic and Gastrointestinal Cancers', *Cancers*. Cancers (Basel), 14(14). doi: 10.3390/CANCERS14143524.

Matusewicz, L., Czogalla, A. and Sikorski, A. F. (2020). 'Attempts to use statins in cancer therapy: An update', *Tumor Biology*. SAGE Publications Ltd, 42(7), pp. 1–9. doi: 10.1177/1010428320941760.

Mayengbam, S. S., Singh, A., Pillai, A. D. and Bhat, M. K. (2021). 'Influence of cholesterol on cancer progression and therapy', *Translational Oncology*. Elsevier, 14(6), p. 101043. doi: 10.1016/J.TRANON.2021.101043.

Megías-Vericat, J. E., García-Robles, A., Company-Albir, M. J., Fernández-Megía, M. J., Pérez-Miralles, F. C., López-Briz, E., Casanova, B. and Poveda, J. L. (2017). 'Early experience with compassionate use of 2 hydroxypropyl-beta-cyclodextrin for Niemann-Pick type C disease: review of initial published cases', *Neurological sciences : official journal of the Italian Neurological Society and of the Italian Society of Clinical Neurophysiology*. Neurol Sci, 38(5), pp. 727–743. doi: 10.1007/S10072-017-2833-9.

Miller, A. L., Garcia, P. L., Gamblin, T. L., Vance, R. B. and Yoon, K. J. (2020). 'Development of gemcitabine-resistant patient-derived xenograft models of pancreatic ductal adenocarcinoma', *Cancer Drug Resistance*. OAE Publishing Inc, 3(3), p. 572. doi: 10.20517/CDR.2020.35.

Mistafa, O. and Stenius, U. (2009). 'Statins inhibit Akt/PKB signaling via P2X7 receptor in pancreatic cancer cells', *Biochemical Pharmacology*. Elsevier, 78(9), pp. 1115–1126. doi: 10.1016/J.BCP.2009.06.016.

Mitrofanova, A., Molina, J., Varona Santos, J., Guzman, J., Morales, X. A., Ducasa, G. M., Bryn, J., Sloan, A., Volosenco, I., Kim, J. J., Ge, M., Mallela, S. K., Kretzler, M., Eddy, S., Martini, S., Wahl, P., Pastori, S., Mendez, A. J., Burke, G. W., Merscher, S. and Fornoni, A. (2018). 'Hydroxypropyl-β-cyclodextrin protects from kidney disease in experimental Alport syndrome and focal segmental glomerulosclerosis', *Kidney International*. Elsevier B.V., 94(6), pp. 1151–1159. doi: 10.1016/j.kint.2018.06.031.

Mizrahi, J. D., Surana, R., Valle, J. W. and Shroff, R. T. (2020). 'Pancreatic cancer', *The Lancet*. Lancet Publishing Group, 395(10242), pp. 2008–2020. doi: 10.1016/S0140-6736(20)30974-0/ASSET/9945DE72-2A4C-414E-922B-01E32C1CDAA9/MAIN.ASSETS/GR2.SML.

Moon, S.H., Huang, C.H., Houlihan, S.L., Regunath, K., Freed-Pastor, W.A., Morris, J.P., Tschaharganeh, D.F., Kastenhuber, E.R., Barsotti, A.M., Culp-Hill, R., Xue, W., Ho, Y.J.,

Baslan, T., Li, X., Mayle, A., de Stanchina, E., Zender, L., Tong, D.R., D'Alessandro, A., Lowe, S.W. and Prives, C. (2019). 'p53 Represses the Mevalonate Pathway to Mediate Tumor Suppression', *Cell*. NIH Public Access, 176(3), p. 564. doi: 10.1016/J.CELL.2018.11.011.

Namba, Y., Sogawa, C., Okusha, Y., Kawai, H., Itagaki, M., Ono, K., Murakami, J., Aoyama, E., Ohyama, K., Asaumi, J. I., Takigawa, M., Okamoto, K., Calderwood, S. K., Kozaki, K. ichi and Eguchi, T. (2018). 'Depletion of lipid efflux pump ABCG1 triggers the intracellular accumulation of extracellular vesicles and reduces aggregation and tumorigenesis of metastatic cancer cells', *Frontiers in Oncology*. Frontiers Media S.A., 8(OCT). doi: 10.3389/fonc.2018.00376.

Narimatsu, A., Kambara, T., Abe, H., Uematsu, T., Tokura, Y., Suzuki, I., Sakamoto, K., Takei, K., Nishihara, D., Nakamura, G., Kokubun, H., Yuki, H., Betsunoh, H. and Kamai, T. (2019). '5-Fluorouracil-based adjuvant chemotherapy improves the clinical outcomes of patients with lymphovascular invasion of upper urinary tract cancer and low expression of dihydropyrimidine dehydrogenase', *Oncology Letters*. Spandidos Publications, 17(5), pp. 4429–4436. doi: 10.3892/ol.2019.10086.

Niculescu, D. N. ;, Bolocan, A.-G. ;, Andronic, A. ;, Grumezescu, O. ;, Bîrlˇ, A. M. ;, An, R., Cîrcioban, L., Pinzaru, I., Trandafirescu, C., Păduraru, D. N., Niculescu, A.-G., Bolocan, A., Andronic, O., Grumezescu, A. M. and Bîrlă, R. (2022). 'An Updated Overview of Cyclodextrin-Based Drug Delivery Systems for Cancer Therapy', *Pharmaceutics*. MDPI, 14(8), p. 1748. doi: 10.3390/PHARMACEUTICS14081748.

Nie, X., Li, C., Hu, S., Xue, F., Kang, Y. J. and Zhang, W. (2017). 'An appropriate loading control for western blot analysis in animal models of myocardial ischemic infarction', *Biochemistry and Biophysics Reports*. Elsevier, 12, pp. 108–113. doi: 10.1016/J.BBREP.2017.09.001.

Noë, M. and Brosens, L. A. A. (2016). 'Pathology of Pancreatic Cancer Precursor Lesions', *Surgical Pathology Clinics*. W.B. Saunders, 9(4), pp. 561–580. doi: 10.1016/J.PATH.2016.05.004.

Nowakowski, A. B., Wobig, W. J. and Petering, D. H. (2014). 'Native SDS-PAGE: High Resolution Electrophoretic Separation of Proteins With Retention of Native Properties Including Bound Metal Ions', *Metallomics : integrated biometal science*. NIH Public Access, 6(5), p. 1068. doi: 10.1039/C4MT00033A.

Oni, T. E., Biffi, G., Baker, L. A., Hao, Y., Tonelli, C., Somerville, T. D. D., Deschênes, A., Belleau, P., Hwang, C. I., Sánchez-Rivera, F. J., Cox, H., Brosnan, E., Doshi, A., Lumia, R. P., Khaledi, K., Park, Y., Trotman, L. C., Lowe, S. W., Krasnitz, A., Vakoc, C. R., Tuveson, D. A. (2020). 'SOAT1 promotes mevalonate pathway dependency in pancreatic cancer', *Journal of Experimental Medicine*. Rockefeller University Press, 217(9). doi: 10.1084/jem.20192389.

Onodera, R., Motoyama, K., Okamatsu, A., Higashi, T., Kariya, R., Okada, S. and Arima, H. (2013). 'Involvement of cholesterol depletion from lipid rafts in apoptosis induced by methyl-β-cyclodextrin', *International Journal of Pharmaceutics*. Elsevier, 452(1–2), pp. 116–123. doi: 10.1016/J.IJPHARM.2013.04.071.

Ortega Duran, M., Shaheed, S. ul, Sutton, C. W. and Shnyder, S. D. (2024). 'A Proteomic Investigation to Discover Candidate Proteins Involved in Novel Mechanisms of 5-Fluorouracil Resistance in Colorectal Cancer', *Cells*. Multidisciplinary Digital Publishing Institute (MDPI), 13(4). doi: 10.3390/cells13040342.

Orth, M., Metzger, P., Gerum, S., Mayerle, J., Schneider, G., Belka, C., Schnurr, M. and Lauber, K. (2019). 'Pancreatic ductal adenocarcinoma: biological hallmarks, current status, and future perspectives of combined modality treatment approaches', *Radiation Oncology 2019 14:1*. BioMed Central, 14(1), pp. 1–20. doi: 10.1186/S13014-019-1345-6.

Osmak, M. (2012). 'Statins and cancer: Current and future prospects', *Cancer Letters*. Elsevier, 324(1), pp. 1–12. doi: 10.1016/J.CANLET.2012.04.011.

Otieno, B. A., Krause, C. E. and Rusling, J. F. (2016). 'Bioconjugation of Antibodies and Enzyme Labels onto Magnetic Beads', *Methods in Enzymology*. Academic Press, 571, pp. 135–150. doi: 10.1016/BS.MIE.2015.10.005.

Palamaris, K., Felekouras, E. and Sakellariou, S. (2021). 'Epithelial to Mesenchymal Transition: Key Regulator of Pancreatic Ductal Adenocarcinoma Progression and Chemoresistance', *Cancers*. Multidisciplinary Digital Publishing Institute (MDPI), 13(21). doi: 10.3390/CANCERS13215532.

Park, J. H., Pyun, W. Y. and Park, H. W. (2020). 'Cancer Metabolism: Phenotype, Signaling and Therapeutic Targets', *Cells*. Multidisciplinary Digital Publishing Institute (MDPI), 9(10). doi: 10.3390/CELLS9102308.

Peake, K. B. and Vance, J. E. (2012). 'Normalization of cholesterol homeostasis by 2-hydroxypropyl-β- cyclodextrin in neurons and glia from Niemann-Pick C1 (NPC1)-deficient mice', *Journal of Biological Chemistry*. Elsevier, 287(12), pp. 9290–9298. doi: 10.1074/jbc.M111.326405.

Peetla, C., Vijayaraghavalu, S. and Labhasetwar, V. (2013). 'Biophysics of Cell Membrane Lipids in Cancer Drug Resistance: Implications for Drug Transport and Drug Delivery with Nanoparticles', *Advanced drug delivery reviews*. NIH Public Access, 65(0), pp. 1686–1698. doi: 10.1016/J.ADDR.2013.09.004.

Pillay, R. (2024). *Investigating the role of KS-01 as Anti-Cancer Agent in Colorectal Cancer*. PhD thesis. University of the Witwatersrand.

Plazzo, A. P., Höfer, C. T., Jicsinszky, L., Fenyvesi, É., Szente, L., Schiller, J., Herrmann, A. and Müller, P. (2012). 'Uptake of a fluorescent methyl-β-cyclodextrin via clathrin-dependent endocytosis', *Chemistry and Physics of Lipids*. Elsevier, 165(5), pp. 505–511. doi: 10.1016/J.CHEMPHYSLIP.2012.03.007.

Po, A., Citarella, A., Catanzaro, G., Besharat, Z. M., Trocchianesi, S., Gianno, F., Sabato, C., Moretti, M., De Smaele, E., Vacca, A., Fiori, M. E. and Ferretti, E. (2020). 'Hedgehog-GLI signalling promotes chemoresistance through the regulation of ABC transporters in colorectal cancer cells', *Scientific Reports 2020 10:1*. Nature Publishing Group, 10(1), pp. 1–14. doi: 10.1038/s41598-020-70871-9.

Principe, D. R., Underwood, P. W., Korc, M., Trevino, J. G., Munshi, H. G. and Rana, A. (2021). 'The Current Treatment Paradigm for Pancreatic Ductal Adenocarcinoma and Barriers to Therapeutic Efficacy', *Frontiers in Oncology*. Frontiers Media S.A. doi: 10.3389/fonc.2021.688377.

Qiu, N., Li, X. and Liu, J. (2017). 'Application of cyclodextrins in cancer treatment', *Journal of Inclusion Phenomena and Macrocyclic Chemistry 2017 89:3*. Springer, 89(3), pp. 229–246. doi: 10.1007/S10847-017-0752-2.

Qiu, Z., Yuan, W., Chen, T., Zhou, C., Liu, C., Huang, Y., Han, D. and Huang, Q. (2016). 'HMGCR positively regulated the growth and migration of glioblastoma cells', *Gene*. Elsevier, 576(1), pp. 22–27. doi: 10.1016/J.GENE.2015.09.067.

Quiroz-Figueroa, K., Vitali, C., Conlon, D. M., Millar, J. S., Tobias, J. W., Bauer, R. C., Hand, N. J. and Rader, D. J. (2021). 'TRIB1 regulates LDL metabolism through CEBPα-mediated effects on the LDL receptor in hepatocytes', *The Journal of Clinical Investigation*. American Society for Clinical Investigation, 131(22). doi: 10.1172/JCI146775.

Ramirez, C. M., Taylor, A. M., Lopez, A. M., Repa, J. J. and Turley, S. D. (2020). 'Delineation of metabolic responses of Npc1−/−nih mice lacking the cholesterol-esterifying enzyme SOAT2 to acute treatment with 2-hydroxypropyl-β-cyclodextrin', *Steroids*. Elsevier, 164, p. 108725. doi: 10.1016/J.STEROIDS.2020.108725.

Rebelo, A., Kleeff, J. and Sunami, Y. (2023). 'Cholesterol Metabolism in Pancreatic Cancer', *Cancers*. Multidisciplinary Digital Publishing Institute (MDPI), 15(21), p. 5177. doi: 10.3390/CANCERS15215177.

Reed, R., Holmes, D., Weyers, J. and Jones, A. (2016). *Practical Skills In Biomolecular Sciences*. Fifth. Harlow, England; New York: Pearson.

Riscal, R., Skuli, N. and Simon, M. C. (2019). 'Even Cancer Cells Watch Their Cholesterol!', *Molecular Cell*. Cell Press, 76(2), pp. 220–231. doi: 10.1016/J.MOLCEL.2019.09.008.

Rodriguez-Ruiz, V., Maksimenko, A., Salzano, G., Lampropoulou, M., Lazarou, Y. G., Agostoni, V., Couvreur, P., Gref, R. and Yannakopoulou, K. (2017). 'Positively charged cyclodextrins as effective molecular transporters of active phosphorylated forms of gemcitabine into cancer cells', *Scientific Reports*. Nature Publishing Group, 7(1). doi: 10.1038/s41598-017-08727-y.

Rogatsky, E. (2021). 'Pandora box of BCA assay. Investigation of the accuracy and linearity of the microplate bicinchoninic protein assay: Analytical challenges and method modifications to minimize systematic errors', *Analytical Biochemistry*. Academic Press, 631, p. 114321. doi: 10.1016/J.AB.2021.114321.

Rosenbaum, A. I., Zhang, G., Warren, J. D. and Maxfield, F. R. (2010). 'Endocytosis of beta-cyclodextrins is responsible for cholesterol reduction in Niemann-Pick type C mutant cells', *Proceedings of the National Academy of Sciences of the United States of America*. National Academy of Sciences, 107(12), pp. 5477–5482. doi: 10.1073/PNAS.0914309107/SUPPL_FILE/PNAS.200914309SI.PDF.

Roy, S. and Kumar, V. (2014). *A Practical Approach on SDS PAGE for Separation of Protein*, *International Journal of Science and Research*. Available at: www.ijsr.net.

Ruiz, C. F., Montal, E. D., Haley, J. A., Bott, A. J. and Haley, J. D. (2020). 'SREBP1 regulates mitochondrial metabolism in oncogenic KRAS expressing NSCLC', *FASEB journal : official publication of the Federation of American Societies for Experimental Biology*. NIH Public Access, 34(8), p. 10574. doi: 10.1096/FJ.202000052R.

Sag, D., Cekic, C., Wu, R., Linden, J. and Hedrick, C. C. (2015). 'The cholesterol transporter ABCG1 links cholesterol homeostasis and tumour immunity', *Nature Communications*. Nature Publishing Group, 6. doi: 10.1038/ncomms7354.

Saha, S. T., Abdulla, N., Zininga, T., Shonhai, A., Wadee, R. and Kaur, M. (2023). '2-Hydroxypropyl-β-cyclodextrin (HPβCD) as a Potential Therapeutic Agent for Breast Cancer', *Cancers*. MDPI, 15(10), p. 2828. doi: 10.3390/CANCERS15102828/S1.

Saiki, Y., Yoshino, Y., Fujimura, H., Manabe, T., Kudo, Y., Shimada, M., Mano, N., Nakano, T., Lee, Y., Shimizu, S., Oba, S., Fujiwara, S., Shimizu, H., Chen, N., Nezhad, Z. K., Jin, G., Fukushige, S., Sunamura, M., Ishida, M., Motoi, F., Egawa, S., Unno, M. and Horii, A. (2012). 'DCK is frequently inactivated in acquired gemcitabine-resistant human cancer cells', *Biochemical and biophysical research communications*. Biochem Biophys Res Commun, 421(1), pp. 98–104. doi: 10.1016/J.BBRC.2012.03.122.

Sandilya, A. A., Natarajan, U. and Priya, M. H. (2020). 'Molecular View into the Cyclodextrin Cavity: Structure and Hydration', *ACS Omega*. American Chemical Society, 5(40), pp. 25655–25667. doi: 10.1021/ACSOMEGA.0C02760/ASSET/IMAGES/MEDIUM/AO0C02760_M006.GIF.

Sarvepalli, D., Ur Rashid, M., Ur Rahman, A., Ullah, W., Hussain, I., Hasan, B., Jehanzeb, S., Khan, A. K., Jain, A. G., Khetpal, N. and Ahmad, S. (2019). 'Gemcitabine: A Review of Chemoresistance in Pancreatic Cancer', *Critical reviews in oncogenesis*. Crit Rev Oncog, 24(2), pp. 199–212. doi: 10.1615/CRITREVONCOG.2019031641.

Schneider, C. A., Rasband, W. S. and Eliceiri, K. W. (2012). 'NIH Image to ImageJ: 25 years of image analysis', *Nature Methods 2012 9:7*. Nature Publishing Group, 9(7), pp. 671–675. doi: 10.1038/nmeth.2089.

Schulz, B., Leitner, E., Schreiber, T., Lindner, T., Schwarz, R., Aboutara, N., Ma, Y., Escobar, H. M., Palme, R., Hinz, B., Vollmar, B. and Zechner, D. (2024). 'Sex Matters–Insights from Testing Drug Efficacy in an Animal Model of Pancreatic Cancer', *Cancers*. Multidisciplinary Digital Publishing Institute (MDPI), 16(10). doi: 10.3390/cancers16101901.

Sharma, B. and Agnihotri, N. (2019). 'Role of cholesterol homeostasis and its efflux pathways in cancer progression', *The Journal of Steroid Biochemistry and Molecular Biology*. Pergamon, 191, p. 105377. doi: 10.1016/J.JSBMB.2019.105377.

Sherman, M. H. and Beatty, G. L. (2023). 'Tumor Microenvironment in Pancreatic Cancer Pathogenesis and Therapeutic Resistance', *Annual Review of Pathology: Mechanisms of Disease*. Annual Reviews , 18(1), pp. 123–148. doi: 10.1146/ANNUREV-PATHMECHDIS-031621-024600.

Singh, P., Saxena, R., Srinivas, G., Pande, G. and Chattopadhyay, A. (2013). 'Cholesterol Biosynthesis and Homeostasis in Regulation of the Cell Cycle', *PLOS ONE*. Public Library of Science, 8(3), p. e58833. doi: 10.1371/JOURNAL.PONE.0058833.

Sitarska, D., Tylki-Szymańska, A. and Ługowska, A. (2021). 'Treatment trials in Niemann-Pick type C disease', *Metabolic Brain Disease*. Springer, 36(8), p. 2215. doi: 10.1007/S11011-021-00842-0.

Smith, L. C., Pownall, H. J. and Gotto, A. M. (1978). 'The plasma lipoproteins: structure and metabolism.', *Annual review of biochemistry*, 47, pp. 751–757. doi: 10.1146/annurev.bi.47.070178.003535.

De Sousa Cavalcante, L. and Monteiro, G. (2014). 'Gemcitabine: Metabolism and molecular mechanisms of action, sensitivity and chemoresistance in pancreatic cancer', *European Journal of Pharmacology*. Elsevier, 741, pp. 8–16. doi: 10.1016/J.EJPHAR.2014.07.041.

Sozen, E. and Ozer, N. K. (2017). 'Impact of high cholesterol and endoplasmic reticulum stress on metabolic diseases: An updated mini-review', *Redox Biology*. Elsevier, 12, p. 456. doi: 10.1016/J.REDOX.2017.02.025.

Stuart, S. E., Clawson, G. A., Rottman, F. M. and Patterson, R. J. (1977). 'RNA transport in isolated myeloma nuclei. Transport from membrane-denuded nuclei.', *Journal of Cell Biology*. The Rockefeller University Press, 72(1), pp. 57–66. doi: 10.1083/JCB.72.1.57.

Suh, J. M., Son, Y., Yoo, J. Y., Goh, Y., Seidah, N. G., Lee, S. and Bae, Y. S. (2021). 'Proprotein convertase subtilisin/kexin Type 9 is required for Ahnak-mediated metastasis of melanoma into lung epithelial cells', *Neoplasia*. Elsevier, 23(9), pp. 993–1001. doi: 10.1016/J.NEO.2021.07.007.

Sum, A. K. and De Pablo, J. J. (2003). 'Molecular Simulation Study on the Influence of Dimethylsulfoxide on the Structure of Phospholipid Bilayers', *Biophysical Journal*. Biophysical Society, 85(6), pp. 3636–3645. doi: 10.1016/S0006-3495(03)74781-X.

Sung, H., Ferlay, J., Siegel, R. L., Laversanne, M., Soerjomataram, I., Jemal, A. and Bray, F. (2021). 'Global Cancer Statistics 2020: GLOBOCAN Estimates of Incidence and Mortality Worldwide for 36 Cancers in 185 Countries', *CA: A Cancer Journal for Clinicians*. American Cancer Society, 71(3), pp. 209–249. doi: 10.3322/CAAC.21660.

Sweeney, R., Richards, K. E. and Hill, R. (2017). 'Gemcitabine-Induced Exosome Hypersecretion Increases the Chemoresistance and Migration of Pancreatic Cancer Cells', *The FASEB Journal*, 31(S1). doi: 10.1096/fasebj.31.1_supplement.775.20.

Tarling, E. J. and Edwards, P. A. (2011). 'ATP binding cassette transporter G1 (ABCG1) is an intracellular sterol transporter', *Proceedings of the National Academy of Sciences of the United States of America*. National Academy of Sciences, 108(49), pp. 19719–19724. doi: 10.1073/PNAS.1113021108/SUPPL_FILE/PNAS.201113021SI.PDF.

Tsuchiya, M., Hosaka, M., Moriguchi, T., Zhang, S., Suda, M., Yokota-Hashimoto, H., Shinozuka, K. and Takeuchi, T. (2010). 'Cholesterol Biosynthesis Pathway Intermediates and Inhibitors Regulate Glucose-Stimulated Insulin Secretion and Secretory Granule Formation in Pancreatic β-Cells', *Endocrinology*. Oxford Academic, 151(10), pp. 4705–4716. doi: 10.1210/EN.2010-0623.

Tu, T., Zhang, H. and Xu, H. (2023). 'Targeting sterol-O-acyltransferase 1 to disrupt cholesterol metabolism for cancer therapy', *Frontiers in Oncology*. Frontiers Media SA. doi: 10.3389/fonc.2023.1197502.

Vance, J. E. and Karten, B. (2014). 'Niemann-Pick C disease and mobilization of lysosomal cholesterol by cyclodextrin', *Journal of Lipid Research*. American Society for Biochemistry and Molecular Biology Inc., 55(8), pp. 1609–1621. doi: 10.1194/JLR.R047837/ASSET/5A5F521B-21D0-472C-A61F-9F3A5AB8F192/MAIN.ASSETS/GR2.JPG.

Váradi, J., Hermenean, A., Gesztelyi, R., Jeney, V., Balogh, E., Majoros, L., Malanga, M., Fenyvesi, E., Szente, L., Bácskay, I., Vecsernyés, M., Fehér, P., Ujhelyi, Z., Vasvári, G., Árvai, I., Rusznyák, Á., Balta, C., Herman, H. and Fenyvesi, F. (2019). 'Pharmacokinetic Properties of Fluorescently Labelled Hydroxypropyl-Beta-Cyclodextrin', *Biomolecules 2019, Vol. 9,*

Page 509. Multidisciplinary Digital Publishing Institute, 9(10), p. 509. doi: 10.3390/BIOM9100509.

Vasseur, S. and Guillaumond, F. (2016). 'LDL Receptor: An open route to feed pancreatic tumor cells', *Molecular and Cellular Oncology*. Taylor and Francis Ltd., 3(1). doi: 10.1080/23723556.2015.1033586.

Vona, R., Iessi, E. and Matarrese, P. (2021). 'Role of Cholesterol and Lipid Rafts in Cancer Signaling: A Promising Therapeutic Opportunity?', *Frontiers in Cell and Developmental Biology*. Frontiers, 0, p. 468. doi: 10.3389/FCELL.2021.622908.

Walenbergh, S. M. A., Houben, T., Hendrikx, T., Jeurissen, M. L. J., van Gorp, P. J., Vaes, N., Damink, S. W. M. O., Verheyen, F., Koek, G. H., Lütjohann, D., Grebe, A., Latz, E. and Shiri-Sverdlov, R. (2015). 'Weekly treatment of 2-hydroxypropyl-β-cyclodextrin improves intracellular cholesterol levels in LDL receptor knockout mice', *International Journal of Molecular Sciences*. MDPI AG, 16(9), pp. 21056–21069. doi: 10.3390/ijms160921056.

Wang, C., Liu, B., Xu, X., Zhuang, B., Li, H., Yin, J., Cong, M., Xu, W. and Lu, A. (2016). 'Toward targeted therapy in chemotherapy-resistant pancreatic cancer with a smart triptolide nanomedicine', *Oncotarget*. Impact Journals, LLC, 7(7), p. 8360. doi: 10.18632/ONCOTARGET.7073.

Wang, L. L., Zheng, W. S., Chen, S. H., Han, Y. X. and Jiang, J. D. (2016). 'Development of rectal delivered thermo-reversible gelling film encapsulating a 5-fluorouracil hydroxypropyl-β-cyclodextrin complex', *Carbohydrate Polymers*. Elsevier, 137, pp. 9–18. doi: 10.1016/J.CARBPOL.2015.10.042.

Wang, L., Li, S., Luo, H., Lu, Q. and Yu, S. (2022). 'PCSK9 promotes the progression and metastasis of colon cancer cells through regulation of EMT and PI3K/AKT signaling in tumor cells and phenotypic polarization of macrophages', *Journal of Experimental and Clinical Cancer Research*. BioMed Central Ltd, 41(1), pp. 1–21. doi: 10.1186/S13046-022-02477-0/FIGURES/9.

Wang, S., Huang, S. and Sun, Y. L. (2017). 'Epithelial-Mesenchymal Transition in Pancreatic Cancer: A Review', *BioMed Research International*. Hindawi Limited, 2017. doi: 10.1155/2017/2646148.

Wang, W., Li, W., Zhang, D., Mi, Y., Zhang, J. and He, G. (2024). 'The Causal Relationship between PCSK9 Inhibitors and Malignant Tumors: A Mendelian Randomization Study Based on Drug Targeting', *Genes*. Multidisciplinary Digital Publishing Institute (MDPI), 15(1). doi: 10.3390/genes15010132.

Wang, W., Liu, B., Sun, S., Lan, L., Chen, Y., Han, S., Li, X. and Li, Z. (2020). 'Downregulation of miR-486-5p enhances the anti-tumor effect of 5-fluorouracil on pancreatic cancer cells', *OncoTargets and Therapy*. Dove Medical Press Ltd., 13, pp. 1649–1659. doi: 10.2147/OTT.S231153.

Wang, X., Xie, Jing, Lu, X., Li, H., Wen, C., Huo, Z., Xie, Junjie, Shi, M., Tang, X., Chen, H., Peng, C., Fang, Y., Deng, X. and Shen, B. (2017). 'Melittin inhibits tumor growth and decreases resistance to gemcitabine by downregulating cholesterol pathway gene CLU in pancreatic ductal adenocarcinoma', *Cancer Letters*. Elsevier, 399, pp. 1–9. doi: 10.1016/J.CANLET.2017.04.012.

Wang, Y., Cai, L., Li, H., Chen, H., Yang, T., Tan, Y., Guo, Z. and Wang, X. (2023). 'Overcoming Cancer Resistance to Platinum Drugs by Inhibiting Cholesterol Metabolism', *Angewandte Chemie International Edition*. John Wiley & Sons, Ltd, 62(42), p. e202309043. doi: 10.1002/ANIE.202309043.

Wei, W., Wang, J., Hu, Y., Chen, S. and Liu, J. (2022). 'Emodin reverses resistance to gemcitabine in pancreatic cancer by suppressing stemness through regulation of the epithelial-mesenchymal transition', *Experimental and Therapeutic Medicine*. Spandidos Publications, 25(1). doi: 10.3892/etm.2022.11706.

Wen, Y. A., Xiong, X., Zaytseva, Y. Y., Napier, D. L., Vallee, E., Li, A. T., Wang, C., Weiss, H. L., Evers, B. M. and Gao, T. (2018). 'Downregulation of SREBP inhibits tumor growth and initiation by altering cellular metabolism in colon cancer', *Cell Death & Disease*. Nature Publishing Group, 9(3). doi: 10.1038/S41419-018-0330-6.

Wu, Y., Si, R., Tang, H., He, Zhen, Zhu, H., Wang, L., Fan, Y., Xia, S., He, Zelai and Wang, Q. (2015). 'Cholesterol reduces the sensitivity to platinum-based chemotherapy via upregulating ABCG2 in lung adenocarcinoma', *Biochemical and Biophysical Research Communications*. Academic Press, 457(4), pp. 614–620. doi: 10.1016/J.BBRC.2015.01.035.

Xiao, M., Xu, J., Wang, W., Zhang, B., Liu, J., Li, J., Xu, H., Zhao, Y., Yu, X. and Shi, S. (2023). 'Functional significance of cholesterol metabolism in cancer: from threat to treatment', *Experimental and Molecular Medicine*. Springer Nature, pp. 1982–1995. doi: 10.1038/s12276-023-01079-w.

Xu, B., Li, S., Fang, Y., Zou, Y., Song, D., Zhang, S. and Cai, Y. (2021). 'Proprotein Convertase Subtilisin/Kexin Type 9 Promotes Gastric Cancer Metastasis and Suppresses Apoptosis by Facilitating MAPK Signaling Pathway Through HSP70 Up-Regulation', *Frontiers in Oncology*. Frontiers Media S.A., 10, p. 609663. doi: 10.3389/FONC.2020.609663/BIBTEX.

Xu, D., Li, Y., Yang, F., Sun, C. R., Pan, J., Wang, L., Chen, Z. P., Fang, S. C., Yao, X., Hou, W. T., Zhou, C. Z. and Chen, Y. (2022). 'Structure and transport mechanism of the human cholesterol transporter ABCG1', *Cell Reports*. Elsevier B.V., 38(4). doi: 10.1016/j.celrep.2022.110298.

Xu, H., Zhou, S., Tang, Q., Xia, H. and Bi, F. (2020). 'Cholesterol metabolism: New functions and therapeutic approaches in cancer', *Biochimica et Biophysica Acta - Reviews on Cancer*. Elsevier B.V. doi: 10.1016/j.bbcan.2020.188394.

Xu, W., Yang, Z. and Lu, N. (2015). 'A new role for the PI3K/Akt signaling pathway in the epithelial-mesenchymal transition', *Cell Adhesion & Migration*. Taylor & Francis, 9(4), p. 317. doi: 10.1080/19336918.2015.1016686.

Yamaguchi, R. and Perkins, G. (2017). 'Deconstructing Signaling Pathways in Cancer for Optimizing Cancer Combination Therapies', *International Journal of Molecular Sciences*. Multidisciplinary Digital Publishing Institute (MDPI), 18(6). doi: 10.3390/IJMS18061258.

Yan, A., Jia, Z., Qiao, C., Wang, M. and Ding, X. (2020). 'Cholesterol metabolism in drug-resistant cancer (Review)', *International Journal of Oncology*. Spandidos Publications, 57(5), pp. 1103–1115. doi: 10.3892/IJO.2020.5124/HTML.

Yancey, P. G., Rodrigueza, W. V., Kilsdonk, E. P. C., Stoudt, G. W., Johnson, W. J., Phillips, M. C. and Rothblat, G. H. (1996). 'Cellular cholesterol efflux mediated by cyclodextrins. Demonstration Of kinetic pools and mechanism of efflux', *The Journal of biological chemistry*. J Biol Chem, 271(27), pp. 16026–16034. doi: 10.1074/JBC.271.27.16026.

Yi, J., Zhu, J., Wu, J., Thompson, C. B. and Jiang, X. (2020). 'Oncogenic activation of PI3K-AKT-mTOR signaling suppresses ferroptosis via SREBP-mediated lipogenesis', *Proceedings of the National Academy of Sciences of the United States of America*. National Academy of Sciences, 117(49), pp. 31189–31197. doi: 10.1073/PNAS.2017152117/-/DCSUPPLEMENTAL.

Yin, N., Wang, Y., Liu, Y., Niu, R., Zhang, S., Cao, Y., Lv, Z., Song, S., Liu, X. and Zhang, H. (2023). 'A Cholesterol Metabolic Regulated Hydrogen-Bonded Organic Framework (HOF)-Based Biotuner for Antibody Non-Dependent Immunotherapy Tailored for Glioblastoma', *Advanced Materials*. John Wiley & Sons, Ltd, 35(44), p. 2303567. doi: 10.1002/ADMA.202303567.

Yin, T., Wei, H., Gou, S., Shi, P., Yang, Z., Zhao, G. and Wang, C. (2011). 'Cancer Stem-Like Cells Enriched in Panc-1 Spheres Possess Increased Migration Ability and Resistance to Gemcitabine', *International Journal of Molecular Sciences 2011, Vol. 12, Pages 1595-1604*. Molecular Diversity Preservation International, 12(3), pp. 1595–1604. doi: 10.3390/IJMS12031595.

Yin, X., Xu, R., Song, J., Ruze, R., Chen, Y., Wang, C. and Xu, Q. (2022). 'Lipid metabolism in pancreatic cancer: emerging roles and potential targets', *Cancer Communications*. John Wiley and Sons Inc, pp. 1234–1256. doi: 10.1002/cac2.12360.

Yokoo, M., Kubota, Y., Motoyama, K., Higashi, T., Taniyoshi, M., Tokumaru, H., Nishiyama, R., Tabe, Y., Mochinaga, S., Sato, A., Sueoka-Aragane, N., Sueoka, E., Arima, H., Irie, T. and Kimura, S. (2015). '2-Hydroxypropyl-β-Cyclodextrin Acts as a Novel Anticancer Agent',

PLOS ONE. Public Library of Science, 10(11), p. e0141946. doi: 10.1371/JOURNAL.PONE.0141946.

Young, J. D., Yao, S. Y. M., Baldwin, J. M., Cass, C. E. and Baldwin, S. A. (2013). 'The human concentrative and equilibrative nucleoside transporter families, SLC28 and SLC29', *Molecular aspects of medicine*. Mol Aspects Med, 34(2–3), pp. 529–547. doi: 10.1016/J.MAM.2012.05.007.

Yu, Yi, Dong, J. T., He, B., Zou, Y. F., Li, X. S., Xi, C. H. and Yu, Yuan (2019). 'LncRNA SNHG16 induces the SREBP2 to promote lipogenesis and enhance the progression of pancreatic cancer', *Future Oncology*. Future Medicine Ltd., 15(33), pp. 3831–3844. doi: 10.2217/fon-2019-0321.

Yue, S., Li, J., Lee, S. Y., Lee, H. J., Shao, T., Song, B., Cheng, L., Masterson, T. A., Liu, X., Ratliff, T. L. and Cheng, J. X. (2014). 'Cholesteryl ester accumulation induced by PTEN loss and PI3K/AKT activation underlies human prostate cancer aggressiveness', *Cell metabolism*. Cell Metab, 19(3), pp. 393–406. doi: 10.1016/J.CMET.2014.01.019.

Zeng, S., Pöttler, M., Lan, B., Grützmann, R., Pilarsky, C. and Yang, H. (2019). 'Chemoresistance in Pancreatic Cancer', *International Journal of Molecular Sciences*. Multidisciplinary Digital Publishing Institute (MDPI), 20(18). doi: 10.3390/IJMS20184504.

Zhang, C., Zhu, N., Li, H., Gong, Y., Gu, J., Shi, Y., Liao, D., Wang, W., Dai, A. and Qin, L. (2022). 'New dawn for cancer cell death: Emerging role of lipid metabolism', *Molecular Metabolism*. Elsevier GmbH. doi: 10.1016/j.molmet.2022.101529.

Zhang, D., Lu, P., Zhu, K., Wu, H. and Dai, Y. (2021). 'TFCP2 Overcomes Senescence by Cooperating With SREBP2 to Activate Cholesterol Synthesis in Pancreatic Cancer', *Frontiers in Oncology*. Frontiers Media S.A., 11. doi: 10.3389/fonc.2021.724437.

Zhang, F., Gao, J., Liu, X., Sun, Y., Liu, L., Hu, B., Wang, Z., Shi, J., Guo, W. and Zhang, S. (2023). 'LATS-regulated nuclear-cytoplasmic translocation of SREBP2 inhibits hepatocellular carcinoma cell migration and invasion via epithelial-mesenchymal transition', *Molecular carcinogenesis*. Mol Carcinog, 62(7), pp. 963–974. doi: 10.1002/MC.23538.

Zhang, Q., Zhao, Y. P., Liao, Q., Hu, Y., Xu, Q., Zhou, L. and Shu, H. (2011). 'Associations between gene polymorphisms of thymidylate synthase with its protein expression and chemosensitivity to 5-fluorouracil in pancreatic carcinoma cells', *Chinese Medical Journal*, 124(2), pp. 262–267. doi: 10.3760/CMA.J.ISSN.0366-6999.2011.02.021.

Zhang, S. Z., Zhu, X. D., Feng, L. H., Li, X. L., Liu, X. F., Sun, H. C. and Tang, Z. Y. (2021). 'PCSK9 promotes tumor growth by inhibiting tumor cell apoptosis in hepatocellular carcinoma', *Experimental Hematology and Oncology*. BioMed Central Ltd, 10(1), pp. 1–11. doi: 10.1186/S40164-021-00218-1/FIGURES/5.

Zhang, Z., Zhang, H., Liao, X. and Tsai, H. I. I. (2023). 'KRAS mutation: The booster of pancreatic ductal adenocarcinoma transformation and progression', *Frontiers in Cell and Developmental Biology*. Frontiers Media SA. doi: 10.3389/fcell.2023.1147676.

Zhao, B., Luo, C., Zhang, M., Xing, F., Luo, S., Fu, S. and Sun, X. (2020). 'Knockdown of phosphatase and tensin homolog (PTEN) inhibits fatty acid oxidation and reduces very low density lipoprotein assembly and secretion in calf hepatocytes', *Journal of Dairy Science*. Elsevier Inc., 103(11), pp. 10728–10741. doi: 10.3168/JDS.2019-17920/ATTACHMENT/3A38C24C-E5BD-4736-B527-658A7A7ECDFA/MMC1.PDF.

Zhao, J., Shi, X., Dong, C., Liu, R., Su, L. and Cao, C. (2022). '5-fluorouracil suppresses stem cell-like properties by inhibiting p38 in pancreatic cancer cell line PANC-1', *Folia Histochemica et Cytobiologica*. Via Medica, 60(1), pp. 55–65. doi: 10.5603/FHC.a2022.0004.

Zhao, Y., He, L., Wang, T., Zhu, L. and Yan, N. (2021). '2-hydroxypropyl-β-cyclodextrin regulates the epithelial to mesenchymal transition in breast cancer cells by modulating cholesterol homeostasis and endoplasmic reticulum stress', *Metabolites*. MDPI, 11(8). doi: 10.3390/metabo11080562.

Zhu, M., Zhao, Q., Zhang, W., Xu, H., Zhang, B., Zhang, S., Duan, Y., Liao, C., Yang, X. and Chen, Y. (2023). 'Hydroxypropyl-β-cyclodextrin inhibits the development of triple negative breast cancer by enhancing antitumor immunity', *International Immunopharmacology*, 125(Part A), p. 111168. doi: 10.1016/j.intimp.2023.111168.

Zhu, X., Yang, J., Zhu, W., Yin, X., Yang, B., Wei, Y. and Guo, X. (2018). 'Combination of Berberine with Resveratrol Improves the Lipid-Lowering Efficacy', *International Journal of Molecular Sciences*. Multidisciplinary Digital Publishing Institute (MDPI), 19(12). doi: 10.3390/IJMS19123903.

Zimmer, S. *et al.* (2016). 'Cyclodextrin promotes atherosclerosis regression via macrophage reprogramming', *Science Translational Medicine*. American Association for the Advancement of Science, 8(333). doi: 10.1126/SCITRANSLMED.AAD6100/SUPPL_FILE/8-333RA50_TABLE_S4.ZIP.

8 APPENDIX

8.1 Mice Xenograft Study

8.1.1 Cell Culture

The mycoplasma free PANC-1 cell line (Cellonex, SA) was used for the PDAC mice xenograft study as it has been widely used to study PDAC and is well reported in literature to successfully form tumours (Aghevlian *et al.*, 2020; Kamitani *et al.*, 2022; Feng *et al.*, 2023; Y Liu *et al.*, 2023). The PANC-1 cell line was established from the primary tumour of a 65-year old male (Deer *et al.*, 2010). PANC-1 cells contain the characteristics of drug resistant PC cells, making it a reliable cell line for preclinical research (Gradiz *et al.*, 2016).

All cell culture was performed by the PhD candidate in preparation for the xenograft study. Briefly, PANC-1 cells were cultured in Dulbecco's Modified Eagle medium (DMEM) (Sigma Aldrich, UK) supplemented with 1% (v/v) Penicillin-Streptomycin (Sigma Aldrich, UK) and 10% (v/v) Foetal Bovine Serum (FBS) (Celtic Molecular Diagnostics, SA and Biowest, UK). Cell cultures were maintained at a temperature of 37°C in a humidified incubator with 5% carbon dioxide (CO_2) to mimic physiological conditions. Once cells reached a confluency of around 80-90%, cells were subjected to trip-LE™ (Thermo Fisher Scientific, USA) and counted using the Invitrogen Countess 2 Automated Cell Counter (Thermo Fisher Scientific, USA) which employs the Neubauer method to assess cell density. Utilizing an automated cell counter enhanced efficiency and reduced the likelihood of subjective interpretations or human errors in cell quantification, when compared to traditional cell counting methods using the haemocytometer. Thereafter, the cells (± 3.5 million cells per mouse) were prepared for injection in a 1:1 ratio of culture media and saline (Adcock Ingram, SA). Afterwards, 120 µL cell suspensions were aliquoted into 1.5 mL Eppendorf tubes and kept on a heating block at 37°C to maintain temperature for mice inoculation.

8.1.2 Xenograft Mice Model Study

Mice xenografts provide a platform to test the therapeutic effect of a drug on tumour growth (Gould *et al.*, 2015). In this study, 30 non-obese diabetic (NOD) severe combined immunodeficiency (SCID) mice (comprising of males and females) were used. NOD/SCID mice are genetically immunodeficient and commonly used for cancer cell line derived xenografts (CDXs) (Hudson *et al.*, 1998). The NOD/SCID mice were acclimatised for two

weeks and allowed to reach the desired weight of 20-21 g for female mice and 20-22 g for male mice. PANC-1 cells were prepared as described in section 3.1.1 and each mouse received a subcutaneous injection in the left flank. The subcutaneous engraftment of tumour cells allowed for tumour visibility and to closely monitor tumour growth, whilst only imposing minimum trauma on the mice (Kong *et al.*, 2020). Mice were assessed daily for general health concerns. Additionally, mice were weighed and tumour volumes were measured thrice weekly using a calliper and calculated using Equation 2 below.

$$Volume = \frac{1}{2} \times L \times W \times H$$

Equation 2: Calculation of tumour volume

Calliper measurements for length, width and height were used to calculate tumour volume. The equation was adopted from Tomayko and Reynolds, 1989, with the assumption that the tumour has an ellipsoid shape.

Once tumours reached a volume of 100 mm^3, treatments were initiated. The mice were divided into seven treatment groups and detailed treatment regimens can be seen in Table 1. All treatments were prepared to a final volume of 200 µL and kept covered in foil on a heating block at 24°C. GEM was dissolved in saline and administered once a week at a concentration of 30 mg/kg. 5-FU was dissolved in 4% dimethyl-sulfoxide (DMSO) and administered twice a week at a concentration of 30 mg/kg. HPβCD was dissolved in saline and administered twice a week at a concentration of 3000 mg/kg. Combination treatments included GEM & HPβCD, as well as the 5-FU & HPβCD and they were administered twice a week at their respective concentrations (Table 1). All treatments were administered by IP injection to the right flank opposite to that of the tumour, to simulate the clinical setting where chemotherapy is not administered directly into the tumour itself. After completion of 10 treatments, mice were euthanized with pentobarbital (150 mg/kg). Blood samples were collected immediately after euthanasia in gold-top blood collection tubes for serum cholesterol analysis. These tubes contain a serum separator gel which aids in separating blood serum from the blood cells. Thereafter, organs and tumours were harvested. Organs were separately sealed in cryovials and snap-frozen in liquid nitrogen. Tumours were measured and weighed, then cut into three sections and stored by three different means for downstream analysis; (1) 4% formaldehyde

(Sigma Aldrich, UK), (2) RNAlater® (Thermo Fisher Scientific, USA) and (3) snap frozen in liquid nitrogen. All snap frozen samples were transported on dry ice and stored at - 80°C. The snap frozen Tumour tissue was used for all downstream experiments in this study.

Regrettably, several mice were euthanized or passed away prior to the conclusion of the experiment due to health concerns. Before Tumour inoculation, one mouse (Mouse 11, Table A1) passed away due to a gastrointestinal infection. Moreover, unexpected challenges emerged with the female mice who received GEM single and GEM & HPβCD combination treatments. It was determined that the initial concentration of GEM at 100 mg/kg was too toxic, and as a result, three mice from the GEM & HPβCD combination treatment group perished due to gastrointestinal issues (Table A1). The remaining fourth mouse from the GEM & HPβCD combination had to be euthanized due to stereotypical behaviour (Table A1). To address the loss of all the mice in the GEM & HPβCD combination treatment group, the three mice used as replacements were from control groups. In subsequent weeks, three mice from the GEM single treatment were also found deceased due to similar gastrointestinal problems. There were no extra mice to be used as replacements for the GEM single treatment group, and ultimately, this group consisted of the only one remaining mouse. Additionally, the GEM dosage was reduced to 30 mg/kg to decrease toxicity. These unforeseen circumstances led to disparities in the sample size between the treatment groups, and ultimately, the GEM treatment group had to be omitted from statistical analysis.

8.2 Mice eliminated from the study

Table A1: Mice eliminated from the study

Date of termination	Mouse ID	Gender	Treatment Regimen	Number of doses	Reason for termination
27/07/2023	11	Male	n/a	n/a	Found deceased. Post-mortem report suggests gastrointestinal infection.
04/09/2023	17	Female	GEM (100 mg/kg) & HPβCD (3000 mg/kg)	2	Found deceased.
	19	Female		2	Euthanized due to stereotypical behaviour.
	27	Female		2	Found deceased.
06/09/2023	26	Female		3	Found deceased.
	22	Female	GEM (100 mg/kg)	3	Found deceased.
09/09/2023	24	Female		3	Found deceased.
11/09/2023	16	Female		4	Found deceased.

8.3 Gene expression

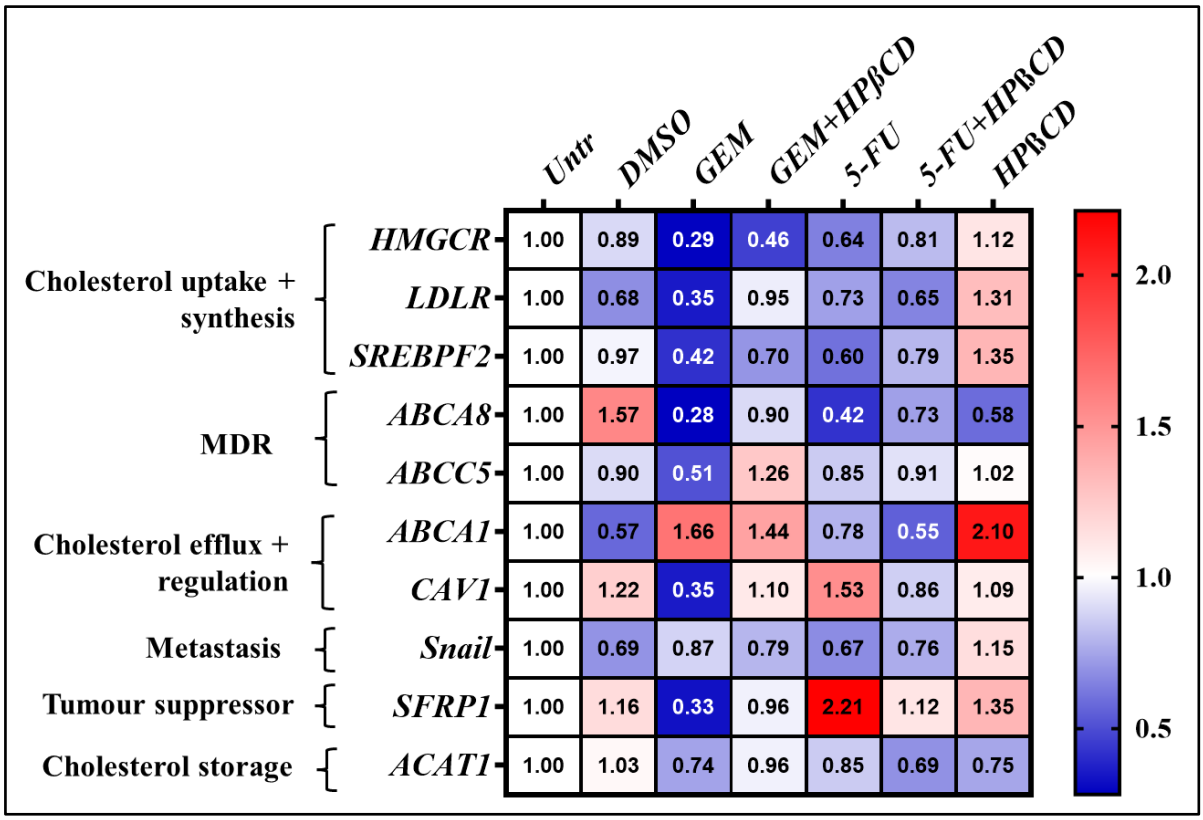


Figure A1: Genetic changes in multi-drug resistance, cholesterol homeostasis, tumour suppression and metastasis

The heatmap portrays the log2 fold change of genes involved in multi-drug resistance (*ABCA8* and *ABCC5*), cholesterol homeostasis (*HMGCR, LDLR, SREBPF2, ABCA1, CAV1* and *ACAT1*), tumour suppression (*SFRP1*) and metastasis (*SNAIL*) in tumour tissue. Each gene is represented on the y-axis with each treatment group on the x-axis. A positive log2 fold change (increase) is represented by red, no change is represented by white and a negative log2 fold change (decrease) is represented by blue compared to the untreated. Data was provided by Tasvi Daya (PhD candidate).

8.4 Mouse serum analysis of total cholesterol

Mice serum cholesterol served as an indication of the physiological cholesterol balance in the body, to provide a holistic insight to cholesterol homeostasis beyond that of the tumour cells. Normal mice serum cholesterol ranges from 80-100 mg/dL.

Table A2: Total serum cholesterol

Treatment Group	Mouse ID	Number of doses (/10)	Total serum cholesterol (mg/dL)
Untreated	2	na	63
	3	na	<18
	5	na	52
	10	na	51
HPβCD	18	10	<18
	20	10	50
	25	10	41
	28	10	32
5-FU	1	10	80
	6	10	83
	9	10	66
	13	10	98
5-FU & HPβCD	4	10	71
	7	10	-
	12	10	86
	14	10	69
GEM	23	6	<24
GEM & HPβCD	21	3	<18
	29	4	<24
	30	4	<18
DMSO	8	10	91
	15	10	88

8.5 Tumour volume and relative protein expression of vehicle control DMSO

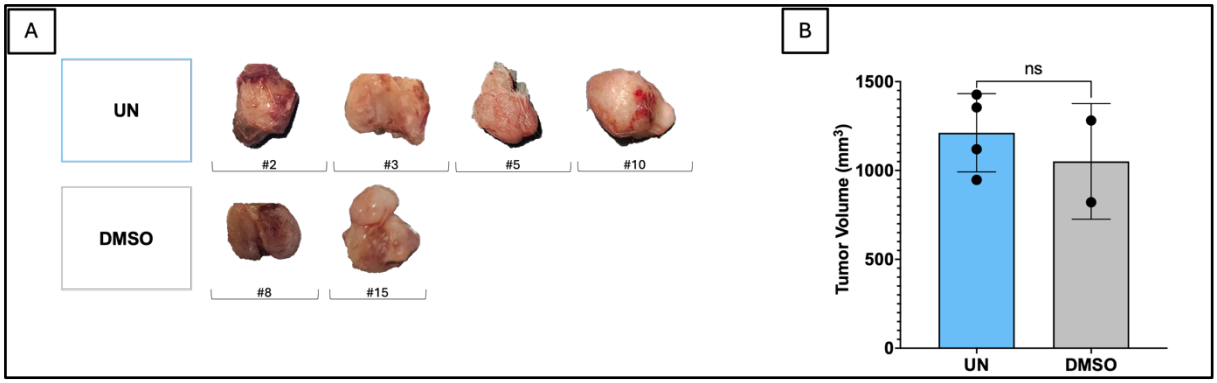


Figure A2: Tumour volume for DMSO vehicle control

(A) Images of excised subcutaneous tumours. (B) Average tumour volume showing similar tumour size was observed for the UN control and DMSO control groups. DMSO exhibits a 13% decrease in tumour volume compared to UN, which was not significant. Data shown as mean ± SD. The data was analysed using a Brown-Forsythe ANOVA test followed by a Dunnett's multiple comparisons test to compare individual differences to the UN control.

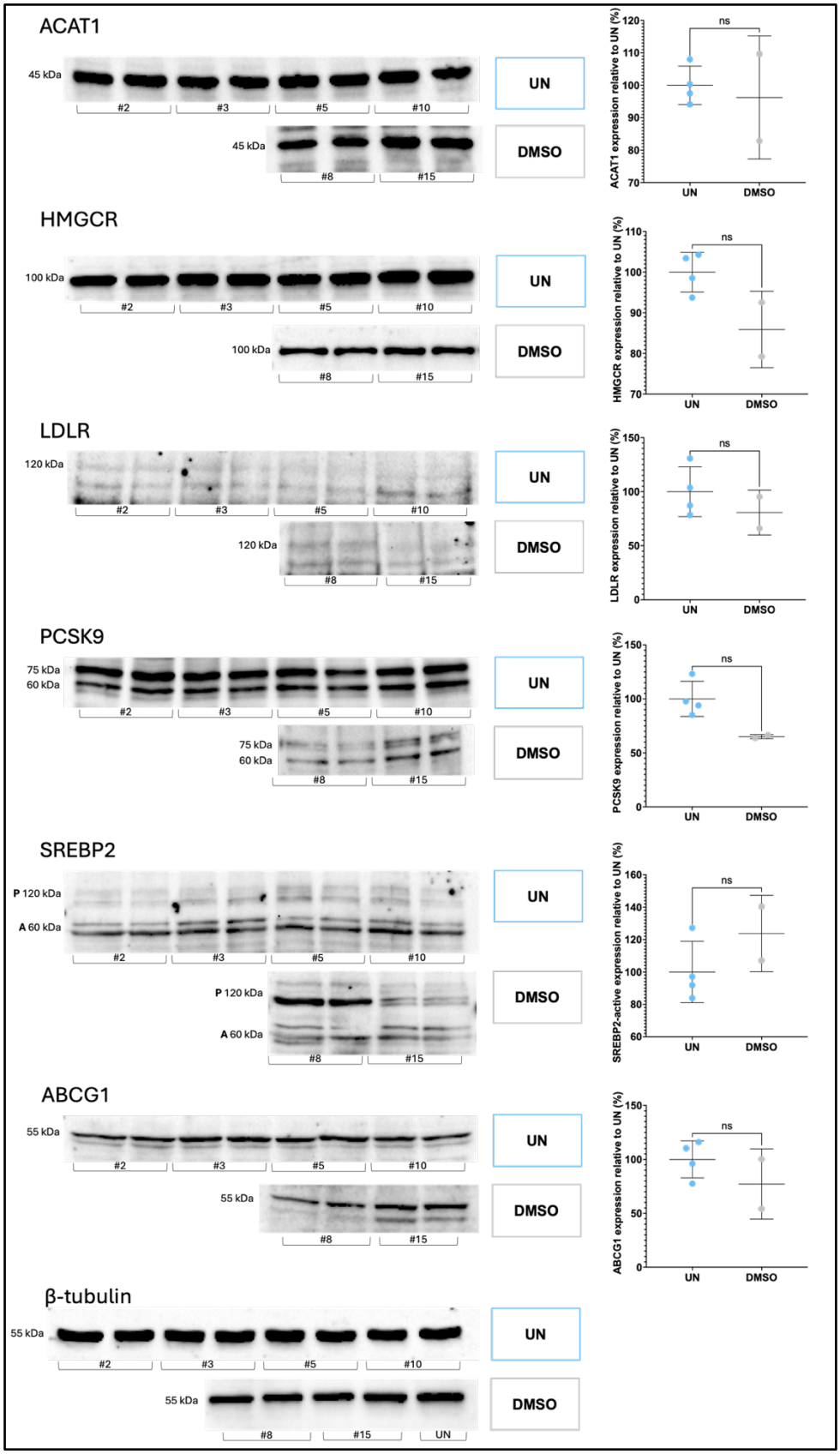


Figure A3: Relative protein expression for DMSO vehicle control

Representative Western blots comparing the protein expression of DMSO relative to the UN control for: ACAT1 (–3%), HMGCR (–14%), LDLR (–19%), PCSK9 (–34%), SREBP2

(+24%) and ABCG1 (–22%). B-tubulin was used as a loading control to normalize expression to that of the UN control, which is visible in the far right lane on the DMSO blot. No significant differences were observed for protein expression between DMSO and the UN control. Data shown as mean ± SD. The data was analysed using a Brown-Forsythe ANOVA test followed by a Dunnett's multiple comparisons test to compare individual differences.